



**Faculty of Engineering and Technology
Joint Master in Electrical Engineering**

**Assessment of Voltage Stability in Active
Distribution Networks**

Submitted By

Alaa Ibrahim Abubaker

Supervisor

Dr. Jaser Sa'ed

July, 2023



Faculty of Engineering and Technology
Joint Master in Electrical Engineering (JMEE)

**Assessment of Voltage Stability in Active
Distribution Networks**

تقييم استقراريه الجهد في شبكات التوزيع الفعّالة

Submitted By

Alaa Ibrahim Abubaker

Supervisor

Dr. Jaser Sa'ed

This Thesis was submitted in partial fulfillment of the requirements for the Master's Degree in Electrical Engineering From the Faculty of Engineering and Technology at Birzeit University, Palestine

Committee

Dr. Jaser Sa'ed
Dr. Muhammad Abu-Khaizaran
Dr. Abdalkarim Awad

July 4, 2023

Assessment of Voltage Stability in Active Distribution Networks

تقييم استقراريه الجهد في شبكات التوزيع الفعّالة

Submitted By

Alaa Ibrahim Abubaker

Approved By the Examining Committee

Dr. Jaser Sa'ed

Dr. Muhammad Abu-Khaizaran

Dr. Abdalkarim Awad

July 4, 2023

DECLARATION

I declare that this thesis entitled “Assessment of Voltage Stability in Active Distribution Networks” is the result of my own research except as cited in the references. It is being submitted to the Master’s Degree in Electrical Engineering from the Faculty of Engineering and Technology at Birzeit University, Palestine. The thesis has not been accepted for any degree and is not concurrently submitted in candidature of any other degree.

Signature:

Name:

Date:

ACKNOWLEDGMENT

First and foremost, I want to thank Almighty ALLAH for getting this work done.

I would like to express my deepest gratitude to all those who have contributed to the completion of my master's thesis. Firstly, I would like to extend my heartfelt appreciation to my academic advisor, Dr. Jaser Sa'ed, for his guidance, expertise, and valuable insights. His dedication and patience in providing constructive feedback and steering me in the right direction have been instrumental in shaping the final outcome of this research.

I am also grateful to my committee members, Dr. Muhammad Abu-Khaizaran and Dr. Abdalkarim Awad, for their advice and mentoring and for their time, expertise, and valuable suggestions. Their insightful comments and critical evaluation have significantly enriched the quality of my work.

I would like to express my sincere gratitude to my family, father, mother, brothers, sisters, and friends for their unwavering support throughout the journey of completing my master's thesis. Their love, encouragement, and understanding have been my constant motivation. Finally, I want to dedicate this thesis to my beloved family.

ABSTRACT

Voltage stability is critical to power systems, ensuring electrical grids' reliable and secure operation. With the increasing integration of renewable energy sources and distributed generation, active networks have become more complex, requiring a reevaluation of existing voltage stability indices.

The research presented in this thesis begins by reviewing the fundamental concepts of voltage stability and its importance in power systems. The thesis proposes a comprehensive reassessment of voltage stability indices in passive and active networks to address voltage stability.

First, it presents a comprehensive overview of various voltage stability indices. It discusses detailed information about each index, including its name, abbreviation, calculation method, assumptions, basic concept, steady-state characteristics, threshold, instability conditions, advantages, and disadvantages. Then various voltage stability indices in passive networks are examined, where it compares the effectiveness of voltage stability indices in predicting voltage instability in power systems, highlighting their strengths and limitations and the coherence between indices in the same category and their theoretical foundation. After that, it compares various voltage stability indices, evaluates their performance under different operating conditions like load variation, and explores the relationship between Distribution Generators (DGs), load changes, and VSIs.

Furthermore, it evaluates line stability indices and their role in identifying weak buses for the placement DGs, where the study considers Type I, Type II, Type III, and Type IV DG models, accounting for changes in voltage profile and minimizing power losses and maximizing voltage stability margin (VSM) to enhance power system performance. The proposed technique is tested and validated on IEEE 12-bus and 30-bus systems,

showing significant savings in annual energy loss, reduced system power losses, and improved voltage profiles for Type I and Type III DG at optimal power factor. The MATLAB code is developed using VSIs to assess stability and successfully applies it to standard IEEE test systems.

In summary, this thesis explores the different aspects of voltage stability in power distribution systems, including analyzing and evaluating voltage stability indices to take preventive measures to protect against voltage collapse, such as identifying the optimal location and sizing of DG units. The results contribute to the understanding and improvement of voltage stability in power systems, and the comprehensive review of existing voltage stability indices serves as the basis for future work in this field and helps professionals to choose the most suitable indices for various applications.

المستخلص

يعدّ استقرار الجهد أمراً بالغ الأهمية لأنظمة الطاقة، مما يضمن التشغيل الموثوق والأمن للشبكات الكهربائية. مع زيادة تكامل مصادر الطاقة المتجددة والمولدات، أصبحت الشبكات النشطة أكثر تعقيداً، مما يتطلب إعادة تقييم مؤشرات استقرار الجهد الحالية.

تبدأ الأطروحة بمراجعة المفاهيم الأساسية لاستقرار الجهد وأهميته في أنظمة الطاقة. ثم تقترح الأطروحة إعادة تقييم شاملة لمؤشرات استقرار الجهد الحالية في الشبكات التقليدية (الشبكات التي تعتمد بشكل حصري على محطات التوليد الكبيرة) والشبكات النشطة التي تدمج مصادر توليد الطاقة الموزعة (مثل الخلايا الشمسية وطاقة الرياح) داخل شبكة الكهرباء العامة عوضاً عن الاعتماد بشكل حصري على محطات التوليد الكبيرة، لمعالجة استقرار الجهد.

أولاً، يتم تقديم نظرة عامة شاملة على مختلف مؤشرات استقرار الجهد. ثم يتم مناقشة معلومات مفصلة عن كل مؤشر، بما في ذلك اسمه، واختصاره، وطريقة الحساب، والافتراضات، والمفهوم الأساسي، واستقراره، والقيمة الحرجة، وظروف عدم استقراره، وفوائده، وعيوبه. ثم يتم فحص مؤشرات استقرار الجهد المختلفة في الشبكات التقليدية، حيث يتم مقارنة فعالية مؤشرات استقرار الجهد في التنبؤ بعدم استقرار الجهد في أنظمة الطاقة، مع تسليط الضوء على نقاط قوتها ونقاط ضعفها والاتساق بين المؤشرات من نفس الفئة وأسسها النظرية. بعد ذلك، يقارن بين مختلف مؤشرات استقرار الجهد، ويقوم أدائها في ظل ظروف تشغيل مختلفة مثل تغيير الأحمال.

بالإضافة إلى ذلك، سيتم تقييم مؤشرات استقرار الجهد ودورها في تحديد خطوط النقل الكهربائية الضعيفة؛ ومن ثم تحديد العقد (نقاط الربط) الضعيفة لوضع DGs، حيث تأخذ الدراسة في الاعتبار أنواع مختلفة من DG، من النوع الأول والثاني والثالث والرابع، مع مراعاة تحسين ملف الجهد للشبكة وتقليل خسائر الطاقة وزيادة هامش استقرار الجهد (VSM) لتحسين أداء نظام الطاقة.

تم اختبار المنهجية المقترحة واعتمادها على أنظمة IEEE 12-Bus و IEEE 30-Bus، وباستخدام برنامج MATLAB. تم تطوير كود لحساب مؤشرات استقرار الجهد (VSIs) لتقييم الاستقرار، وتم تطبيقه بنجاح على أنظمة اختبار IEEE القياسية.

باختصار، تستكشف هذه الأطروحة الجوانب المختلفة لاستقرار الجهد في أنظمة توزيع الطاقة، بما في ذلك تحليل مؤشرات استقرار الجهد وتقييمها بهدف اتخاذ التدابير الاحترازية للحماية من انهيار الجهد، كتحديد الموضع الأمثل وحجم وحدات DG، حيث تساهم النتائج في فهم وتحسين استقرار الجهد في أنظمة الطاقة، وتعمل المراجعة الشاملة لمؤشرات استقرار الجهد الحالية كأساس للعمل المستقبلي في هذا المجال، وتساعد المهنيين في اختيار أنسب المؤشرات للتطبيقات المتنوعة.

TABLE of CONTENTS

ACKNOWLEDGMENT	I
ABSTRACT	II
المستخلص.....	IV
TABLE of CONTENTS	V
LIST of TABLES	VII
LIST of FIGURES	VIII
LIST OF ABBREVIATIONS.....	XII
CHAPTER 1: Introduction.....	1
1.1 Background	1
1.2 Problem Statement	3
1.3 Research Objectives	4
1.4 Importance and Expected Impact	5
1.5 Contribution.....	6
1.6 Research Methodology.....	7
CHAPTER 2: Literature Review.....	9
CHAPTER 3: Power System Voltage Stability	18
3.1 Introduction	18
3.2 Definition and Classification of Power System Stability	18
3.3 Voltage Stability Definition	20
3.4 Voltage Stability Classification.....	22
3.4.1 Large-Disturbance Voltage Stability	22
3.4.2 Small-Disturbance Voltage Stability	22
3.4.3 Short-Term Voltage Stability	22
3.4.4 Long-Term Voltage Stability.....	22
3.5 Voltage Stability Analysis.....	23
CHAPTER 4: Voltage Stability Indices	29
4.1 Theory and VSIs Formulation:.....	29
4.2 Voltage Stability Indices Classification	30
4.3 Voltage Stability Indices	31
4.3.1 Fast Voltage Stability Index (FVSI)	32
4.3.2 Line Stability Index (Lmn).....	33
4.3.3 Line Stability Factor (LQP).....	35
4.3.4 Line Stability Index (Lp) Or Line Voltage Stability Index (LVSI).....	36

4.3.5 Novel Line Stability Index (NLSI)	37
4.3.6 Voltage Collapse Proximity Index (VCPI)	37
4.3.7 New Voltage Stability Index (NVSI)	40
4.3.8 Voltage Stability Indicator (VSI ₂).....	41
4.3.9 Power Transfer Stability Index (PTSI).....	41
4.3.10 Voltage Reactive Power Index (VQI _{Line})	42
4.3.11 Voltage Stability Load Index (VSLI).....	44
4.3.12 Voltage Vulnerability Index (VVI).....	44
4.3.13 Line Collapse Proximity Index (LCPI).....	45
4.3.14 Power Stability Index (PSI).....	47
4.3.15 Voltage Stability Index (VSI)	48
4.3.16 Line Voltage Stability Index (LVSI).....	49
4.3.17 Voltage Collapse Proximity Index (VCPI ₁)	50
4.3.18 Voltage Stability Margin (VSMs)	50
CHAPTER 5: Results and Discussions	53
5.1 Introduction	53
5.2 Description of Test System	53
5.3 Assessment of Voltage Stability Indices in a Distribution Networks for Prediction of Voltage Collapse.....	57
5.4 Methodology to Calculate Voltage Stability Indices.....	58
5.5 Voltage Stability Indices	59
5.6 PV and QV Curve.....	81
CHAPTER 6: Optimal Placement of Distributed Generation (DG) Based on Voltage Stability Indices	86
6.1 Introduction	86
6.2 Types and Sizing of DG	87
6.3 VSIs in DG Placement.....	89
6.4 Simulation Results and Evaluation.....	90
6.4.1 IEEE 12-Bus Test Network.....	90
6.4.2 IEEE 33-Bus Test Network.....	100
CHAPTER 7: Conclusions and Recommendations for Future Work.....	118
7.1 Conclusions	118
7.2 Recommendations for Future Work	121
Appendix A.	122
References	125

LIST of TABLES

Table 4.1 Characteristics of VSIs.....	51
Table 5.1 The top critical line for each voltage stability index (ranking one) for base case loading.	66
Table 5.2 The top critical line for each voltage stability index (ranking one) for PQ incremental loading at all buses.	79
Table 6.1 Results of IEEE 12-Bus System.	95
Table 6.2 Comparison of results with Type I DG injection at different buses.	95
Table 6.3 Results of IEEE 30-Bus System for bus 26.	101
Table 6.4 Results of IEEE 30-Bus System for bus 30.	103
Table A.1 Bus data for IEEE 12-bus system.....	122
Table A.2 Line data for IEEE 12-bus system.....	122
Table A.3 Bus data for IEEE 30-bus system.....	123
Table A.4 Line data for IEEE 30-bus system.....	124

LIST of FIGURES

Figure 3.1 Classification of power system stability	19
Figure 3.2 P-V curve with stable and unstable operating points.	24
Figure 3.3 Voltage stability margin.....	25
Figure 3.4 P-V curve for different power factor loads.....	26
Figure 3.5 Q-V curve for different load real powers	27
Figure 4.1 The two-bus representation of radial distribution network	29
Figure 4.2 Concepts of the voltage stability indices	52
Figure 4.3 Impedance dependent and independent voltage stability indices.....	52
Figure 5.1 Single line diagram of IEEE 12-bus distribution test system.	56
Figure 5.2 Single line diagram of IEEE 30-bus distribution test system.	56
Figure 5.3 Flowchart depicting the computation method for VSIs and detection of weak lines in a real-time power system.	58
Figure 5.4 VSIs of each branch in the IEEE 12-bus network under base case condition, branch 4 is critical.....	60
Figure 5.5 VSIs of each branch in the IEEE 12-bus network under base case condition, branch 7 is critical.....	60
Figure 5.6 VSI & PSI of each branch in the IEEE 12-bus system under base case condition, branch 8 is critical.....	61
Figure 5.7 LVSI, VCPI(1) and VSMs of each branch in the IEEE 12-bus system under base case condition	61
Figure 5.8 VSIs of all 33 kV transmission lines for IEEE 30-bus network under base case condition.	62
Figure 5.9 VSIs of all 132 kV transmission lines for IEEE 30-bus network under base case condition.....	63
Figure 5.10 VSIs of all 33 kV transmission lines for IEEE 30-bus network under base case condition.....	63
Figure 5.11 VSIs of all 132 kV transmission lines for IEEE 30-bus network under base case condition.....	64
Figure 5.12 VSI & PSI of all 33 kV transmission lines for IEEE 30-bus network under base case condition.	64
Figure 5.13 VSI & PSI of all 132 kV transmission lines for IEEE 30-bus network under base case condition.	65
Figure 5.14 LVSI, VCPI(1), and VSMs value of all 33 kV transmission lines for IEEE30-bus network under base case condition.	65
Figure 5.15 LVSI, VCPI (1), and VSMs value of all 132 kV transmission lines	

for IEEE-30 bus network under base case condition.	66
Figure 5.16 load buses for IEEE 12-bus system (a) under base case condition (b) under heavy PQ loading.....	68
Figure 5.17 Voltage profile for IEEE 12-bus system under heavy PQ loading at all buses.....	68
Figure 5.18 VSIs for each line in IEEE 12-bus under heavy PQ loading at all buses.....	69
Figure 5.19 LQP & NVSI for each line in IEEE 12-bus under heavy PQ loading at all buses.....	69
Figure 5.20 VSI & PSI for each line in IEEE 12-bus under heavy PQ loading at all buses.....	69
Figure 5.21 LVSI, VCPI(1),and VSMs for each line in IEEE 12-bus under heavy PQ loading at all buses.	70
Figure 5.22 The index values for different VSIs with respect to PQ loading in IEEE 12-bus system. (a),(c) Line 4(4-5) - (b),(d) Line 8(8-9).....	70
Figure 5.23 FVSI under heavy PQ loading for IEEE 12-bus, top critical lines.	71
Figure 5.24 LQP under heavy PQ loading for IEEE 12-bus, top critical lines.	71
Figure 5.25 PSI under heavy PQ loading for IEEE 12-bus, top critical lines.	72
Figure 5.26 VSMs under heavy PQ loading for IEEE 12-bus, top critical lines.	72
Figure 5.27 load buses for IEEE 30-bus system (a) under base case condition (b) under heavy PQ loading.....	73
Figure 5.28 Voltage profile for IEEE 30-bus system under heavy PQ loading at all buses.....	73
Figure 5.29 VSIs of 33 kV transmission lines for IEEE 30-bus network under heavy PQ loading at all buses.	74
Figure 5.30 VSIs of 132 kV transmission lines for IEEE 30-bus network under heavy PQ loading at all buses.	74
Figure 5.31 VSIs of 33 kV transmission lines for IEEE 30-bus network under heavy PQ loading at all buses.	75
Figure 5.32 VSIs of 132 kV transmission lines for IEEE 30-bus network under heavy PQ loading at all buses.	75
Figure 5.33 VSI and PSI of all 33 kV transmission lines for IEEE 30-bus network under heavy PQ loading.	75
Figure 5.34 VSI and PSI of all 132 kV transmission lines for IEEE 30-bus network under heavy PQ loading.	76
Figure 5.35 LVSI, VCPI(1), and VSMs of all 33 kV transmission lines for IEEE30-bus under heavy PQ loading.	76
Figure 5.36 LVSI, VCPI(1), and VSMs of all 132 kV transmission lines in	

IEEE30-bus under heavy PQ. loading.....	76
Figure 5.37 values for different VSIs with respect to PQ loading for line 38 (27-30) in IEEE 30 bus system.	77
Figure 5.38 VSIs under PQ loading in IEEE 30-bus, top critical lines of all 33 kV transmission lines.	77
Figure 5.39 VSIs under PQ loading in IEEE 30-bus, top critical lines of all 33 kV transmission lines.	78
Figure 5.40 PSI & VSI under PQ loading in IEEE 30-bus, top critical lines of all 33 kV transmission lines.....	78
Figure 5.41 LVSI, VCPI(1), and VSMs under PQ loading in IEEE 30-bus, top critical lines of all 33 kV transmission lines.....	79
Figure 5.42 P-V curve of a load bus in the IEEE 12-bus	82
Figure 5.43 Q-V curve of a load bus in the IEEE 12-bus	82
Figure 5.44 P-V curve of all 33 kV buses for IEEE 30-bus.	83
Figure 5.45 Q-V curve of all 33 kV buses for IEEE 30-bus.....	84
Figure 5.46 P-V curve of all 132 kV buses for IEEE 30-bus.....	85
Figure 5.47 P-V curve of all 132 kV buses for IEEE 30-bus.....	85
Figure 6.1 Active power losses vs. PL for different DG types	91
Figure 6.2 Voltage profile of each bus in the IEEE 12-bus system – (Type 1 DG injection at bus 5,8,9).	93
Figure 6.3 Voltage profile of each bus in the IEEE 12-bus system – (optimum PL% for each Type of DG at 9).	94
Figure 6.4 Voltage profile of each bus in the IEEE 12-bus - (different DG types vs. different penetration levels).....	94
Figure 6.5 P-V curves at bus 9 for different DG types vs. optimum (PL%) for each type.	96
Figure 6.6 Q-V curves at bus 9 for different DG types vs. optimum (PL%) for each type.	96
Figure 6.7 P-V curves at bus 9 for different penetration level-type 1 DG.....	97
Figure 6.8 Q-V curves at bus 9 for different penetration level- type 1 DG.....	97
Figure 6.9 VSIs of each lines for IEEE 12-bus under injection DG(Type1 at bus 9, size = 230.55 + j214.65 kVA)	98
Figure 6.10 LVSI, VCPI(1),and VSMs of each lines for IEEE 12-bus under injection DG	99
Figure 6.11 VSI and PSI of each lines for IEEE 12-bus under injection DG.....	99
Figure 6.12 Active power losses vs. PL for different DG types of 33kV buses.....	100
Figure 6.13 Voltage profile of each bus in the IEEE 30-bus – (optimum PL%	

for each Type of DG at bus 30).....	103
Figure 6.14 Voltage profile of each bus in the IEEE 30-bus system – (Type3 DG injection at bus 26,30).	103
Figure 6.15 Voltage profile of each bus in the IEEE 30-bus - (different DG types vs. different penetration levels).....	105
Figure 6.16 P-V curves at bus 30 (33kV buses) - (different DG types vs. PL%).....	107
Figure 6.17 Q-V curves at bus 30 (33kV buses) - (different DG types vs. PL%).....	107
Figure 6.18 P-V curves at bus 30 (33kV buses) – (type 3 DG vs. different PL%).....	108
Figure 6.19 Q-V curves at bus 30 (at 33kV buses) – (type 3 DG vs. different PL%).....	109
Figure 6.20 Voltage profile vs. different PL% at bus 30, type3 DG.....	110
Figure 6.21 VSIs of all 33 kV transmission lines, Base case.....	110
Figure 6.22 VSIs of all 33 kV transmission lines, PL = 5%, type3 DG	111
Figure 6.23 VSIs of all 33 kV transmission lines, PL = 10%, type3 DG	113
Figure 6.24 VSIs of all 33 kV transmission lines, PL = 30%, type3 DG	114
Figure 6.25 VSIs of all 33 kV transmission lines, PL = 30%, type1 DG	115
Figure 6.26 VSIs of all 33 kV transmission lines, PL = 23%, type2 DG	116
Figure 6.27 VSIs of all 33 kV transmission lines, PL = 30%, type 4 DG.....	117

LIST OF ABBREVIATIONS

Abbreviation	Full word
ANN	Artificial Neural Networks
BPF	Bus Participation Factor
BVSI	Line Voltage Stability Index
CBI	Critical Boundary Index
CPF	Continuous Power Flow
DERs	Distributed Energy Resources
DG	Distributed Generator
DN	Distributed Network
DS	Distribution System
DSOs	Distribution System Operators
D-STATCOM	Distribution Static Synchronous Compensator
DVS	Dynamic Voltage Stability
FACTS	Flexible AC Transmission Systems
FVSI	Fast Voltage Stability Index
ITLTI	Integrated Transmission Line Transfer Index
LCPI	Line Collapse Proximity Index
LM	Load ability Margin
Lmn	Line Stability Index
LQP	Line Stability Factor
LVSI	Line Voltage Stability Indices
LVSI / L_p	Line Voltage Stability Index / Line Stability Index
MG	Microgrid's
MSCA	Modified Sine Cosine Algorithm
MVSI	Modern Voltage Stability Index
NLSI	Novel Line Stability Index
NVSI	New Voltage Stability Index
OPF	Optimal Power Flow

OPSO	Oscillatory Particle Swarm Optimization
PDS	Passive Distribution System
PLI	Power Loss Index
PMUs	Phasor Measurement Units
PSI	Power Stability Index
PTSI	Power Transfer Stability Index
RDN	Radial Distribution Network
RESs	Renewable Energy Sources
RPC	Reactive Power Compensation
RPC	Reactive Power Compensation
SC	Shunt Capacitors
SSO	Salp Swarm Optimization
STVS	Short-Term Voltage Stability
SVC	Static Var Compensator
SVSI	Simplified Voltage Stability Index
VCPI	Voltage Collapse Proximity Index
VCPI	Voltage Collapse Proximity Index
VSI	Voltage Stability Index
VSI_s	Voltage Stability Indices
VSLI	Voltage Stability Load Index
VSMI	Voltage Stability Margin Index
VSMs	Voltage Stability Margin
VVI	Voltage Vulnerability Index
VQI_{Line}	Voltage Reactive Power Index
VRI_{sys}	System Voltage Recovery Index
VSI₂	Voltage Stability Indicator
V_{cr}	Critical Voltage

CHAPTER 1: Introduction

1.1 Background

The daily electricity demand increase has forced power systems to operate close to their stability limits. Voltage instability leads to voltage collapses in the distribution power system. Collapse occurs in the entire power system, or a part of a system called a blackout system. So many voltage stability and voltage collapse prediction methods have been presented to help power system operators take proper corrective action to prevent voltage collapse. The IEEE power system engineering committee and CIGRE have defined voltage stability as: "Voltage stability refers to the ability of a power system to maintain steady voltages at all buses in the system after being subjected to a disturbance from a given initial operating condition" [1]. It is influenced by a complex interplay of factors, including generation and load characteristics, system configuration, control devices, and overall system behavior. When voltage stability is compromised, the voltage magnitude and angle deviate from their desired values, potentially leading to a cascade of failures and voltage instability.

Voltage collapse is primarily attributed to escalating loads, leading to a progressive decline in voltage magnitude until a sudden and rapid transformation occurs. The problem of voltage collapse can be clarified as the power system's incapacity to furnish the necessary reactive power or an increase of reactive power consumption by the system itself [2]. Additionally, inadequate maintenance and insufficient investments in infrastructure upgrades for power system networks can exacerbate voltage stability problems.

With the increasing integration of Distributed Generators (DGs) into power grids, voltage stability has become an even more significant concern. Due to the integration of distributed

generation, and energy storage, the distribution networks turn from passive systems to active ones. The typical distribution system that feeds solely from a distribution substation that services one or more primary feeders is called the Passive Distribution System (PDS). The power flows from the distribution substation to users, which means only one direction for the power flow [3].

PDS is a distribution network model that serves loads through feeders based on centralized generation without integrating distributed generators. Moreover, unlike the traditional distribution network, the smart grid, or active distribution network, includes centralized and distributed power generation produced by dispatchable and renewable energy sources. Moreover, it can be characterized by a unidirectional and bidirectional power flow [4]. DGs have changed the distribution network's operation from passive with centralized generation to active with distributed generation and bidirectional power flow. A global definition “Active Distribution Networks are distribution networks that have systems in place to control a combination of distributed energy resources (generators, loads, and storage). Distribution System Operators (DSOs) have the possibility of managing the electricity flow using flexible network topology. Distributed Energy Resources (DERs) take some degree of responsibility for system support, which will depend on a suitable regulatory environment connection agreement” [3].

DGs, such as renewable energy sources (e.g., solar and wind) and small-scale cogeneration units, offer numerous benefits, including lower transmission losses, improved grid stability, and environmental sustainability. However, their intermittent nature and decentralized spread offer unique challenges to voltage stability. Additionally, the location and power of DGs in the distribution network can significantly affect voltage profiles. Improper placement and size of

DGs may lead to overvoltage or undervoltage conditions, risking the quality and dependability of the power supply.

A survey of the literature on methodologies or procedures to analyse voltage collapse indicates that many analytical tools based on different ideas have been presented to predict voltage collapse, such as traditional method P-V and Q-V curves [5]. The status of voltage stability in a power system can be known using voltage stability indices. Especially with modern power grids' rising complexity and magnitude, it is essential to develop effective methodologies for monitoring, assessing, and quantifying voltage stability. Voltage stability indices are essential instruments that help power system operators and planners to analyse the stability margins and identify potential voltage stability issues. So, the voltage stability indices are introduced to evaluate the voltage stability limit. Voltage stability indices are tools for gauging the proximity of a given operating point to voltage collapse, load ability, security limits, and overall performance of the system. Many indices have been proposed in the literature to assess voltage stability [6]. One of the essential applications of the Voltage Stability Indices (VSIs) is identifying the weak lines and buses in the power systems [7], which can be used for placement Distributed Generation (DG) and determine its size since DG can offer both benefits and detriments to the network, relating power losses and voltage profiles enhancement. Moreover, the static voltage stability indices have been used to measure the distance from the current operating point to the voltage collapse point [8].

1.2 Problem Statement

The research problem is to investigate, compare, and evaluate voltage stability indices. These indices are essential for predicting and assessing the voltage security and stability of power systems operating near their stability limits. The existing voltage stability indices are different

in the variables of the equations that capture the sensitivity towards different loading conditions and factors such as active power, reactive power, the angular difference between sending and receiving bus voltage, line resistance, and shunt admittance. Furthermore, there is a need for comparison studies between the existing voltage stability indices to evaluate their basis, performance, and general behavior thoroughly.

The research problem provides researchers with a general outline for selecting suitable voltage stability indices for various applications, such as solving optimization problems related to distributed generators' best location and size. Moreover, the effectiveness of the proposed indices in assessing voltage stability, finding stressed lines, and determining weak buses, is essential to consider the variables and loading conditions to ensure accurate and reliable voltage stability assessment.

Furthermore, integrating renewable energy sources into power systems challenges voltage stability. Proper placement of DGs in distribution systems is essential for maintaining voltage stability. Therefore, this research problem also includes studying and assessing the effect of DG placement on voltage stability based on the suggested indicators.

In summary, the study problem includes the assessment of voltage stability indices that account for variables and loading conditions. It involves comparing suggested indices, providing instructions for selecting appropriate indices for various applications, exploring the application of indices in improving DG placement, and studying the impact of DG placement on the voltage stability.

1.3 Research Objectives

This research aims to review various indices for voltage stability assessment and investigate

and analyze various voltage stability indices used in power systems. Moreover, it seeks to understand the underlying principles, advantages, and limitations of different indices to assess their effectiveness in traditional power networks without integration DG.

The study uses VSIs to detect weak lines and buses. Countermeasures are triggered to mitigate voltage instability once the weak lines and buses are identified. The study then uses the VSIs to identify specific areas for Distributed Generation (DG) placement and sizing. This information can be used to enhance voltage stability and maximize the benefits of DG integration. The study also seeks to develop comprehensive methodologies and control strategies to enhance voltage stability.

The research will study and evaluate Voltage Stability Indices (VSIs) in diverse scenarios, analyzing their performance under various operating conditions, including load variation scenarios.

The study will employ comprehensive power system modeling and simulation techniques to achieve these objectives using multiple IEEE benchmark systems, including 12-bus and 30-bus test systems, designed and simulated within the MATLAB environment.

1.4 Importance and Expected Impact

Distributed Generation has emerged as a favored option in the energy sector due to its ability to reduce greenhouse gas emissions [9]. Additionally, it offers significant economic advantages, such as cost-effective electricity and enhanced power reliability. Despite these environmental and economic benefits, careful consideration and assessment of the technical aspects related to integrating DG into the power grid are essential [10]. This integration introduces new challenges in terms of system planning and operation [11]. The random

connection of DG units can result in various technical impacts on the grid, including voltage rise, reverse power flow, power quality issues, and reliability, stability, and safety considerations during steady-state and dynamic operations.

The rapid growth of power demand pushes power systems to operate near their stability limits. This has led to an increased focus on voltage stability, which is the ability of a power system to maintain acceptable voltage levels under different operating conditions. One of the leading causes of voltage collapse is an imbalance between reactive power generation and consumption. Distributed Generation (DG) systems can help to improve voltage stability by providing reactive power support to the grid to avoid voltage collapse.

1.5 Contribution

The thesis presents the following contributions:

1. The primary aim of this thesis is to contribute to reviewing various voltage stability indices and investigating their effectiveness in traditional power networks without integration DG. The research seeks to understand these indices' underlying principles, advantages, and limitations to assess their effectiveness in voltage stability assessment.
2. Using VSIs to detect weak lines and buses to identify suitable locations and sizes for Distributed Generation (DG) placement.
3. Studying and evaluating VSIs in diverse scenarios, analyzing their performance under various operating conditions.
4. The study evaluates the performance of voltage stability indices in diverse scenarios, considering various operating conditions, including load variations. Comprehensive power system modeling and simulation techniques are employed using multiple IEEE benchmark systems to achieve these objectives.

5. Studying the impact of DG on voltage stability in active distribution systems.
6. Assessing voltage stability indices for active distribution networks.
7. Improving voltage profiles and load factors, reducing power losses and on-peak operating costs, improving system integrity, reliability, and efficiency, and improving power system behaviour and performance through integration with DG.
8. Classifying voltage stability indices in the active distribution network will help power system operators take corrective action to prevent voltage collapse.
9. The thesis will provide new insights into DG's optimal placement and sizing in power systems to improve voltage stability.

1.6 Research Methodology

In this thesis, the methodology employed can be divided into four stages, as follows:

1. **Literature Survey:** The first stage involves conducting a comprehensive literature survey on various aspects of voltage stability, voltage stability indices in Distributed Networks (DNs) without Distributed Generation (DG) units, and then assessment indices in active distribution networks with DG units. The study also covers defining and categorizing power system voltage stability and comparing and classifying voltage stability indices in power system networks.
2. **Derivation and Formulation of Voltage Stability Indices:** The second stage focuses on mathematically deriving Voltage Stability Indices (VSIs) based on the characteristics of the voltage collapse point, utilizing a two-bus model for assessing the system's stability. Then these formulations are implemented in the MATLAB environment to evaluate voltage stability within the power system and assess the effectiveness of the voltage stability indices in distribution networks.

3. **Evaluation of Voltage Stability in Active Power System Networks:** The third stage includes evaluating voltage stability indices in active power system networks by adding DG units into IEEE network systems. This stage aims to study the effects of DG units on voltage stability and assess the performance of the suggested voltage stability indices under active network conditions.
4. **Simulation, Comparison, and Analysis:** The fourth stage focuses on performing simulations to evaluate and compare the suggested voltage stability indices. The simulation results are reported in the thesis, and a detailed analysis is done to evaluate the performance of several voltage stability indices in passive and active networks. Finally, the contributions and outcomes of the research are summarized and discussed.

By following the suggested research methodology, the thesis aims to provide a comprehensive assessment of voltage stability in active networks and demonstrate their effectiveness through simulation studies, where the thesis is organized as follows: Chapter 2 presents a comprehensive study of voltage stability and indices of voltage stability in a literature survey. Whilst, Chapter 3 provides an introduction to power system voltage stability. Chapter 4 briefly analyses the theory behind the indices and their formulation. Chapter 5 assesses voltage stability indices and provides results and discussions. Chapter 6 looks for the optimal Distributed Generation (DG) placement based on voltage stability indices. Finally, in Chapter 7, the results and recommendations for future work are presented and clarified.

CHAPTER 2: Literature Review

Every power network possesses a finite capacity to cater to a specific maximum load volume. However, an escalation in load demand weakens the system, causing it to operate under stressed conditions. If the load surpasses a certain threshold, a cascade of voltage collapse can occur, rendering the system unstable and leading to an eventual blackout. Consequently, it becomes paramount to identify the stress conditions of the network during the planning stage. A report crafted by a joint task force established by the CIGRE Study Committee 38 and the IEEE Power System Dynamic Performance Committee ventures to confront the vexing conundrum surrounding stability definition and classification in power systems. With unwavering determination, this report aspires to delineate power system stability with utmost precision, bestowing upon it a systematic framework for classification while simultaneously exploring the interconnectedness with allied facets such as power system reliability and security [1]. The paper delves into the intricate tapestry of voltage instability conditions within distribution networks [12].

Delves into future power systems' challenges regarding voltage stability, particularly emphasizing the impact of emerging technological solutions. The discussion encompasses major factors influencing voltage stability, the necessity to model them, and the requirement for new simulation tools. Additionally, the interdependency between future power systems and other infrastructures is examined [13].

Numerous indices in the existing literature assess the system's health and gauge its proximity to the instability region. The explores the application of selected indices on two conventional electrical systems [14].

Delves into the vast expanse of Voltage Stability Indices (VSIs) from multifaceted perspectives, encompassing concepts, assumptions, critical values, and equations [15]. Moreover, they aid in discerning the most suitable VSI for diverse applications such as Distributed Generation (DG) placement and sizing, as well as voltage stability assessment. The casts a spotlight upon the intrinsic nature of each category of indices, revealing their functional prowess in specific applications, irrespective of their respective drawbacks, and it aptly dismisses the feasibility of employing Jacobian matrix-based indices for online applications [16]. The initial phase of this study navigates the intricacies of voltage stability analysis in electrical power distribution systems. A formula is devised to compute the Voltage Stability Index (VSI) for all nodes within the distribution network. Exploration of a typical radial distribution network shows that the node the minimum VSI value is the most sensitive. Subsequently, the study advances into its second phase, wherein critical values of total real and total reactive power loads are determined for various cases [17]. Compares the efficacy of voltage stability indices in illuminating the proximity of voltage instability within a power system. Three simple voltage stability indices are introduced, their effectiveness juxtaposed against recently proposed indices like Index-L and Diagonal element dependent index (I_{ds}). This comparative analysis unfolds across a broad spectrum of system operating conditions, encompassing the manipulation of load power factors and feeder X/R ratios [18]. The meticulous examination differentiates numerous Line Voltage Stability Indices (LVSI) types to ascertain their effectiveness in identifying the weakest lines within the power system. Additionally, the paper introduces the practical implementation of real-time voltage stability monitoring by utilizing Artificial Neural Networks (ANN) [19]. Aspires to appraise the performance of four extant voltage stability indices when confronted with alterations in reactive and real power loads [20]. Notably, the total power loss is observed in each scenario.

A novel line voltage stability index emerges, revolutionizing the landscape of voltage stability assessment by presenting an efficient technique [21].

Through meticulous analysis, unveils a comprehensive study encompassing qualitative and quantitative dimensions focused on measurement-based centralized voltage stability monitoring approaches employing Thevenin equivalents [22].

Delves into the fundamental aspects of voltage stability indices, specifically focusing on determining the maximum load ability and identifying weak buses using line indices. The efficacy of these techniques is elucidated through numerical analysis employing the Line Stability Index (L_{mn}) and the Fast Voltage Stability Index (FVSI), considering base loading and heavy reactive loading scenarios. The findings from this research offer valuable insights for optimizing the placement of FACTS devices to enhance voltage stability margins [23].

In the pursuit of comprehending the intricacies surrounding voltage instability, an integrated and efficacious framework for voltage stability assessment was submitted [24]. The approach introduced in this research harnesses the Fast Voltage Stability Index (FVSI) to identify weak buses under various loading scenarios.

The precarious scenario arises when reactive loads surpass generation capacity, leading to a voltage drop that permeates the grid. The Fast Voltage Stability Index (FVSI) and Line Stability Index (L_{mn}) were used to identify the loads to be shed in the event of an undervoltage condition [25].

A novel index called the Modern Voltage Stability Index (MVSI) is proposed, which offers a more precise means of predicting voltage collapse. The MVSI identifies weak buses and critical lines while partially disregarding line resistance. To validate the efficacy of the proposed index,

this investigation undertakes a comprehensive comparison between the existing stability indices, namely L_{mn} , FVSI, LQP, NLSI, VSLI, NVSI, and the MVSI [26].

Evaluates an array of voltage stability indices, including the L-Index, Voltage Collapse Proximity Index (VCPI), Novel Line Stability Index (NLSI), Fast Voltage Stability Index (FVSI), and the Bus Participation Factor (BPF) [27]. This meticulous analysis unfolds by subjecting the system to gradual variations in reactive power load at each load bus until the precipice of voltage collapse is reached. The highest bus value of the indices mentioned above is the voltage collapse bus.

Real-time voltage stability assessment based on Phasor Measurement Units (PMUs) has emerged as a novel concept to mitigate the risks associated with voltage instability and potential collapse. Within this research, an array of voltage stability indices has been considered, including the Line Stability Index (L_{mn}), Fast Voltage Stability Index (FVSI), Line Stability Factor (LQP), Line Index (L-index), Voltage Collapse Proximity Index (VCPI(P) and VCPI(Q)), Line Voltage Stability Index (LVSI), and Critical Voltage (V_{cr}) in [28].

Short-Term Voltage Stability (STVS) indices were enhanced [29]. Specifically, the Voltage Recovery Index (VRI) is subject to meticulous refinement, addressing inherent limitations ingrained in its original formulation. New index derived known as the system Voltage Recovery Index (VRI_{sys}) is designed to assess STVS at the system level quantitatively.

A Line Voltage Stability Index (LVSI) has been proposed as an assessment tool to evaluate the voltage stability state and stress conditions of transmission lines [30]. The proposed index can be utilized to estimate the stability margin of the power system.

Within this context, introduces an enhanced voltage stability index by drawing upon existing

indices, which primarily rely on active and reactive power variations within a power system [31]. The primary objective of the computational technique employed in this research is to gauge the critical boundaries, leading to the introduction of the Critical Boundary Index (CBI). The derivation of this improved index utilizes the LAGRANGE CONSTANT computational method.

A novel approach is developed to identify vulnerable lines in [32]. The method hinges upon practical line ABCD parameters, the power factor at the receiving end, and the power angle between the sending and receiving ends. The Integrated Transmission Line Transfer Index (ITLTI) novel concept is formulated for a radial transmission system and applied to a large-scale system. The ITLTI index offers a more comprehensive perspective, making it a promising online voltage stability assessment solution.

The study presents a machine-learning approach to forecast the long-term voltage stability margin, specifically referred to as the Load Ability Margin (LM) [33].

Introducing an improved indicator, the Simplified Voltage Stability Index (SVSI) is presented, designed to estimate the voltage stability margin in electric power systems [34]. The index employs voltage measurements and certain assumptions from the Thevenin model. The proposed technique incorporates information about the current operating conditions, considering only voltage phasor measurements and the power system's topology. The validation process involved comparing the proposed index with other established voltage stability indexes. Simulation results indicate that the proposed index reliably indicates power system voltage stability. Furthermore, it presents a simpler and computationally less demanding alternative to the compared indices.

The research focuses on improving voltage stability in power systems by using a line voltage

stability index based on Optimal Power Flow (OPF) [35]. The Line Voltage Stability Index (LVSI), which traditionally identifies the most critical line in the system, ranging from 0 (no load) to 1 (voltage collapse), is employed as part of the constraints to prevent voltage collapse and as the objective function to enhance system stability. The Salp Swarm Optimization (SSO) algorithm is employed to solve the OPF problems. The investigation of voltage stability improvement under two conditions: stressed load condition, where the load demand is increased, and line outage contingency condition, where the most critical line is subjected to an outage.

The research introduces a Novel Line Voltage Stability Index (BVSI) to identify weak lines and buses across various loading conditions and network configurations [36]. The findings of this research aim to provide a general guideline for researchers in selecting the appropriate VSIs for various applications, particularly in solving optimization problems like Distributed Generation (DG) and Reactive Power Compensation (RPC) placement, optimal power flow, optimal reactive power dispatch, and optimal network reconfiguration for different loading scenarios and networks. The results demonstrate the effectiveness of the proposed index in assessing the voltage stability state and stress condition of lines. Additionally, the proposed approach successfully identifies potential candidate buses for DG location and sizing.

The integration of Distributed Generators (DGs) in distribution networks through optimal allocation is a significant challenge faced by power system engineers aiming to enhance stability and achieve economical operation. This article presents a comprehensive analysis of the impacts of optimal allocation and the number of DGs on both steady-state and transient performances of distribution networks. An Oscillatory Particle Swarm Optimization (OPSO) algorithm is employed to determine the optimal allocation of DGs by minimizing various

objective functions related to total transmission losses, voltage regulation, and power performance index [37]. Two penetration scenarios are considered, and DGs' optimal sizes and locations are obtained and presented as results. Moreover, the impact of the penetration level of photovoltaic and wind energy sources on transient performance is analyzed using detailed nonlinear models of synchronous machines and DG sources.

A comprehensive overview of a myriad of VSIs is meticulously unfurled, offering an extensive repository of resources tailored to researchers, students, and industry stakeholders. Each VSI is meticulously scrutinized, encompassing diverse facets such as nomenclature, calculation methodology, underlying assumptions, fundamental concepts, steady-state behavior, threshold criteria, instability markers, as well as the strengths and weaknesses of each index [38]. Furthermore, the study delves into the intricate interplay between renewable energy sources (RESs), load variations, and VSIs, while investigating the inherent stability challenges power systems face.

The research provides a comprehensive overview of the rotational inertia and strength services within electric power grids incorporating Renewable Energy Sources (RESs) [39]. The objective is to characterize the impact of these services on stability indices and synthesize the prerequisites for the secure integration of RES. The evaluation of steady-state voltage and transient frequency stability indices is conducted. The findings of this study serve a dual purpose: firstly, they provide clarifications regarding stability indices, and secondly, they shed light on the interconnectedness of system services such as inertia and system strength.

The voltage stability of transmission networks incorporating wind energy sources was investigated, employing P-V and P-Q curves as analytical tools [40]. Weak buses, identified through P-V curves, are considered potential connection points for the wind generator.

Additionally, graphical representations of the voltage stability region for each candidate bus are presented to identify the optimal location for the wind energy source. The influence of the renewable energy source is evaluated by comparing the active power margin at a specific load bus for various wind penetration levels.

Moreover, introduces different methodologies to identify and address guidelines for Distributed Generation (DG) integration in mesh-type networks, which are expected to be crucial in managing future power systems [41]. Efficient integration of DG involves analyzing numerous influencing factors; thus, comprehensive planning becomes essential for addressing future challenges in power systems.

The utilization of the Modified Sine Cosine Algorithm (MSCA) was introduced to augment the performance of DNs by integrating multiple DG technologies [42]. The objective is to optimize active power losses, expedite voltage stability index calculations, and minimize overall costs. Notably, the penetration level of DGs and the operational constraints of DG units' power factors are considered.

An innovative approach was presented to place and size Distributed Generation (DG) systems, specifically focusing on ensuring voltage stability and reducing total power losses. The primary objective of this method is to guarantee voltage stability in the presence of load fluctuations, all while selecting optimal sites for DG deployment and determining their power capacities [43]. First, vulnerable buses are identified utilizing the Voltage Stability Margin Index (VSMI). The optimal size of the DG unit is then computed using a curve-fitting approximation implemented in MATLAB.

Two novel indices were introduced, namely the Power Loss Index (PLI) and Power Stability Index (PSI), for the placement of Distribution Static Synchronous Compensator

(D-STATCOM) on a bus, aimed at reducing line losses and enhancing the voltage profile of the system under consideration [44].

Two novel techniques have been introduced to determine the optimal placement of Flexible AC Transmission Systems (FACTS) devices in the network [45]. The primary objective is to enhance the voltage profile, augment power transfer capability, and improve overall power transmission efficiency. The techniques presented herein are the Power Stability Index (PSI) and the Fast Voltage Stability Index (FVSI). These indices are derived from data obtained through load flow analysis conducted.

Upon transitioning from a Microgrid's (MG) normal operation to its island operating mode in the face of resilient contingencies, the Dynamic Voltage Stability (DVS) becomes alarmingly compromised. The Static Var Compensator (SVC) device fortified with Flexible AC Transmission Systems (FACTS) technology emerges as a concentrated solution, offering rapid and efficient reactive power compensation. To unlock the dynamic performance potential of voltage within the MG, the optimal placement of the SVC assumes paramount significance. Thus, the research propounds an optimization algorithm. The proposed algorithm computes indices that quantitatively evaluate voltage's dynamic performance by discretizing voltage signals over time [46].

CHAPTER 3: Power System Voltage Stability

3.1 Introduction

Since the 1920s power system stability has been recognized as an important problem for secure system operation [47], [48]. The primary problem is transient instability in most systems in the past. However, different forms of system instability have emerged, such as voltage stability, frequency stability, and rotor angle stability. Power systems have operated under more tension in the last two decades than they usually had. These problems and tension have emerged because they have evolved power systems through sustainable interconnect growth, increased operation in highly stressed conditions, increased use of induction machines, high penetration DGs in power network systems, and new technologies and controls. Under these tense conditions, a new type of unstable behavior can exhibit in a power system like voltage instability.

3.2 Definition and Classification of Power System Stability

An IEEE/CIGRE joint task force defined power system stability as "The ability of an electric power system, for a given initial operating condition, to regain a state of operating equilibrium after being subjected to a physical disturbance, with most system variables bounded so that practically the entire system remains intact" [1].

The power system is considered a highly nonlinear system that acts in a constantly changing environment, so the system's stability depends on the initial operating conditions and the nature of the disturbance when exposed to disturbance.

IEEE power system dynamic performance committee and CIGRE study committee 38 set up a joint task force and proposed various definitions and classifications related to power system stability [1].

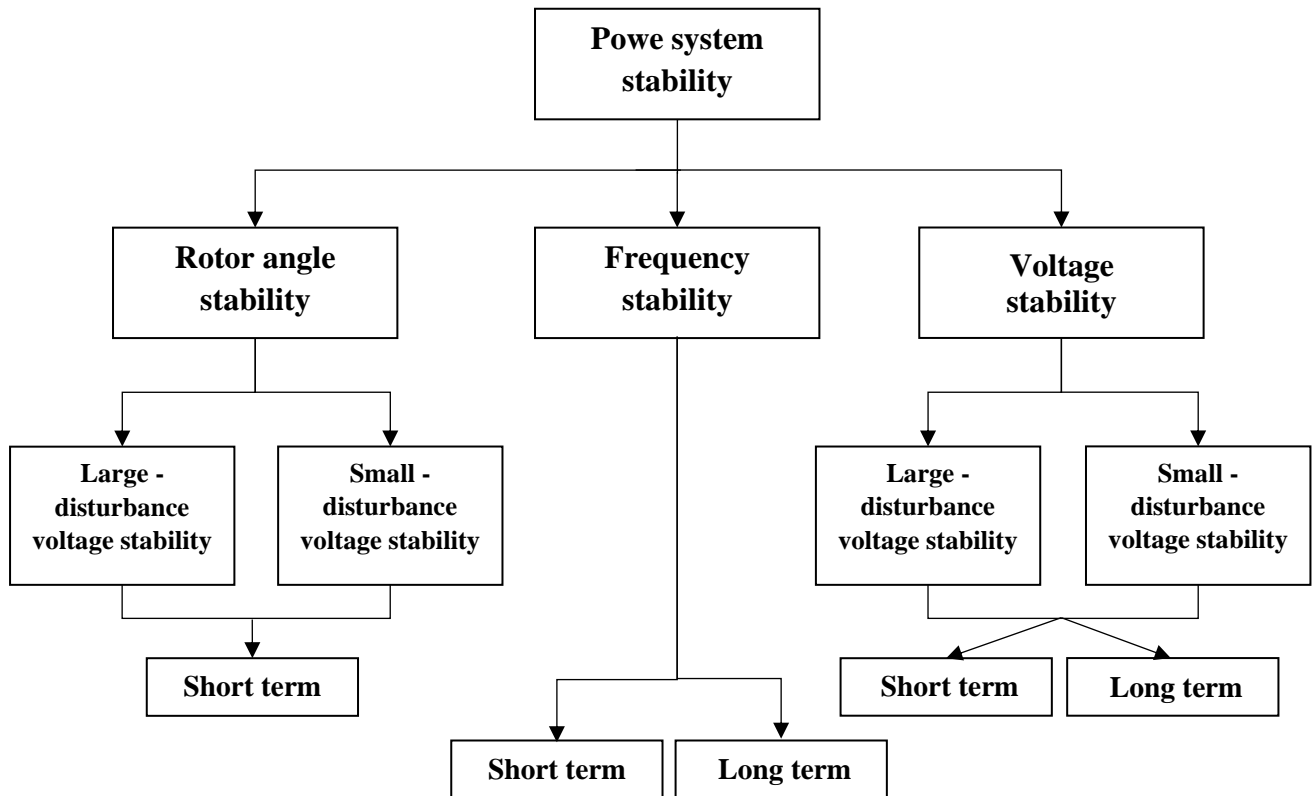


Figure 3.1 Classification of power system stability

Figure 3.1 show the classification of power system stability Focuses on the classification of power system stability mainly on one variable (for example, voltage, frequency, angle) to greatly facilitate stability analysis. Figure 3.1 shows that power stability can be categorized into different types, namely:

- Angle stability
- Frequency (short and long-term) stability
- Voltage stability

The power stability system was classified into the categories mentioned above based on the following considerations [1]:

- The physical nature of the resulting instability model is indicated by the primary system variable in which instability can be observed.
- The size of the disturbance influences the method of calculation and prediction of stability.
- The devices, processes, and period must be considered to assess stability.

So, a power system operating condition is described according to the previous classification (physical quantities). For example, voltage magnitude and phase angle at each bus and the active/reactive power flowing in each line. Can say the system is in a steady state if these quantities are constant over time. However, if they are not constant, the system is a disturbance. The power systems are subjected to a small or large disturbance. The continually occurring load changes are represented minor disturbances; the system must be able to adapt to the changing circumstances and operate satisfactorily. A short circuit on a transmission line or loss of a source generator is represented a significant disturbance; the system also must be able to adapt to large disturbances. The significant disturbance may lead to structural changes in the power system because of the isolation of the faulted components.

For a power system's excellent design and operation, it is essential to understand different kinds of instability and how they are associated. This chapter will focus on and provide an overview of the voltage stability problem where voltage instability has become a significant research area in the field of power systems in recent years, following several voltage instability events worldwide [49],[50].

3.3 Voltage Stability Definition

Voltage stability has been defined by the IEEE power system engineering committee as follows: "Voltage stability refers to the ability of a power system to maintain steady voltages at all buses in the system after being subjected to a disturbance from a given initial operating condition. It depends on the ability to maintain/restore equilibrium between load demand and load supply from the power system. Instability that may result occurs in the form of a progressive fall or rise of voltages of some buses. A possible outcome of voltage instability is loss of load in an area, or tripping of transmission lines and other elements by their protective systems leading to cascading outages" [1], [50], [51].

The IEEE/CIGRE Joint Task Force provides another definition for voltage stability: "Voltage

stability refers to the ability of a power system to maintain steady voltages at all buses in the system after being subjected to a disturbance from a given initial operating condition." [1].

Unbalance between load demand and load supply causes unstable voltage, mainly an imbalance of reactive power. This may occur because of a sudden change in load demand, like a loss of load in an area or a transmission line tripping, limiting load supply capacity. Voltage instability occurs in the form of a gradual fall or increase in the voltages for some buses.

Voltage stability can be a local or global phenomenon. It is a local phenomenon when voltage stability issues affect just a particular bus or bus in a specific area and do not affect the entire system. It is a global phenomenon when voltage stability issues affect many system buses, which can also cause angle stability issues and hence can affect the entire system. Some voltage stability issues can begin as a local problem and then progress to a global stability problem.

Voltage instability has been the cause of many significant blackouts in the world [52]. Voltage instability leads to progressive voltage falls. Used the term " Voltage Collapse" instead of voltage stability in literature. However, this term is more complex than voltage instability. It is the process by which the sequence of events accompanying voltage instability leads to a blackout or abnormally low voltages in a significant part of the power system [1], [53]. Low voltage profiles, heavy reactive power flows, insufficient reactive support, and heavily loaded systems are the critical signs of voltage collapse.

Because of several voltage collapse accidents in recent years, the issue of voltage instability has gotten much attention.

Accidents and problems of voltage instability and collapse have led to several major system blackouts in various countries [49],[54]. One of these incidents occurred in the French on January 12, 1987, resulting in a widespread blackout; the other incident occurred on July 23, 1987, in Tokyo, Japan.

3.4 Voltage Stability Classification

Voltage stability was classified by the IEEE/CIGRE task force into four categories [1],[50]: significant disturbance voltage stability, small disturbance voltage stability, short-term voltage stability, and long-term voltage stability, Figure 3.1 above shows these classifications, voltage stability is classified according to the time frame too (long-term or short-term voltage stability) and classified according to disturbance (significant disturbance or small disturbance voltage stability). Below is a summary of these classifications.

3.4.1 Large-Disturbance Voltage Stability

This means the ability of systems to maintain constant voltages after being subjected to significant disturbances like loss of generation or circuit contingencies and system faults. The system and load characteristics and the interactions of continuous and discrete controls and protections determine this ability. The study period under interest may extend from a few seconds to tens of minutes.

3.4.2 Small-Disturbance Voltage Stability

This means the ability of systems to maintain constant voltage after being subjected to minor disturbances like growing changes in the load. This type of stability is affected by the characteristics of the loads, discrete controls at a given time, and continuous controls.

3.4.3 Short-Term Voltage Stability

It includes dynamics of fast-acting load components like induction motors, HVDC converters, and electronically controlled loads. The study period of interest is about a few seconds. Moreover, the analysis needs to solve appropriate system differential equations.

3.4.4 Long-Term Voltage Stability

Involves slower equipment, acting like thermostatically controlled loads, tap-changing transformers, and generator current limiters. The duration of the study may extend to a few or

many minutes, and Long-term simulations are needed to analyze the system's dynamic performance.

3.5 Voltage Stability Analysis

Many factors can cause voltage instability, such as reactive power constraints, increased loading, load characteristics, and on-load tap changer dynamics [55]. As the power system networks grow, there is a great need to study and analyze the voltage stability system. Static (short time frame) or dynamic (long time frame) considerations can be used to study and investigate voltage stability [56]. To study static voltage stability, steady-state methods, such as the power flow model, are used in the analysis, while studying dynamic stability uses non-linear differential and algebraic equations to describe analysis, such as dynamics generator and tap changing transformers. The static analysis method is used in much work to determine voltage stability. Different methods have been used in the static voltage stability analysis like the PV and QV curves, optimization, continuation load flow, model, etc. [57].

P-V and Q-V Curves

The P-V (Active Power-Voltage) and Q-V (Reactive Power-Voltage) curves are used to monitor power system operation under different operating conditions and give important information about the loading of the system and voltage stability

From P-V and Q-V curves can be identified voltage stability analysis, voltage collapse, and voltage stability margin in feeders [49], [53], and [58]. There is a close relation between voltage stability and variation of the reactive power demand of a particular bus and its variance with the voltage. The relation between voltage and active power can be an essential tool to monitor feeder voltage stability [58], [59]. P-V and Q-V curves are considered conventional analytical tools. These curves are essential tools for analyzing and designing power systems, as they provide insights into the system's voltage stability, load flow, and reactive power control. Engineers can identify potential problems and optimize the power system's performance by

analyzing the P-V and Q-V curves.

P-V and Q-V curves are graphical representations of the behavior of a power system in terms of active and reactive power, respectively, at different voltage levels. Power flow analysis helps track changes in system voltages as loads vary.

Moreover, the PV curve is a common application to plot the voltage at a particular bus as the load varies from the base case to a loadability limit (often known as ‘the point of maximum loadability’).

Figure 3.2 shows that the PV curve is sometimes called the “nose curve” for its shape. If the load is increased to the loadability limit and then decreased back, it is possible to trace the entire power-voltage or "P-V" curve. Only the operating points above the nose point (critical point) represent satisfactory operating conditions.

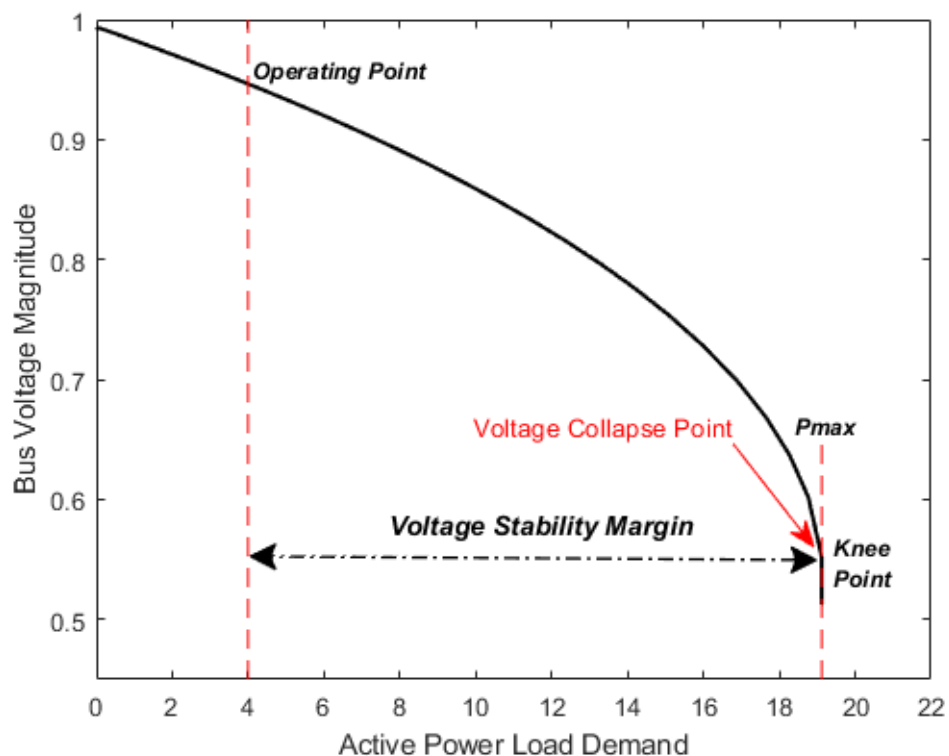


Figure 3.2 P-V curve with stable and unstable operating points [58]

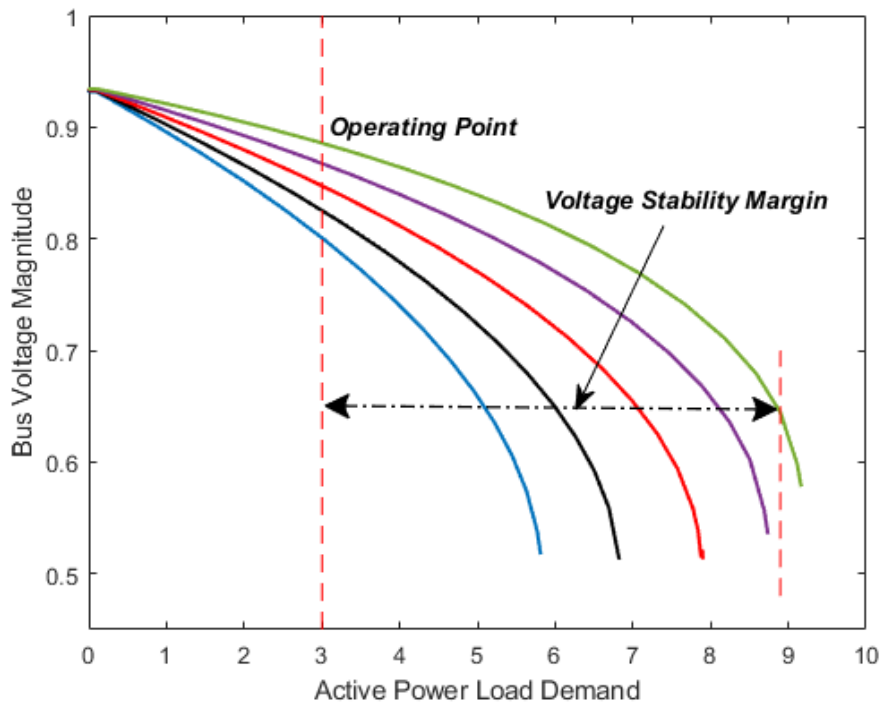


Figure 3.3 Voltage stability margin

At the knee point in Figure 3.2, the derivative ($dV_R/dP_L = 0$) is equal to zero; the P-V curve above the knee point has a negative slope (dV_R/dP_L), indicating that the differences in real power and voltage are in opposite directions, and the curve below the knee has a positive slope (dV_R/dP_L). As power increases, voltage decreases until it reaches a critical point, at which point the voltage collapses.

The voltage stability margin refers to the distance between the operating voltage and the voltage collapse point on the P-V curve. In other words, it is the amount by which the voltage can be decreased before the power system becomes unstable and collapses. The greater the voltage stability margin, the more stable the power system is, and the less likely it is to experience voltage collapse. Therefore, it is important to carefully monitor and maintain the voltage stability margin to ensure a secure and reliable power system operation [60]. VSM is shown in Figure 3.3.

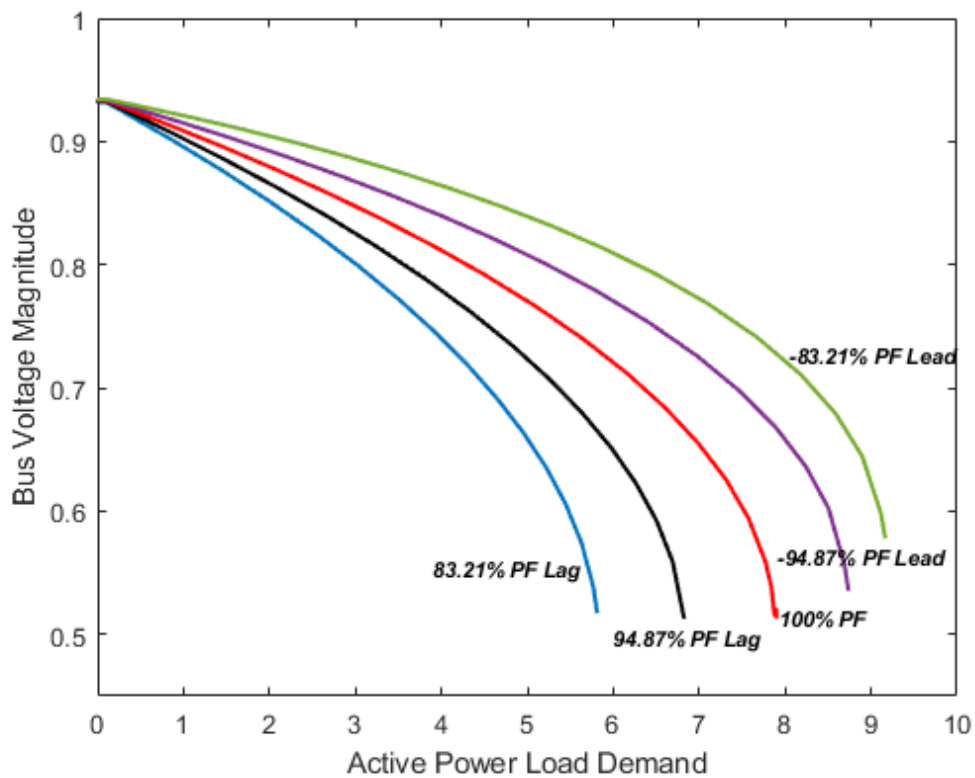


Figure 3.4 P-V curve for different power factor loads

The P-V curves for loads with various power factors are shown in Figure 3.4. The lagging and leading power factors are related to the phase relationship between the voltage and current of a load. A lagging power factor occurs when the current lags behind the voltage in phase, and a leading power factor occurs when the current leads the voltage in phase. The power factor of a load affects the shape and position of the PV curve, as well as the voltage stability margin.

The PV curve is shifted to the left for a lagging power factor, indicating a decrease in the voltage stability margin. This is because a lagging power factor causes an increase in the reactive power demand, which reduces the available voltage for the load. On the other hand, a leading power factor shifts the PV curve to the right, indicating an increase in the voltage stability margin. This is because a leading power factor reduces the reactive power demand, increasing the load's available voltage.

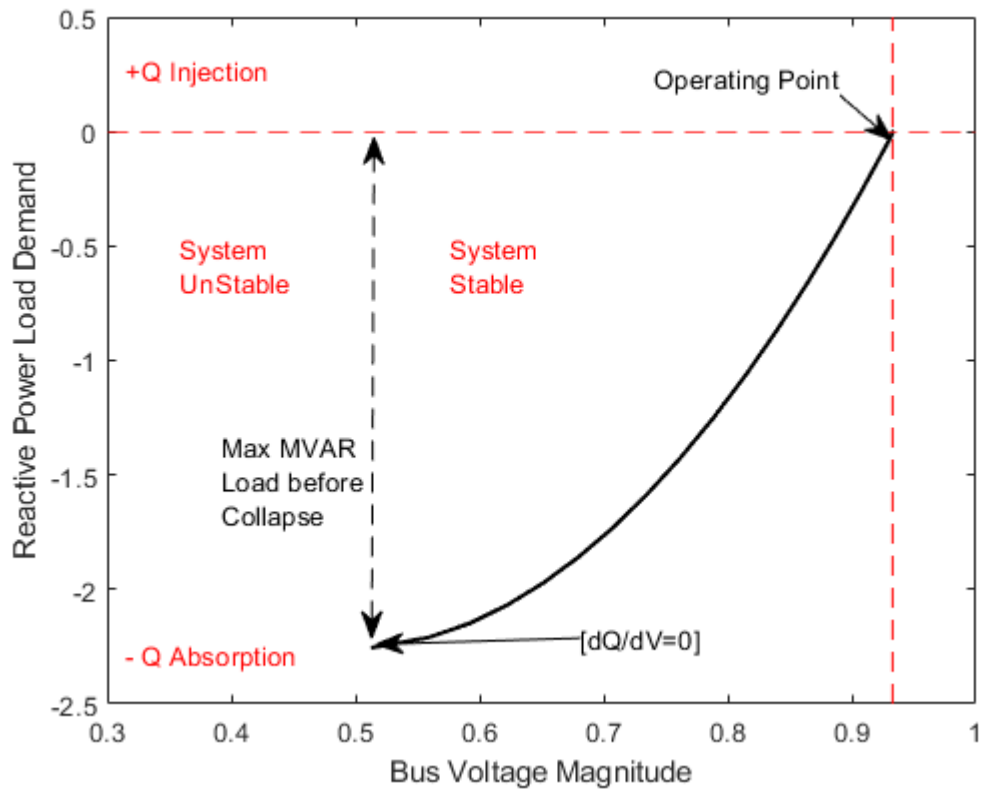


Figure 3.5 Q-V curve for different load real powers [58]

Therefore, it is essential to maintain a power factor close to unity, which maximizes the available power for a given voltage and ensures a stable and efficient power system operation. Figure 3.5 shows the Q-V curve, The Q-V curve in power systems is a graphical representation of the reactive power (Q) and voltage (V) relationship at a specific bus in the electrical network. Q-V Analysis studies show how variations in reactive power (Q) affect the voltages (V) in the system. The y-axis is the reactive power injection, and the x-axis is the bus terminal voltage in the V-Q curve. The x-intercept of the V-Q curve represents the operating point of the system. The part where $Q_{injection} < 0$ represents an increase in MVAR load. The bottom of the curve represents the maximum increase in the load MVAR (MVAR Margin) at this bus before voltage collapse occurs.

The bottom of the curve defines the voltage stability limit, which represents the locus of the knee point of the Q-V curve where the derivative (dQ/dV_R) is equal to zero; This point is

known as the voltage collapse point, and it represents the limit beyond which the power system cannot maintain stable voltage levels. The system becomes unstable at this point, and voltage collapse may occur, leading to power outages and system failures. Therefore, it is essential to maintain a stable voltage level within the system and operate within the stable region of the Q-V curve. This can be achieved by using reactive power compensation devices, such as capacitors and reactors, to regulate the reactive power flow and maintain stable voltage levels. By analyzing the Q-V curve, power system engineers can identify the required level of reactive power compensation to keep the power system operating within a stable range of voltage and reactive power. PV and QV curves assess voltage stability and margins to the voltage collapse points [58]. Many utilities use PV-QV curves to calculate loading and reactive margins for voltage-stable power system operation.

CHAPTER 4: Voltage Stability Indices

4.1 Theory and VSIs Formulation:

Voltage stability is concerned with both the static and dynamic behavior of a power system. Researchers had been proposed various Voltage Stability Indices (VSIs) to acquire fast computational voltage stability conditions of a system. These indices can be used to perform static and dynamic analyses of voltage stability. This thesis is focused on studying voltage stability indices assessment mainly from a static analysis behavior point of view. The reason is that the dynamic voltage stability analysis deals with the non-linear load and is somewhat difficult to model. The dynamic voltage stability simulation of online applications is still time-consuming. Static voltage stability analysis is accomplished by assuming the system is functioning in a steady state [61]. The basic formulas are used to examine the system voltage stability. Thus, voltage stability indices are derivative by using a simplified power system model shown in Figure 4.1 composed of a two-bus system and a transmission line and it is computed using Thevenin equivalent circuit of the power system referred to a load bus, which can be generalized to an n-line power system. Many efforts focus on analyzing the two-bus system to straightforward analytical derivation and provide insight into the problem adapted to the extensive system is component n-line.

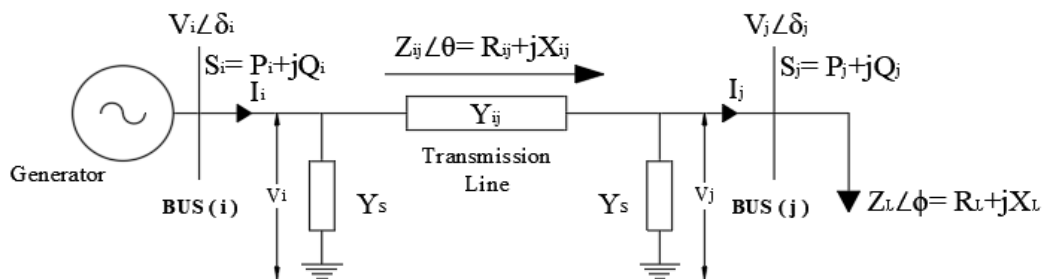


Figure 4.1 The two-bus representation of radial distribution network

A power system is an electrical network containing generators, transmission lines, loads, and voltage controllers. The symbols from Figure 4.1 are explained as follows:

V_i, V_j : Voltage magnitude at the sending and receiving buses, respectively.

I : Current flow. When shunt admittance is neglected so $I = I_i = I_j$.

P_i, P_j : Real power at the sending and receiving bus.

Q_i, Q_j : Reactive power at the sending and receiving bus.

S_i, S_j : Apparent power at the sending and receiving bus.

δ_i, δ_j : Voltage angle at the sending and receiving buses, respectively.

$\delta = \delta_i - \delta_j$: Angle difference between the sending and receiving voltage bus.

P_L, Q_L : Real and reactive load power.

P_L, Q_L : Real and reactive load power at receiving bus.

P_G, Q_G : Real and reactive generated power at receiving bus.

Z_{ij}, Z_L : Line impedance and load impedance.

R_{ij}, X_{ij}, θ : Line resistance, line reactance and line impedance angle.

R_L, X_L, ϕ : Load resistance, load reactance and load impedance angle.

$Y_{ij} = 1/Z_{ij}$: Series admittance.

$Y_s = Y/2$: Shunt admittance.

4.2 Voltage Stability Indices Classification

VSI indices are classified according to the following criteria [62], [63], [64]:

1. Jacobian matrix and system parameters (variables) based VSIs.
2. Bus, line and overall VSIs

VSIs based on a Jacobian matrix can determine the voltage collapse point and the VSM.

However, the computation time is lengthy, and any topological change causes the Jacobian

matrix to change, necessitating a recalculation; consequently, they are unsuitable for real-time voltage stability assessment. Additionally, using VSIs based on the Jacobian matrix increases the execution time of DG placement and sizing problems.

In contrast, VSIs based on system parameters (variables) require less computation and are suitable for real-time applications. The disadvantage of these indices is that they cannot accurately estimate the VSM, so they can only present the most critical lines and buses.

VSIs can also be classified based on their main concepts. These concepts can be used to differentiate between various types of VSIs:

1. Existence of solutions for voltage equation
2. P-V curve
3. Maximum transferable power through a line
4. Maximum power transfer theorem
5. Lyapunov stability theory
6. Jacobian matrix

4.3 Voltage Stability Indices

Many VSIs have been proposed in the literature, and Their classifications were previously discussed during the chapter. In many applications, such as the first step of DG placement and sizing problems, VSIs are used to detect the weakest bus and line of power system or trigger countermeasures against voltage instability.

The function of VSI is to predict the voltage stability of the power system network and determine the weakest bus on the system. All line VSIs are formulated based on the two-bus representation of the system, as shown in Figure 4.1, and shunt admittance (Y_s) is ignored in most of the suggested indices. Therefore, most of the theoretical base of line VSIs is the same, and the difference is in the assumptions used in each index. This section will be discussed VSIs which have been proposed in the literature.

4.3.1 Fast Voltage Stability Index (FVSI)

The Fast Voltage Stability Index (FVSI) is used to detect the critical line in the power system through shows the voltage stability margin of a line. The index was proposed by Ismail Musirin et al [61]. Moreover, it is developed based on the notion of power flow in a single line. The first is obtaining the current equation through a line of two bus representation models as in Figure 4.1 to derive the index. By taking the Sending bus (i) as the reference, the current through line connected between two buses is expressed using Kirchhoff Voltage Law (KVL),

$$I = \frac{V_i \angle \delta_i - V_j \angle \delta_j}{R + jX} \quad (4.1)$$

Where,

$$S_j = V_j I^*, \text{ Rearrange:}$$

$$I = \left(\frac{S_j}{V_j \angle \delta_j} \right)^* = \frac{P_j - jQ_j}{V_j \angle -\delta_j} \quad (4.2)$$

Substituting (4.1) into (4.2),

$$\frac{V_i \angle \delta_i - V_j \angle \delta_j}{R + jX} = \frac{P_j - jQ_j}{V_j \angle -\delta_j} \quad (4.3)$$

$$\text{Where, } \delta_i - \delta_j = \delta$$

Simplify (4.3) as,

$$V_i V_j \angle (\delta) - V_j^2 \angle 0 = (P_j - jQ_j)(R + jX) \quad (4.4)$$

By solving and rearranging (4.4)

$$V_i V_j \cos \delta + j V_i V_j \sin \delta - V_j^2 = [P_j R + Q_j X] + j [P_j X - Q_j R] \quad (4.5)$$

Separating the real and imaginary parts yields,

$$V_i V_j \cos \delta - V_j^2 = P_j R + Q_j X \quad (4.6)$$

$$V_i V_j \sin \delta = P_j X - Q_j R \quad (4.7)$$

Rearranging (4.7) for P_j and substituting into (4.6) yields a quadratic Eq. in V_j^2 ;

This quadratic equation is given by Eq. (4.8):

$$V_j^2 + V_i V_j \left(\frac{R \sin \delta}{X} - \cos \delta \right) + Q_j \left(\frac{R^2 + X^2}{X} \right) = 0 \quad (4.8)$$

The roots of quadratic Eq. become imaginary when the discriminant is less than zero, causing voltage instability in the system. The discriminant ($\Delta = b^2 - 4ac$) must be set greater than or equal to 0, to obtain real roots for quadratic Eq. V_j :

$$b^2 - 4ac \geq 0$$

$$V_i^2 \left(\frac{R \sin \delta - X \cos \delta}{X} \right)^2 - 4Q_j \left(\frac{R^2 + X^2}{X} \right) \geq 0 \quad (4.9)$$

Then, Rearrange (4.9):

$$FVSI_{ij} = \frac{4Z_{ij}^2 Q_j X}{V_i^2 (R \sin \delta - X \cos \delta)^2} \leq 1 \quad (4.10)$$

The angle difference between the sending and receiving voltage buses is assumed to be approximately zero ($\delta \approx 0$) then,

$$R \sin \delta = 0, \text{ and } X \cos \delta = X$$

$$FVSI_{ij} = \frac{4Z_{ij}^2 Q_j}{V_i^2 X} \quad (4.11)$$

The criterion to derive FVSI is to set the discriminant of the roots of the voltage quadratic equation to be greater than or equal to zero. The shunt admittance (Y_s) is neglected in this index.

To maintain a stable transmission line, the FVSI must be below 1. when the value of FVSI is closed to 1.0 for a line, it implies that the line is approaching its instability point. If the value of FVSI is more than 1.0, a sudden voltage drop will occur on one of the buses connected to the line, leading to system collapse.

4.3.2 Line Stability Index (L_{mn})

Line Stability Index (L_{mn}) is formulated from power flow in the line containing the tow-bus system presented Figure 4.1. This index has been suggested by Moghavemmin et al. [65]; this

index uses the same concept as the FVSI index to obtain it, which is necessary for the discriminant of the voltage quadratic equation to be greater than or equal to zero to keep the line in the power system stable. If the discriminant is less than zero, the resultant roots will be imaginary, pointing towards voltage instability. The shunt admittance (Y_s) is neglected in this index. To formulate the index is used apparent power flow is into the line:

$$I = \frac{V_i \angle \delta_i - V_j \angle \delta_j}{Z_{ij} \angle \theta}$$

$$\text{However, } S_j = V_j I^*$$

So,

$$S_j = V_j \angle \delta_j \cdot \left(\frac{V_i \angle -\delta_i - V_j \angle -\delta_j}{Z_{ij} \angle -\theta} \right)$$

$$S_j = \frac{V_i V_j}{Z_{ij}} \angle (\theta - \delta_i + \delta_j) - \frac{V_j^2}{Z_{ij}} \angle \theta \quad (4.12)$$

Here, $\delta = |\delta_i - \delta_j|$ and $S_j = P_j + jQ_j$.

The real and reactive power at the receiving end can be obtained by separating the real and imaginary parts as follows:

$$P_j = \frac{V_i V_j}{Z_{ij}} \cos(\theta - \delta) - \frac{V_j^2}{Z_{ij}} \cos \theta \quad (4.13)$$

$$Q_j = \frac{V_i V_j}{Z_{ij}} \sin(\theta - \delta) - \frac{V_j^2}{Z_{ij}} \sin \theta \quad (4.14)$$

Rearrange (4.14):

$$\sin \theta \cdot V_j^2 - V_i \sin(\theta - \delta) V_j + Q_j Z_{ij} = 0 \quad (4.15)$$

The discriminant of the quadratic Eq.(4.15), ($\Delta = b^2 - 4ac$) must be greater than or equal to 0 in order to obtain real roots for V_j and thus get a real value for the receiving end voltage.

Therefore,

$$(V_i \sin(\theta - \delta))^2 - 4 \sin \theta \cdot Z_{ij} Q_j \geq 0, \quad (4.16)$$

However, $Z_{ij} \angle \theta = R + jX$

Therefore, the $(\sin \theta \cdot Z_{ij} = X)$, can be substituted into (4.16)

$$(V_i \sin(\theta - \delta))^2 - 4XQ_j \geq 0 \quad (4.17)$$

Rearrange (4.17):

$$L_{mn-ij} = \frac{4XQ_j}{\{(V_i \sin(\theta - \delta))^2\}} \leq 1 \quad (4.18)$$

To keep transmission line stable, $L_{mn-ij} \leq 1.0$.

4.3.3 Line Stability Factor (LQP)

The index for Line Stability Factor (LQP) was proposed by Mohamed et al. [66]. To derive the index, the power flow, depicted in Figure 4.1, is considered to be the same concept as obtaining (FVSI), (L_{mn}). The line stability factor can be formulated by deriving the active and reactive power at the receiving bus from equations (4.6) and (4.7):

$$P_j = \frac{Q_j R + V_i V_j \sin \delta}{X} \quad (4.19)$$

$$Q_j = \frac{V_i V_j \cos \delta - V_j^2 - P_j R}{X} \quad (4.20)$$

For lossless line, the $\frac{R}{X} \ll 1$, mean $\frac{R}{X} \approx 0$. therefore, Eq. (4.19) and (4.20) can be simplified to [66]:

$$P_j = \frac{V_i V_j \sin \delta}{X} \quad (4.21)$$

$$\text{Rearrange (4.21), } \sin \delta = \frac{P_j X}{V_i V_j}$$

$$Q_j = \frac{V_i V_j \cos \delta - V_j^2}{X} \quad (4.22)$$

$$\text{Rearrange (4.22), } \cos \delta = \frac{XQ_j + V_j^2}{V_i V_j}$$

Since $\sin^2 \delta + \cos^2 \delta = 1$, So,

$$\left(\frac{P_j X}{V_i V_j}\right)^2 + \left(\frac{XQ_j + V_j^2}{V_i V_j}\right)^2 = 1 \quad (4.23)$$

Rearrange (4.23):

$$V_j^4 + (2XQ_j - V_i^2)V_j^2 + X^2Q_j^2 + X^2P_j^2 = 0 \quad (4.24)$$

To obtain real roots for the quadratic Eq. (4.24), V_j^2 , the discriminant must be greater than or equal to 0.

$$(2XQ_j - V_i^2)^2 - 4(X^2Q_j^2 + X^2P_j^2) \geq 0 \quad (4.25)$$

Rearrange (4.25):

$$4\left(\frac{X}{V_i^2}\right)\left(\frac{P_j^2X}{V_i^2} + Q_j\right) \leq 1 \quad (4.26)$$

The $P_i = -P_j$, because the transmission line is lossless.

$$LQP_{ij} = 4\left(\frac{X}{V_i^2}\right)\left(\frac{P_i^2X}{V_i^2} + Q_j\right) \leq 1 \quad (4.27)$$

To maintain a transmission line stable, it must be kept $LQP \leq 1$. The shunt admittance (Y_s) is neglected too in this index.

4.3.4 Line Stability Index (L_p) Or Line Voltage Stability Index (LVSI)

Moghavvemi et al. has designated the L_p using the same concept as last line VSIs. The system is deemed unstable if L_p is greater than one [67]. A transmission line's L_p is defined as follows:

Rearrang (4.13):

$$\cos \theta \cdot V_j^2 - V_i \cos(\theta - \delta) V_j + P_j Z_{ij} = 0 \quad (4.28)$$

The discriminant ($\Delta = b^2 - 4ac$) must be set greater than or equal to 0, to obtain real roots for quadratic equation V_j above and thus get the real value of the receiving end. Therefore [67]:

$$(V_i \cos(\theta - \delta))^2 - 4 \cos \theta \cdot Z_{ij} P_j \geq 0 \quad (4.29)$$

However, $Z_{ij} \angle \theta = R + jX$,

Therefore, the ($\cos \theta \cdot Z_{ij} = R$), can be substituted into (4.29).

So,

$$(V_i \cos(\theta - \delta))^2 - 4RP_j \geq 0 \quad (4.30)$$

Rearrange (4.31):

$$L_{p-ij} = \frac{4RP_j}{\{(V_i \cos(\theta-\delta))^2\}} \leq 1 \quad (4.31)$$

In this index, the effect of reactive power on voltage stability and line shunt admittance are neglected, and it is assumed that only active power affects the stability of the line voltage.

4.3.5 Novel Line Stability Index (NLSI)

Yazdanpanah-Goharrizi et al. developed a Novel Line Stability Index (NLSI) based on the same concept as L_p . An NLSI value close to one indicates that the line is approaching its stability limit [68].

The index is formulated by rearranging equation (4.6) [68]:

$$V_j^2 - (V_i \cos \delta)V_j + P_jR + Q_jX = 0 \quad (4.32)$$

In order to obtain a real value for the receiving end voltage, V_j , the discriminant of the quadratic equation (4.32), ($\Delta = b^2 - 4ac$), must be set greater than or equal to 0.

Therefore, (NLSI) can be derived as shown below:

$$(V_i \cos \delta)^2 - 4(P_jR + Q_jX) \geq 0 \quad (4.33)$$

Rearrange (4.33):

$$\frac{4(P_jR+Q_jX)}{V_i^2 \cos^2 \delta} \leq 1 \quad (4.34)$$

Since the angle difference between the sending bus and the receiving bus is usually tiny, therefore, $\cos^2 \delta = 1$, so finally have:

$$NLSI_{ij} = \frac{(P_jR+Q_jX)}{0.25V_i^2} \leq 1 \quad (4.35)$$

In this index, the line shunt admittance (Y_s) is neglected, and the angle difference between the sending and receiving voltages is assumed to be very small ($\delta \approx 0$).

4.3.6 Voltage Collapse Proximity Index (VCPI)

Four Voltage Collapse Prediction Indices (VCPIs) that assess the voltage stability of a

transmission line by utilizing its maximum power transfer capacity were introduced by Moghavvemi and colleagues [69]. These indices take into account the maximum active and reactive power transmitted through the line ($P_{j(max)}$ and $Q_{j(max)}$) as well as the maximum power losses ($P_{l(max)}$ and $Q_{l(max)}$) that occur on the line.

The mathematical expressions for these indices derived from Figure 4.1 are as follows [69]:

$$V_i = IZ_{ij}\angle\theta + IZ_L\angle\phi$$

$$I = \frac{V_i}{(Z_{ij} \cos \theta + Z_L \cos \phi) + j(Z_{ij} \sin \theta + Z_L \sin \phi)}$$

$$I = \frac{V_i}{\sqrt{(Z_{ij} \cos \theta + Z_L \cos \phi)^2 + (Z_{ij} \sin \theta + Z_L \sin \phi)^2}} \quad (4.36)$$

Rearrange (4.36):

$$I = \frac{V_i}{\sqrt{Z_{ij}^2 + Z_L^2 + 2Z_{ij}Z_L \cos(\theta - \phi)}} \quad (4.37)$$

Representing the voltage at the receiving bus as:

$$V_j = Z_L \cdot I \quad (4.38)$$

The following is obtained by substituting (4.37) into (4.38):

$$V_j = \frac{Z_L}{Z_{ij}} \cdot \frac{V_i}{\sqrt{1 + (Z_L/Z_{ij})^2 + 2(Z_L/Z_{ij}) \cos(\theta - \phi)}} \quad (4.39)$$

Therefore, the active and reactive power at the receiving end can be described as follows:

$$P_j = V_j I \cos \phi \quad (4.40)$$

$$Q_j = V_j I \sin \phi \quad (4.41)$$

So, the equations (4.40) and (4.41) can be written as follows:

$$P_j = \frac{Z_L}{Z_{ij}^2} \cdot \frac{V_i^2}{[1 + (Z_L/Z_{ij})^2 + 2(Z_L/Z_{ij}) \cos(\theta - \phi)]} \cdot \cos \phi \quad (4.42)$$

$$Q_j = \frac{Z_L}{Z_{ij}^2} \cdot \frac{V_i^2}{[1 + (Z_L/Z_{ij})^2 + 2(Z_L/Z_{ij}) \cos(\theta - \phi)]} \cdot \sin \phi \quad (4.43)$$

The maximum real power that can be delivered to the receiving end can be obtained using the boundary condition $\partial P_j / \partial Z_L = 0$, that leads into $(Z_L / Z_{ij}) = 1$.

By substituting $(Z_L / Z_{ij}) = 1$ in Equations (4.42) and (4.43), the maximum transferable power, $P_{j(max)}$ is obtained as follows;

$$P_{j(max)} = \frac{V_i^2}{Z_{ij}(2+2 \cos(\theta-\phi))} \cdot \cos \phi \quad \text{So,}$$

$$P_{j(max)} = \frac{V_i^2}{Z_{ij}} \cdot \frac{\cos \phi}{4 \cos^2\left(\frac{\theta-\phi}{2}\right)} \quad (4.44)$$

By applying the same technique, the maximum transferable reactive power, $Q_{j(max)}$, is given by:

$$Q_{j(max)} = \frac{V_i^2}{Z_{ij}} \cdot \frac{\sin \phi}{4 \cos^2\left(\frac{\theta-\phi}{2}\right)} \quad (4.45)$$

Similarly, the active and reactive power losses in the line are given by:

$$P_l = Z_{ij} I^2 \cos \theta \quad (4.46)$$

$$Q_l = Z_{ij} I^2 \sin \theta \quad (4.47)$$

So, the equations (4.46) and (4.47) can be written as follows:

$$P_l = \frac{1}{Z_{ij}} \cdot \frac{V_i^2}{[1+(Z_L/Z_{ij})^2+2(Z_L/Z_{ij}) \cos(\theta-\phi)]} \cdot \cos \theta \quad (4.48)$$

$$Q_l = \frac{1}{Z_{ij}} \cdot \frac{V_i^2}{[1+(Z_L/Z_{ij})^2+2(Z_L/Z_{ij}) \cos(\theta-\phi)]} \cdot \sin \theta \quad (4.49)$$

The maximum real power in the line $P_{l(max)}$ and the maximum reactive power loss in the line $Q_{l(max)}$ can be obtained by using the boundary condition $(Z_L / Z_{ij}) = 1$.

$$P_{l(max)} = \frac{V_i^2}{Z_{ij}(2+2 \cos(\theta-\phi))} \cdot \cos \theta \quad \text{So,}$$

$$P_{l(max)} = \frac{V_i^2}{Z_{ij}} \cdot \frac{\cos \theta}{4 \cos^2\left(\frac{\theta-\phi}{2}\right)} \quad (4.50)$$

$$Q_{l(max)} = \frac{V_i^2}{Z_{ij}} \cdot \frac{\sin \theta}{4 \cos^2\left(\frac{\theta-\phi}{2}\right)} \quad (4.51)$$

$$VCPI(P) = \frac{P_j}{P_{j(max)}} = \frac{\text{Real power transfer to the receiving end}}{\text{Maximum real power that can be transferred}} \quad (4.52)$$

$$VCPI(Q) = \frac{Q_j}{Q_{j(max)}} = \frac{\text{Reactive power transfer to the receiving end}}{\text{Maximum reactive power that can be transferred}} \quad (4.53)$$

$$VCPI(P_{Loss}) = \frac{P_l}{P_{l(max)}} = \frac{\text{Real power loss in the line}}{\text{Maximum possible real power loss}} \quad (4.54)$$

$$VCPI(Q_{Loss}) = \frac{Q_l}{Q_{l(max)}} = \frac{\text{Reactive power loss in the line}}{\text{Maximum possible reactive power loss}} \quad (4.55)$$

Where the values of P_j , Q_j , P_l , and Q_l are obtained from conventional power flow calculations..

So, the four VCPIs are assessments of the line voltage stability based on the concept of maximum power transfer able through a line.

The experimental findings revealed that $VCPI(P)$ equals $VCPI(Q)$ for any load condition. Hence, only the real or reactive components can be used instead of employing four indices. Specifically, $VCPI(P)$ and $VCPI(P_{Loss})$, which respectively determine the power ratio and loss ratio, can be utilized.

The fundamental cause of voltage collapse is either excessive power transfer through the line or excessive power absorption by the line. As the power demand from the system increases, the power flow through the transmission line rises, resulting in a gradual decline in voltage at the receiving end bus. This rise in power flow also leads to an increase in line losses, consequently causing both $VCPI(P)$ and $VCPI(loss)$ to increase. As the loading conditions approach the critical operating point, both indices approach a value of 1.0.

4.3.7 New Voltage Stability Index (NVSI)

The NVSI was derived by Kanimozhi et al. This index is defined as follows for a transmission line [70]:

$$NVSI = \frac{2X^* \sqrt{P_j^2 + Q_j^2}}{2Q_j X - V_i^2} \quad (4.56)$$

In order to maintain a stable system, the NVSI must be less than 1.0 on all transmission lines.

4.3.8 Voltage Stability Indicator (VSI₂)

To avoid confusion with other notations, the VSI₂ notation has been revised to VSI₂. to avoid confusion with other notations. This index was proposed by T. K. Chattopadhyay et al. [71] and is defined as follows:

$$VSI_2 = \frac{4Q_j(R+X)^2}{X(V_i^2+8RQ_j)} \quad (4.57)$$

The condition should be VSI₂ less than 1. If the magnitude of VSI₂ is greater than 1, the corresponding radial distribution line is highly unstable. For the network to operate safely, the Voltage Stability Indicator (VSI₂) must therefore be less than unity.

4.3.9 Power Transfer Stability Index (PTSI)

The PTSI proposed by Nizam et al. is based on the concept of maximum transferable power through a limited line, similar to the VCPI index [72]:

The apparent power transfer to the receiving end can be obtained by combining Equations (4.37) and (4.39), as follows:

$$S_j = I.V_j \text{ so,}$$

$$S_j = \frac{Z_L}{Z_{ij}^2} \cdot \frac{V_i^2}{[1+(Z_L/Z_{ij})^2+2(Z_L/Z_{ij}) \cos(\theta-\phi)]} \quad (4.58)$$

$$\text{However, } (Z_L/Z_{ij}) = 1$$

The maximum load apparent power is given by:

$$S_{j(max)} = \frac{V_i^2}{Z_{ij}(2+2 \cos(\theta-\phi))} = \frac{V_i^2}{2Z_{ij}(1+\cos(\theta-\phi))} \quad (4.59)$$

a voltage collapse will occur if the ratio, $L_{Sr} = \frac{S_j}{S_{j(max)}} = 1$

By substituting (4.58) and (4.59) into $\frac{S_j}{S_{j(max)}}$, the proposed Power Transfer Stability Index

(PTSI) can be defined as follows.:

$$PTSI = \frac{S_j}{S_{j(max)}} = \frac{S_j \cdot 2Z_{ij}(1 + \cos(\theta - \phi))}{V_i^2} \quad (4.60)$$

This index is based on the same concept as VCPI in which limits the maximum power that can be transferred through a line. For the network's safe operation, the PTSI must be less than unity. When PTSI reaches 1, voltage collapse has taken place. Similar to previous line VSIs, the line shunt admittance is ignored in this index.

4.3.10 Voltage Reactive Power Index (VQI_{Line})

VQI_{Line} was proposed by F.A. Althowibi et al. [73] based on the same concept as L_p . The index is given as follows:

$$I = (V_i \angle \delta_i - V_j \angle \delta_j) \cdot Y_{ij} \angle -\theta$$

$$(S_j) = V_j I^*$$

$$S_j = V_j \angle \delta_j \cdot (V_i \angle -\delta_i - V_j \angle -\delta_j) \cdot Y_{ij} \angle \theta$$

$$S_j = V_i V_j Y_{ij} \angle (\theta - \delta_i + \delta_j) - V_j^2 Y_{ij} \angle \theta \quad (4.61)$$

Where,

$$\delta = |\delta_i - \delta_j| \text{ and } S_j = P_j + jQ_j$$

The real and reactive power at the receiving end can be obtained by separating the real and imaginary parts of Eq. (4.61), as follows::

$$P_j + jQ_j = V_i V_j Y_{ij} \angle (\theta - \delta) - V_j^2 Y_{ij} \angle \theta \quad (4.62)$$

$$P_j = V_i V_j Y_{ij} \cos(\theta - \delta) - V_j^2 Y_{ij} \cos \theta \quad (4.63)$$

$$Q_j = V_i V_j Y_{ij} \sin(\theta - \delta) - V_j^2 Y_{ij} \sin \theta \quad (4.64)$$

By substituting Equation (4.63) into Equation (4.64), a relationship between V_i and Q_j is established, as follows:

$$V_i V_j Y_{ij} \cos(\theta - \delta) - V_j^2 Y_{ij} \cos \theta + jQ_j = V_i V_j Y_{ij} \angle (\theta - \delta) - V_j^2 Y_{ij} \angle \theta \quad (4.65)$$

$$V_i V_j Y_{ij} \cos(\theta - \delta) - V_j^2 Y_{ij} \cos \theta + jQ_j = V_i V_j Y_{ij} \cos(\theta - \delta) + jV_i V_j Y_{ij} \sin(\theta - \delta) - V_j^2 Y_{ij} \cos \theta - jV_j^2 Y_{ij} \sin \theta \quad (4.66)$$

$$jQ_j = jV_i V_j Y_{ij} \sin(\theta - \delta) - jV_j^2 Y_{ij} \sin \theta \quad (4.67)$$

Rearrange (4.67):

$$V_j^2 Y_{ij} \sin \theta - V_i V_j Y_{ij} \sin(\theta - \delta) + Q_j = 0$$

$$V_j^2 - \frac{V_i V_j \sin(\theta - \delta)}{\sin \theta} + \frac{Q_j}{Y_{ij} \sin \theta} = 0 \quad (4.68)$$

If δ is negligible, the equation can be simplified by setting δ to zero. This removes the term $(\sin(\theta - \delta)/\sin \theta = 1)$, and $Y_{ij} \sin \theta = |B_{ij}|$. The following expression results:

$$V_j^2 - V_i V_j + \frac{Q_j}{|B_{ij}|} = 0 \quad (4.69)$$

The discriminant of the quadratic equation V_j (4.69), ($\Delta = b^2 - 4ac$) must be greater than or equal to 0 in order for the equation to have real roots. This is because a real root means that the value of V_j is real. Therefore, the discriminant must be set to a value greater than or equal to 0.

$$V_i^2 - 4 \frac{Q_j}{|B_{ij}|} \geq 0 \text{ So,}$$

$$\frac{4Q_j}{|B_{ij}|} \leq V_i^2 \quad (4.70)$$

Rearrange (4.70),

$$VQI_{Line} = \frac{4Q_j}{|B_{ij}|V_i^2} \leq 1$$

$$VQI_{Line} = \frac{4Q_j}{|B_{ij}|V_i^2} \quad (4.71)$$

Where, $B_{ij} = \text{Im}(Y_{ij}) = \text{Im}(1/R + jX)$

The voltage stability of a power system is considered to be at its limit when the (VQI_{Line}) value approaches 1. A (VQI_{Line}) value of 1 indicates that the power system is in a state of voltage instability.

4.3.11 Voltage Stability Load Index (VSLI)

T. K. Abdul Rahman et al. proposed the Voltage Stability Line Index (VSLI) to assess line voltage stability, based on the principle used in Lp [74] [75].

The VSLI is determined by squaring equations (4.6) and (4.7), and then summing them up to form a quartic Eq. (4.72). This equation describes the connection between voltage and transferred power at the receiving end.

$$V_j^4 - [V_i^2 - 2(P_j R + Q_j X)]V_j^2 + (P_j^2 + Q_j^2)(R^2 + X^2) = 0 \quad (4.72)$$

$$V_j^4 - [V_i^2 - 2(P_j R + Q_j X)]V_j^2 + S_j^2 Z_{ij}^2 = 0 \quad (4.73)$$

The discriminant of the quadratic equation (4.72) must be greater than or equal to 0 in order to obtain real roots for the equation and therefore a real value for the receiving end voltage.

Therefore,

$$\left(V_i^2 - 2(P_j R + Q_j X)\right)^2 - 4(P_j^2 + Q_j^2)(R^2 + X^2) \geq 0 \quad (4.74)$$

Eq. (4.74) can be simplified to the following equation::

$$\frac{4[V_i^2(P_j R + Q_j X) + (P_j R - Q_j X)^2]}{V_i^4} \leq 1 \quad (4.75)$$

By substituting equations (4.6) and (4.7) into (4.75).

$$\frac{4[V_i^2(V_i V_j \cos \delta - V_j^2) + (V_i V_j \sin \delta)^2]}{V_i^4} \leq 1$$

$$VSLI = \frac{4[V_i V_j \cos \delta - V_j^2 \cos^2 \delta]}{V_i^2} \quad (4.76)$$

Maintaining VSLI below 1.0 is essential for ensuring a consistent system. A VSLI value of 1.0 or greater indicates a voltage collapse, which can lead to system instability. Therefore, controlling VSLI is critical for maintaining stable system operations.

4.3.12 Voltage Vulnerability Index (VVI)

The Voltage Vulnerability Index (VVI) is proposed by Andreea-Georgiana et al. [76]. Equation

(4.73) can be expressed in a quadratic form in terms of the unknown variable y .

$$y = V_j^2 :$$

$$y^2 - ay + b^2 = 0 \quad (4.77)$$

Where:

$$a = V_i^2 - 2(P_j R + Q_j X) \quad (4.78)$$

And,

$$b^2 = (P_j^2 + Q_j^2)(R^2 + X^2) = (S_j Z_{ij})^2 \quad (4.79)$$

The voltage stability is ensured if real and positive roots are possessed by the equation (4.77).

Thus, to achieve real and positive roots, the following conditions need to be satisfied:

1. The discriminant must be non-negative: $\Delta = a^2 - 4b^2 \geq 0$.
2. The product of the roots is: $y_1 y_2 = b^2 \geq 0$.
3. The sum of the roots is: $y_1 + y_2 = a$, must be positive: $a \geq 0$.

So, the inequalities are satisfied when:

$$0 \leq \frac{2b}{a} \leq 1 \quad (4.80)$$

Mathematically, the Voltage Vulnerability Index (VVI) can be represented as follows by substituting equations (4.78) and (4.79) into (4.80):

$$VVI = \frac{2Z_{ij}S_j}{[V_i^2 - 2(P_j R + Q_j X)]} \quad (4.81)$$

The VVI index will be computed for each line using equation (4.81). The lines with the highest VVI values are the most vulnerable. When the VVI value exceeds 1, the system loses stability and experience voltage collapse.

4.3.13 Line Collapse Proximity Index (LCPI)

Traditionally, the previous equations for voltage stability indices have overlooked the impact of line shunt admittance and the relative direction of active power flow compared to reactive power flow. As a result, these indices may produce inaccurate predictions in specific scenarios.

The Line Collapse Proximity Index (LCPI) is developed. The LCPI considers the exact transmission line model and the effects of both reactive and active power flow on the system's voltage stability [19] [77].

The (LCPI) index is derived using ABCD parameters of the transmission line. Figure 4.1 displays the pie model of a transmission line for a two-bus system. The relationship among the network parameters can be articulated as follows:

$$\begin{bmatrix} V_i \\ I_i \end{bmatrix} = \begin{bmatrix} A & B \\ C & D \end{bmatrix} \begin{bmatrix} V_j \\ I_j \end{bmatrix} \quad (4.82)$$

Where A, B, C, and D are known as the transmission parameters of the two-port network, and they can be expressed as:

$$A = (1 + Z_{ij}Y_{ij}/2)$$

$$B = Z_{ij}$$

$$C = Y_{ij}(1 + Z_{ij}Y_{ij}/4)$$

$$D = A$$

The sending end voltage V_i of the line can be written as follows, using equation (4.82):

$$V_i \angle \delta_i = A \angle \alpha \cdot V_j \angle \delta_j + B \angle \beta \cdot I_j \angle 0 \quad (4.83)$$

Where A and B are the magnitudes and α and β are the phase angles of the parameters A and B, respectively.

The current at the receiving end of the line is expressed as follows:

$$I_j = (S_j/V_j)^* = (P_j - jQ_j)/V_j \angle -\delta_j \quad (4.84)$$

The value of I_j is substituted into (4.83) to get:

$$V_i \angle \delta_i = A \angle \alpha \cdot V_j \angle \delta_j + B \angle \beta \cdot (P_j - jQ_j)/V_j \angle -\delta_j \quad (4.85)$$

Rearranging (4.85) gives:

$$V_i V_j \angle \delta = A \angle \alpha \cdot V_j^2 \angle 0 + B \angle \beta \cdot (P_j - jQ_j) \quad (4.86)$$

The discriminant of equation (4.86) must be greater than zero for the equation to have real and non-zero roots. This can be achieved by setting the discriminant equal to zero and solving for the roots.

$$(V_i \cos\delta)^2 - 4(A \cos\alpha)(P_j B \cos\beta + Q_j B \sin\beta) \geq 0 \quad (4.87)$$

Rearrange (4.87):

$$\frac{4(A \cos\alpha)(P_j B \cos\beta + Q_j B \sin\beta)}{(V_i \cos\delta)^2} \leq 1 \quad (4.88)$$

The Line Collapse Proximity Index (LCPI) is defined as:

$$LCPI = \frac{4(A \cos\alpha)(P_j B \cos\beta + Q_j B \sin\beta)}{(V_i \cos\delta)^2} \quad (4.89)$$

The Line Collapse Proximity Index (LCPI) considers the magnitudes and relative directions of the real and reactive powers of the receiving end. Furthermore, parameters A and B in equation (4.89) account for the effects of line resistance and shunt admittance, which previous voltage stability indices overlooked. In (4.89), the term $(B \cos\beta)$ corresponds to the resistance of the transmission line. Hence, the first term in (4.89) represents the voltage drop caused by the active power (P_j) flowing through the line. Similarly, the second term $(Q_j B \sin\beta)$ in (4.89) indicates the reactive voltage drop created by the reactive power (Q_j) of the line. If P_j and Q_j flow in the same direction, both terms are additive, while the signs of these terms are opposite when the active and reactive power of the receiving end flow in opposite directions. To maintain the voltage stability of the system, the LCPI index must be less than unity, i.e., $LCPI < 1$.

4.3.14 Power Stability Index (PSI)

The Power Stability Index (PSI) was proposed by M.M. Aman et al. in [78]. The index was derived from a simple two-bus network shown in Figure 4.1.

$$S_L = P_L + jQ_L = V_j I_j^*$$

$$V_j = V_i - I_j Z_{ij} \quad (4.90)$$

Where,

$$I_j = \frac{(P_L - P_G) - j(Q_L - Q_G)}{V_j^*} \quad (4.91)$$

By substituting I_j into Eq. (4.90) and separating the real and imaginary parts gives:

$$(P_L - P_G) = \frac{V_i V_j}{Z_{ij}} \cos(\theta - \delta) - \frac{V_j^2}{Z_{ij}} \cos \theta \quad (4.92)$$

$$(Q_L - Q_G) = \frac{V_i V_j}{Z_{ij}} \sin(\theta - \delta) - \frac{V_j^2}{Z_{ij}} \sin \theta \quad (4.93)$$

Rearranging Eq. (4.92) gives:

$$V_j^2 - V_i V_j \frac{\cos(\theta - \delta)}{\cos \theta} + \frac{(P_L - P_G) Z_{ij}}{\cos \theta} = 0 \quad (4.94)$$

Equation (4.94) is a quadratic equation. For stable status, the equation must have real roots, which means that the discriminant ($\Delta = b^2 - 4ac \geq 0$), must be greater than or equal to zero.

The Power Stability Index (PSI) is given by:

$$PSI = \frac{4R_{ij}(P_L - P_G)}{[|V_i| \cos(\theta - \delta)]^2} \quad (4.95)$$

Under stable conditions, the Power Stability Index (PSI) should be less than one. The closer PSI is to zero, the more stable the system.

4.3.15 Voltage Stability Index (VSI)

V.V.S.N. Murty et al. proposed a voltage stability index that can be calculated from a simple Radial Distribution System (R.D.S.), as illustrated in Figure 4.1 [79]. The mathematical model of the index is shown below:

$$VSI = \frac{4X_{ij}}{V_i^2} \left(\frac{P_L^2}{Q_L} + Q_L \right) \quad (4.96)$$

During stable operation, the VSI value should remain below one. A VSI value closer to zero indicates a more stable system, while a higher VSI value signifies potential instability. Buses

with higher VSI values are more sensitive and should be considered for optimal DG placement to improve system stability.

4.3.16 Line Voltage Stability Index (LVSI)

Saurabh Ratra et al. proposed the Line Voltage Stability Index (LVSI) to assess the voltage stability status and stress conditions of transmission lines [30].

The receiving end active power can be expressed using the ABCD parameters from Eq. (4.82) as follows:

$$P_j = \frac{V_i V_j \cos(\beta - \delta)}{B} - \frac{AV_j^2 \cos(\beta - \alpha)}{B} \quad (4.97)$$

Rearranging Eq. (4.97) results in the formation of a quadratic equation for voltage in the following manner:

$$AV_j^2 \cos(\beta - \alpha) - V_i V_j \cos(\beta - \delta) + BP_j = 0 \quad (4.98)$$

The $(dV_j)/(dP_j)$ can be obtained from equation (4.98).

$$\frac{dV_j}{dP_j} = \frac{-B}{2AV_j \cos(\beta - \alpha) - V_i \cos(\beta - \delta)}$$

For the system to maintain voltage stable the sensitivity must be negative.

$$\frac{-B}{2AV_j \cos(\beta - \alpha) - V_i \cos(\beta - \delta)} < 0$$

$$V_i \cos(\beta - \delta) - 2AV_j \cos(\beta - \alpha) < 0 \quad (4.99)$$

Based on Eq. (4.99), the following condition must be met to prevent voltage collapse in the system:

$$\frac{2AV_j \cos(\beta - \alpha)}{V_i \cos(\beta - \delta)} > 1 \quad (4.100)$$

$$LVSI = \frac{2AV_j \cos(\beta - \alpha)}{V_i \cos(\beta - \delta)} \quad (4.101)$$

The LVSI value is 2 under a no-load condition, indicating a large voltage stability margin. However, as the line loading increases, the LVSI value decreases, signifying a reduced voltage

stability margin. At the maximum loading point, the LVSI value of the line reaches 1, indicating a critical state. Thus, the LVSI index is used to identify critical lines based on their LVSI values. To prevent voltage collapse in a system, the LVSI must be greater than 1.

4.3.17 Voltage Collapse Proximity Index (VCPI_1)

In the system consisting of two buses as illustrated in Figure 4.1, a simple calculation shows that in the critical condition, the generator voltage phasor (V_i) is twice the magnitude of the projection of the load bus voltage phasor (V_j) onto it.

$$V_i > 2V_j \cos \delta$$

Consequently, to evaluate the potential for voltage instability, the proximity of voltage collapse is quantified using the voltage collapse proximity index VCPI (1) [80].

$$VCPI(1) = V_j \cos \delta - 0.5V_i \quad (4.102)$$

When $VCPI(1) \geq 0$, the line voltage is considered stable; otherwise, it is unstable.

4.3.18 Voltage Stability Margin (VSMs)

VSMs was proposed by Guiping et al. [81]. This index is derived based on the same concept as VCPI and PTSI, which are based on the maximum transferable power through a line.

Referring to equation (4.58), the apparent load power (S_j) is derived, and the maximum load apparent power ($S_{j(max)}$) is derived in equation (4.59).

This confirms the well-known fact that the critical level of (Z_L / Z_{ij}) is unity, representing the voltage stability limit. At this critical point, the load power reaches its maximum value.

The voltage stability margin is defined as:

$$VSMs = \frac{S_{j(max)} - S_j}{S_{j(max)}} \quad (4.103)$$

Table 4.1 Characteristics of VSIs.

No.	VSI	Stability Threshold	Equation	Relative Variables	Assumptions
1	FVSI	≤ 1	$FVSI_{ij} = 4Z_{ij}^2 Q_j / V_i^2 X$	Z_{ij}, X, Q_j, V_i	$Y_s \approx 0, \delta = 0,$ $\sin \delta = 0, \cos \delta = 1$ Effect of active power is neglected.
2	L_{mn}	≤ 1	$L_{mn} = 4XQ_j / \{(V_i \sin(\theta - \delta))^2\}$	$X, Q_j, V_i, \theta, \delta$	$Y_s \approx 0$ Effect of active power is neglected.
3	LQP	≤ 1	$LQP_{ij} = 4(X/V_i^2)(P_i^2 X / V_i^2 + Q_j)$	X, Q_j, V_i, P_j	$Y_s \approx 0, R/X \ll 1$ $R \approx 0$
4	L_p	≤ 1	$L_p = 4RP_j / \{(V_i \cos(\theta - \delta))^2\}$	$R, P_j, V_i, \theta, \delta$	$Y_s \approx 0$ Effect of reactive power is neglected.
5	NLSI	≤ 1	$NLSI_{ij} = (P_j R + Q_j X) / 0.25V_i^2 \cos^2(\delta_i - \delta_j)$	$R, X, P_j, Q_j, V_i, \delta$	$Y_s \approx 0,$ $\delta \approx 0$
6	VCPI	≤ 1	$VCPI(P) = P_j / P_{j(max)}, VCPI(Q) = Q_j / Q_{j(max)}$ $VCPI(P_{Loss}) = P_l / P_{l(max)}, VCPI(Q_{Loss}) = Q_l / Q_{l(max)}$	$Z_{ij}, P_j, Q_j, P_l, Q_l,$ V_i, θ, ϕ	Constant power factor, $Y_s \approx 0$
7	NVSI	≤ 1	$NVSI = 2X * \sqrt{P_j^2 + Q_j^2} / [2Q_j X - V_i^2]$	X, P_j, Q_j, V_i	$Y_s \approx 0, R \approx 0s$ Y_s, R are neglected
8	VSI ₂	≤ 1	$VSI = 4Q_j(R + X)^2 / X(V_i^2 + 8RQ_j)$	R, X, Q_j, V_i	$Y_s \approx 0,$ $\delta \approx 0$
9	PTSI	≤ 1	$PTSI = S_j / S_{j(max)}$ $= S_j \cdot 2Z_{ij}(1 + \cos(\theta - \phi)) / V_i^2$	$S_j, Z_{ij}, V_i, \theta, \phi$	$Y_s \approx 0$ $\delta \approx 0$
10	VQI _{Line}	≤ 1	$VQI_{Line} = (4Q_j) / (B V_i^2)$	B, Q_j, V_i	Constant power factor, $Y_s \approx 0$
11	VSLI	≤ 1	$VSLI = 4[V_i V_j \cos(\delta) - V_j^2 \cos(\delta)] / V_i^2$	V_i, V_j, δ	$Y_s \approx 0$
12	VVI	≤ 1	$VVI = 2Z_{ij} S_j / [V_i^2 - 2(P_j R + Q_j X)]$	$Z_{ij}, V_i, R, X, P_j,$ Q_j, S_j	$Y_s \approx 0$ $\delta \approx 0$
13	LCPI	≤ 1	LCPI $= \frac{4 A \cos(\alpha)[P_j B \cos(\beta) + Q_j B \sin(\beta)]}{[V_i \cos(\delta)]^2}$	$P_j, Q_j, V_i,$ $\delta, A, \alpha, B, \beta$	Line is modeled as pie model
14	VSI	≤ 1	$VSI = \frac{4X}{V_i^2} \left(\frac{P_L^2}{Q_L} \right) + Q_L$	X, P_L, Q_L, V_i	$Y_s \approx 0$ $\delta \approx 0$
15	PSI	≤ 1	$PSI = \frac{4R(P_L - P_G)}{[V_i \cos(\theta - \delta)]^2}$	$R, P_L, P_G, V_i, \theta, \delta$	$Y_s \approx 0$
16	VCPI(1)	> 0	$VCPI(1) = V_j \cos \delta - 0.5V_i$	V_j, δ, V_i	Z_{ij} is neglected $Y_s \approx 0$
17	VSM _S	> 0	$VSM_S = \frac{S_{cr} - S_j}{S_{cr}}$ $S_{cr} = \frac{V_i^2}{2Z_{ij}[1 + \cos(\theta - \phi)]}$	$S_j, Z_{ij}, \theta, \phi, V_i$	$Y_s \approx 0$ $\delta \approx 0$ The power factor is constant
18	LVSI	> 1	$LVSI = \frac{2V_i A \cos(\beta - \alpha)}{V_j \cos(\beta - \delta)}$	$V_i, V_j, A, \beta, \alpha, \delta$	Line is modeled as pie model

To facilitate comparative analysis, Table 4.1 presents the principal features of the examined VSIs, including equations, crucial values, and underlying assumptions.

Figure 4.2 shows classify the VSIs based on their underlying concepts, revealing that the majority is founded on the notion that the voltage equation must possess a solution to ensure voltage stability, which means the discriminant of VSIs equations is set to be greater than or equal to zero.

The VSIs are shown in Figure 4.3 based on their dependence on the power system's impedance.

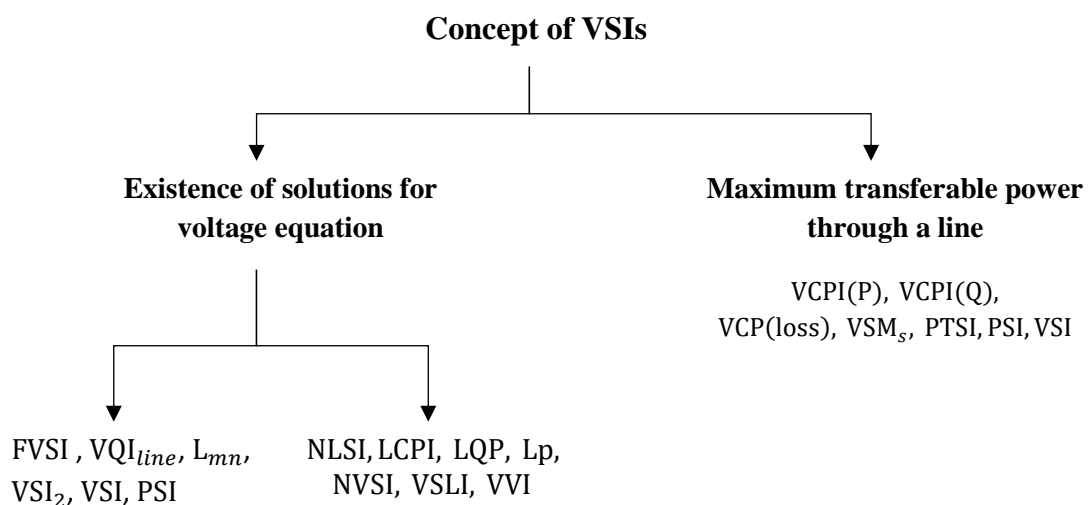


Figure 4.2 Concepts of the voltage stability indices

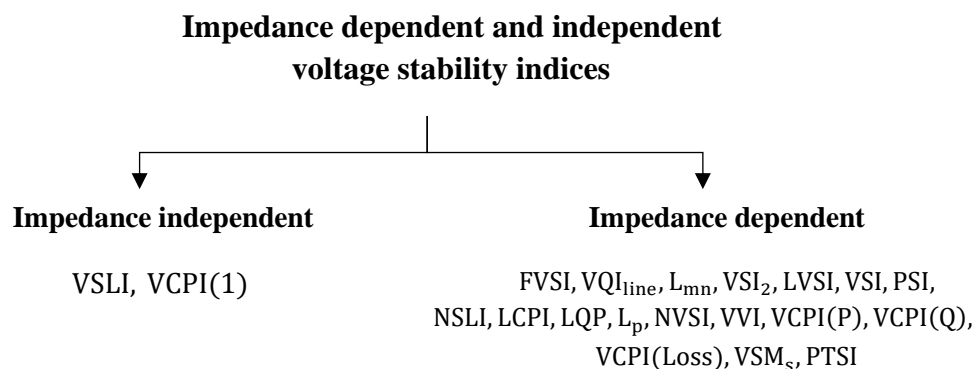


Figure 4.3 Impedance dependent and independent voltage stability indices

CHAPTER 5: Results and Discussions

5.1 Introduction

In this chapter, the results of the tested indices are presented. This thesis presents a comprehensive study of voltage indices of power system networks, focusing on two specific test systems: the radial distribution system IEEE 12-bus and the meshed power network IEEE 30-bus system. The analysis and results presented in this thesis are based on the Newton-Raphson method of power flow solution, which is used for practical systems. A computer software program, MATLAB environment, has been used to perform the simulation. The data of the two systems used in this thesis are sourced from the IEEE database.

In Appendix A of this thesis, detailed descriptions of the system's data, including the system configurations, bus data, generator data, and branch data, have been provided.

5.2 Description of Test System

The distribution networks serve as intermediaries between distribution substations and consumers, facilitating electrical power transfer the last few miles from the transmission or sub-transmission systems to end users. Power transmission within distribution networks occurs through the utilization of overhead wires mounted on poles or buried underground. Distribution networks can be distinguished from transmission networks based on their voltage level and configuration.

The distribution network consists of feeders interconnected in a radial structure, preventing loops formation. This type of network is commonly referred to as a Radial Distribution Network (RDN) or a "star network," where only a single path exists for power flow between the distribution substation and a specific load. In some cases, distribution networks may exhibit a ring or loop topology, allowing for two distinct power flow paths between the distribution substation and the load.

Significant power losses are observed within this segment of the electric power network due to increased branch currents and voltage drops. These losses subsequently result in a reduction in the overall quality and efficiency of power delivery to consumers. Accommodating the continuous growth in electric distribution loads poses a significant challenge for engineers responsible for designing and maintaining the power distribution network, particularly ensuring that the network remains adaptable to load increases without exceeding system constraints.

The flow of loads through electric distribution lines leads to elevated active power losses, increased voltage drops across branches, and a deterioration in the power factor at the load terminals. These issues can be mitigated by implementing reactive power compensation techniques such as Shunt Capacitors (SC) strategic placement or a combination of SC and Distributed Generation (DG) sources. Such measures effectively prevent the problems mentioned above from arising.

Distribution networks typically operate at lower voltages. Generally, lines with voltage ratings up to 35kV are part of the distribution network [82]. The interconnection between distribution networks and transmission or sub-transmission systems occurs at distribution substations. These substations are equipped with transformers to step down the voltage to the primary distribution level, typically ranging from 4kV to 35kV in the United States. Similar to transmission substations, distribution substations feature circuit breakers and monitoring equipment. However, distribution substations typically exhibit lower automation levels than their transmission counterparts. Therefore, the distribution substation is an intermediary between the transmission and distribution systems.

A comprehensive examination of the proposed indices was conducted on two different distribution systems; the first Radial Distribution Network (RDN) is a 12-bus power system model, which serves as a simplified representation of typical electrical power distribution

systems in real-world applications. This model comprises 11 branches and 12 buses, one slack bus and 11 PQ buses. The system voltage is 11kV, and the total active and reactive loads are 435kW and 405kVAR, respectively. Moreover, the system's total real and reactive power loss is 20.7kW and 8.04kVAR, respectively, for the base case. A schematic representation of the single line diagram for this test system can be found in Figure 5.1, with accompanying line and load data in reference [83].

The second system used is IEEE 30-bus test system shown in Figure 5.2. This test system has meshed transmission and distribution network. It consists of 30 buses, six generator buses (PV), twenty-four load buses (PQ), forty-one interconnected branches, six generators, and two shunt capacitors. Under normal loading conditions, the total required loads are 283.4 MW and 126.2MVAR that operate at four different voltage levels; 132 kV, 33 kV, 11 kV and 1 kV [84]. The system is a more complex test system and is designed to represent a typical distribution system with a mix of radial and meshed configurations. It is widely used as a benchmark system in power systems research, as it is small enough to be solved easily yet complex enough to represent real-world power systems.

The voltage stability indices are being examined separately for the 33 kV and 132 kV distribution lines to facilitate a more straightforward analysis. This approach allows a more detailed investigation of the voltage stability characteristics of each line, which may vary depending on their specific operating conditions and network topology. By studying the voltage stability indices for each line separately, insights into the impact of various factors, such as load variations, system topology, and fault conditions, can be gained on the network's voltage stability as a whole.

The configurations of the networks and their branch data are included as supplementary material in the Appendix A section.

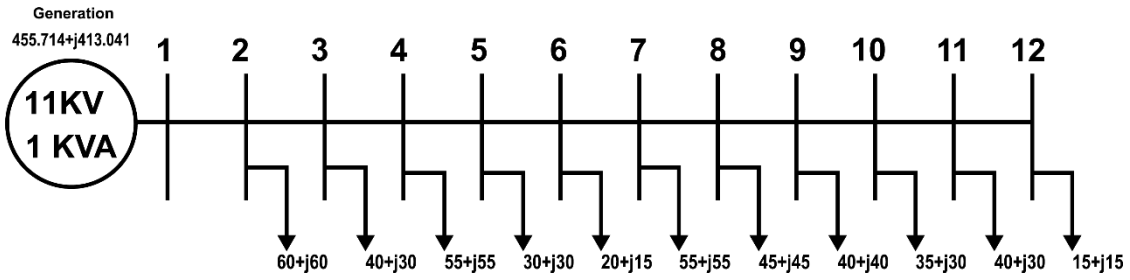


Figure 5.1 Single line diagram of IEEE 12-bus distribution test system [83]

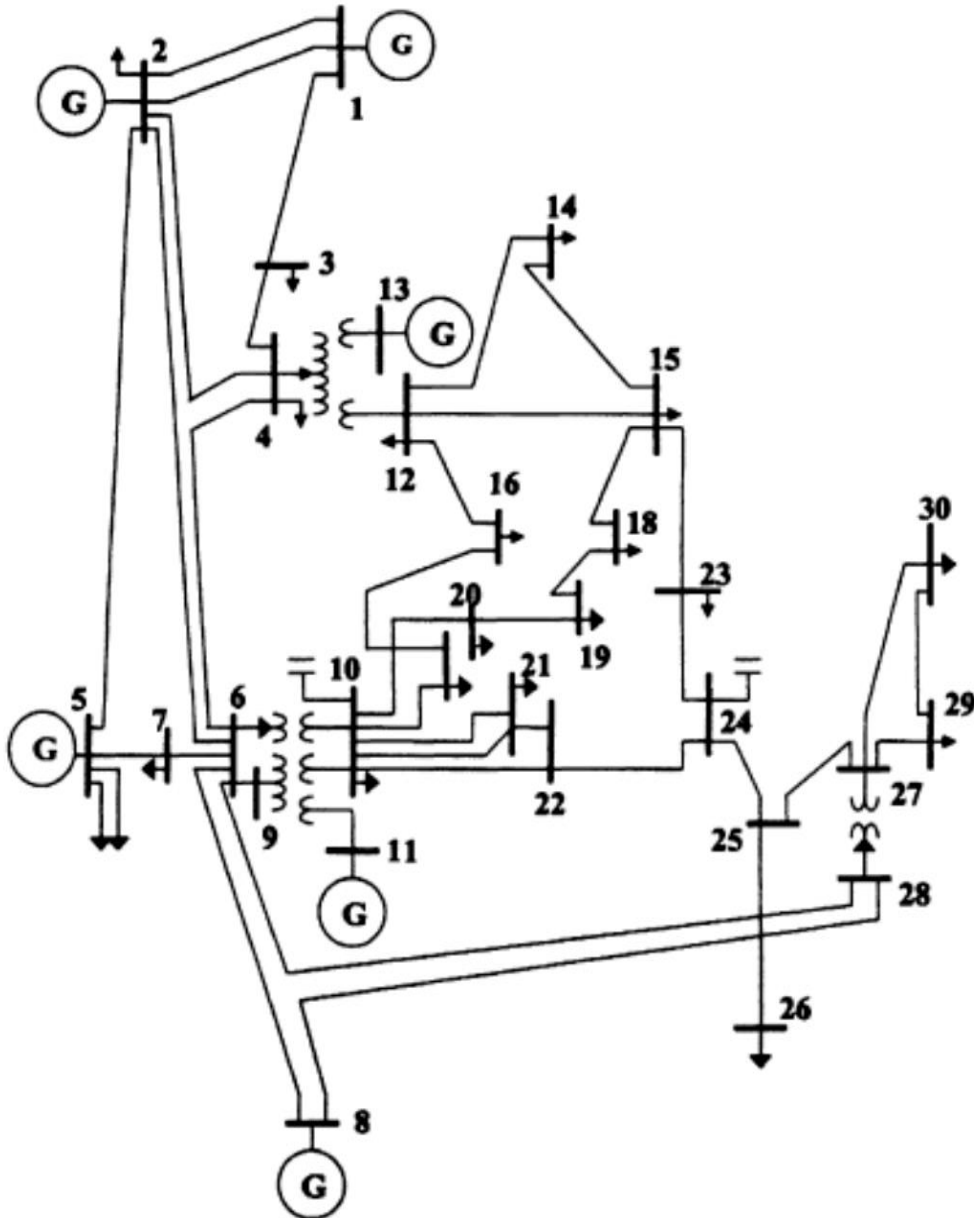


Figure 5.2 Single line diagram of IEEE 30-bus distribution test system [85]

5.3 Assessment of Voltage Stability Indices in a Distribution Networks for Prediction of Voltage Collapse

The voltage stability analysis is carried out by categorizing it as dynamic or static. Static voltage stability analysis approaches are mainly based on the steady-state model, such as the power flow model. In contrast, dynamic analysis is based on nonlinear differential and algebraic equations, such as tap-changing transformers and generator dynamics. Static analysis has recently been applied to investigate the voltage stability problem thoroughly. This analysis is more accurate and less complicated since it requires less calculation time to perform system stability analysis, especially when dealing with short load disruptions.

Identifying weak lines and buses in power networks is an essential application of Voltage Stability Indices (VSIs). Thereby implementing corrective actions to mitigate the risk of voltage instability, particularly in solving optimization problems such as Distributed Generation (DG) and Reactive Power Compensation (RPC) placement. Voltage stability indices can determine a power system's voltage stability state, and the voltage stability assessment within an electrical power system is facilitated through voltage stability indices .

In this chapter, two main scenarios have been simulated and discussed:

First scenario: The base case data for two networks have been analyzed, and then voltage stability indices have been calculated for each branch in the test network. These indicators will be evaluated and have been used to detect the weak bus and choose the optimal location for the installation of DG based on their performance.

Second scenario: An incremental load perturbation analysis has been performed, where the active and reactive load change at all buses have been gradually increased from the base case until their maximum allowable load or maximum loadability, which represents the maximum load that can be injected at the bus without causing a diverges (did not converge) in the power flow solution. Then voltage stability indices were calculated for each branch in the test

network.

5.4 Methodology to Calculate Voltage Stability Indices

In some indices, the effects of relative directions of active and reactive power flow in the line must be considered to predict voltage collapse.

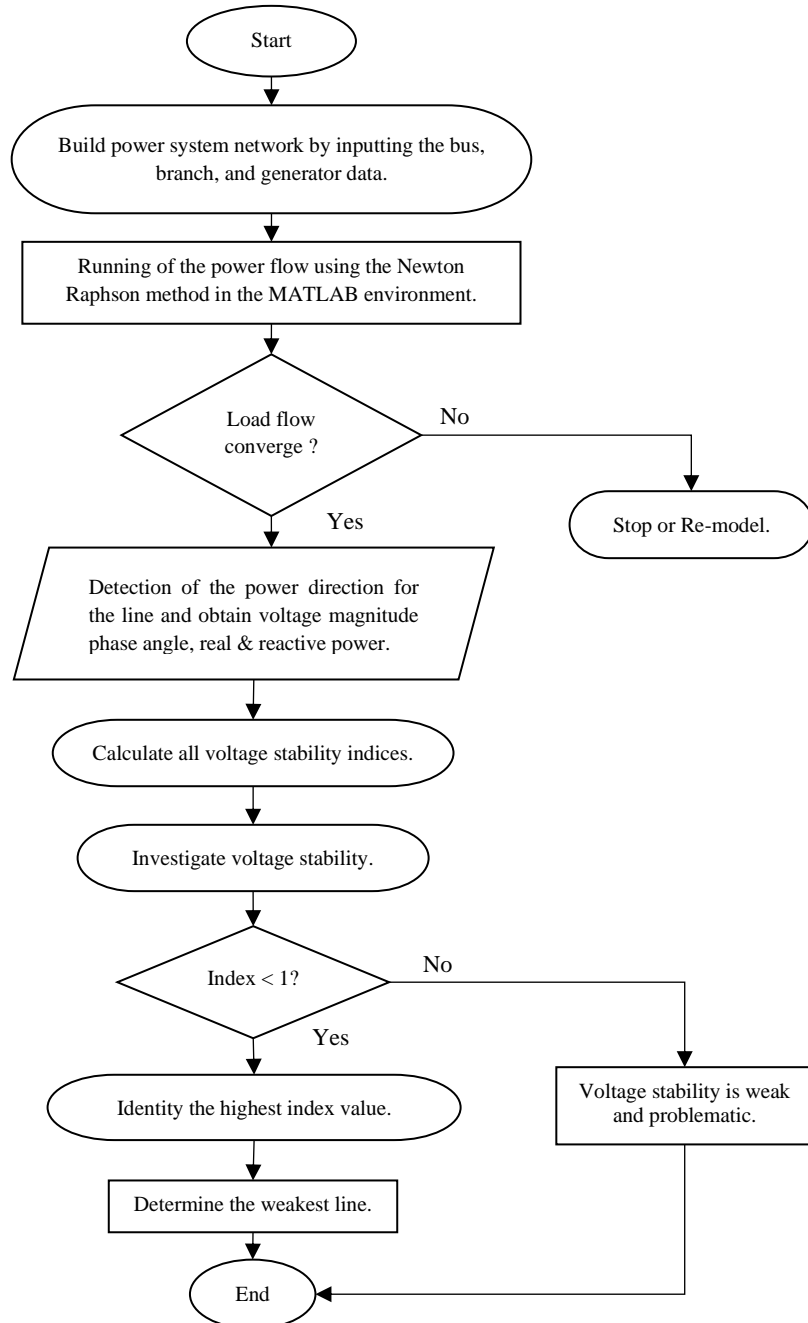


Figure 5.3 Flowchart depicting the computation method for VSIs and detection of weak lines in a real-time power system

Therefore, the direction of the power will be determined after calculating load flow as a methodology proposed for identifying the most vulnerable lines within a power grid, as the authors demonstrate in [77], [86].

Figure 5.3 presents the flowchart delineating the methodology proposed for identifying the most vulnerable lines within a power grid. The approach employs a set of established voltage stability indices on a static load model. The initial stage of this process involves constructing a power system utilizing the MATLAB Simulink tool. The investigation focuses on the IEEE 12-bus and IEEE 30-bus systems to assess weak lines.

5.5 Voltage Stability Indices

The previous chapter introduces a comprehensive review of 19 types of VSIs - [NLSI, LCPI, PTSI, VCPI(p), LQP, L_p , VCPI(loss), NVSI, VSLI, VVI, FVSI, VQI_{line} , VSI_2 , L_{mn} , LVSI, VCPI(1), VSM_s , VSI and PSI] - from where: name, abbreviation, calculating method, assumptions, the central concept, stable condition, critical value, unstable condition.

In this chapter, we will explore these indicators in depth, discussing their advantages and limitations and how they can be used to assess the stability of power systems. We will also examine case studies and real-world examples to illustrate the practical applications of these indicators in power system analysis. Moreover, study the load changes and their effect on voltage stability.

This chapter aims to provide a comprehensive understanding of the various indicators used to measure line voltage stability and how they can be used to improve the performance and reliability of power systems.

Each of these indices must be kept below 1 to maintain voltage stability except VCPI(1), VSM_s must be kept more than 0 to maintain voltage stability, and LVSI must be kept more than 1 to maintain voltage stability; the critical value for each index explain in Table 4.1.

First scenario: Simulation test results for assessing voltage stability and voltage stability indices under base case conditions.

A. IEEE 12-Bus Test Network.

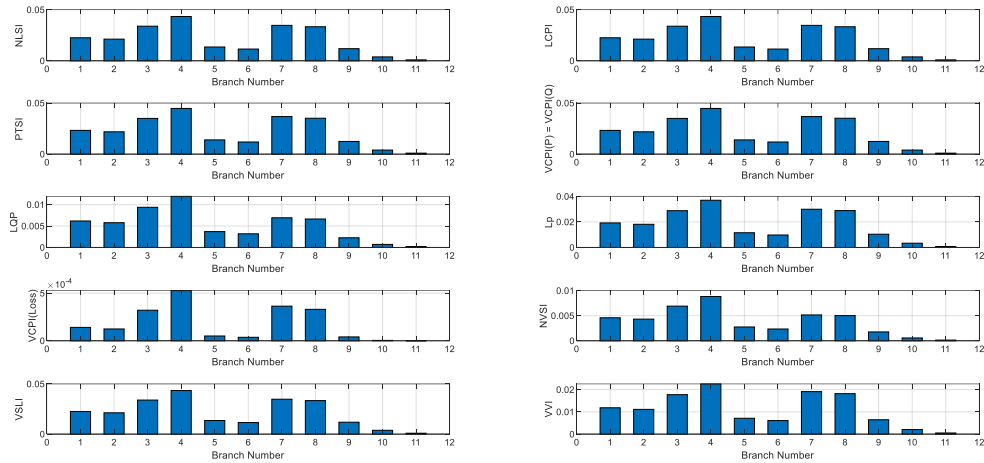


Figure 5.4 VSIs of each branch in the IEEE 12-bus network under base case condition, branch 4 is critical

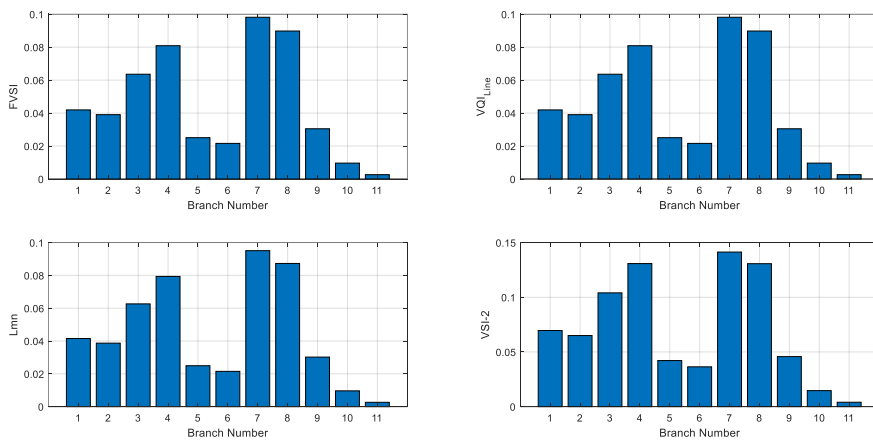


Figure 5.5 VSIs of each branch in the IEEE 12-bus network under base case condition, branch 7 is critical

It is noticeable from the results of the VSIs in Figure 5.4 to Figure 5.6 that under normal loading, the values of all indices are close to zero, and from Figure 5.7, VCPI(1), VSMs are close to 1 and LVSI close to 2, which indicates that the system operates at a stable point. Based on the findings, the highest values are observed at line 4 (4-5) in Figure 5.4, line 7 (7-8) in Figure 5.5, and line 8 (7-9) in Figure 5.6 and Figure 5.7 the index LVSI, and VSMs Line 4 is

considered the critical line because it has the lowest value among the lines. However, for VCPI(1), the critical line is line 8, as it recorded the lowest value. The top critical line for each index is shown in Table 5.1.

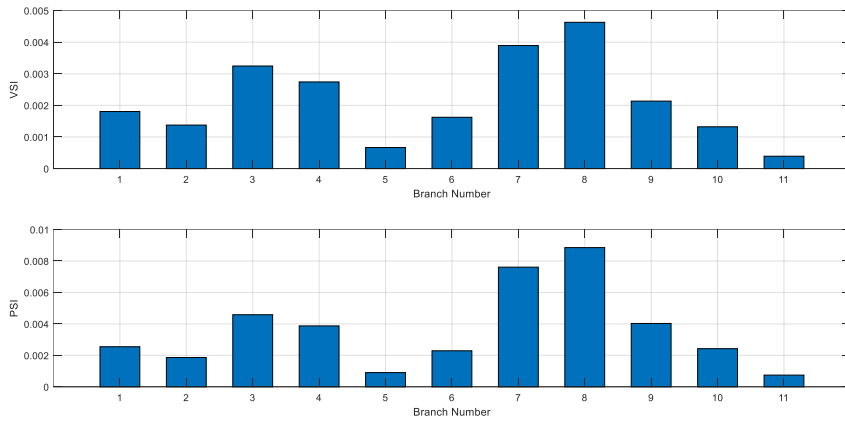


Figure 5.6 VSI & PSI of each branch in the IEEE 12-bus system under base case condition, branch 8 is critical

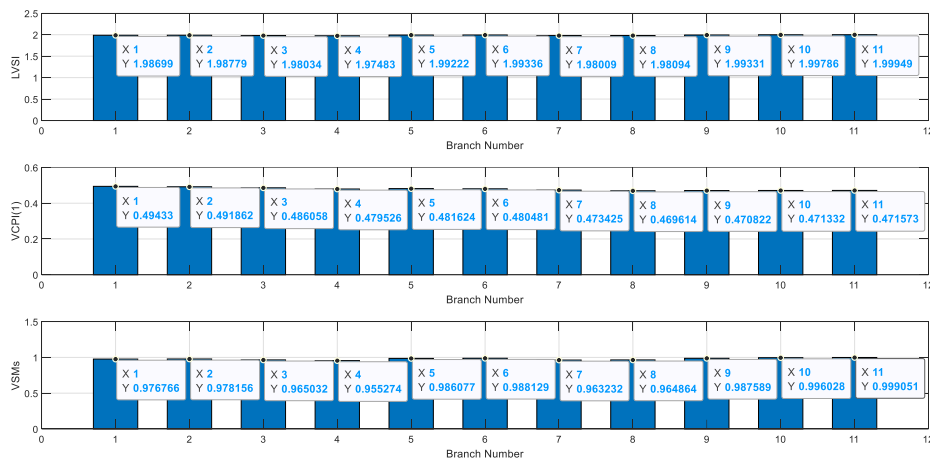


Figure 5.7 LVSI, VCPI(1) and VSM_s of each branch in the IEEE 12-bus system under base case condition

It is observed that all indices in Figure 5.4 take active and reactive power flow into account, except for L_p, is take the active power effect, while the index VSLI takes effects of sending end, receiving end voltage and δ . However, active and reactive power flow effects are ignored. Moreover, all indices in Figure 5.5 consider reactive power flow and neglect the active power flow effects. The VSI index in Figure 5.6 take active and reactive load power into account, and the PSI index takes active load power and active power generation into account. Moreover, the

VSI and PSI take the effect of line reactance and line resistance, respectively, into account, as the eighth line has the highest value of resistance and reactance of the line.

As for VCPI(1) in Figure 5.7, each of sending end and receiving end voltage and δ is taken into account, where the critical condition occurs when the sending end voltage (V_i) is twice greater than the cosine of the (δ) angle multiplied by receiving end voltage (V_j). The index does not need to track the Thevenin equivalent parameters. Therefore, So it is fast in the calculation. Also, in Figure 5.7, index VSM_s have the same concept as VCPI(p) and PTSI. The concept is the maximum power transfer theorem, and the index considers line impedance and the angle of line impedance and load.

B. IEEE 30-Bus Test Network

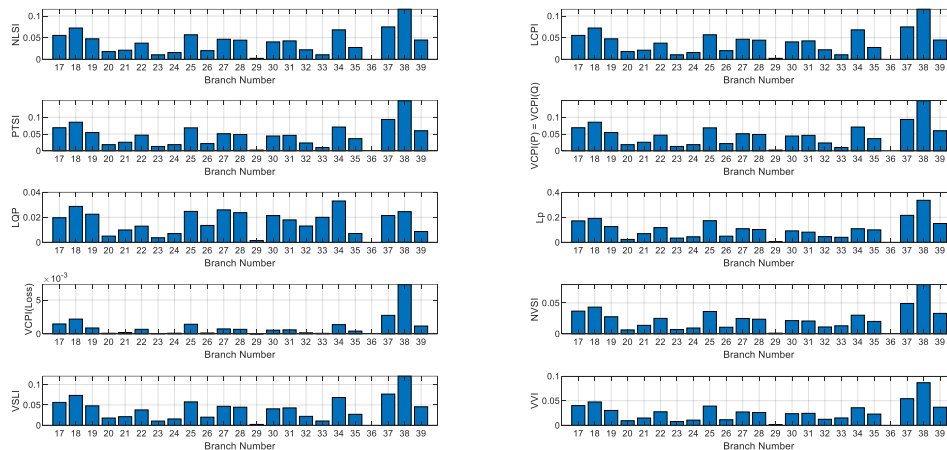


Figure 5.8 VSIs of all 33 kV transmission lines for IEEE 30-bus network under base case condition

Only the results obtained for all the 132kV and 33kV lines are presented in this section. It is noticeable from the results of the VSIs in Figures (5.8, 5.12, 5.14) that under normal loading, it is observed that the highest value of the indices is recorded at line 38 (27-30), except for the LQP index in Figure 5.8 where is the highest critical line value is in line 34 (25-26), and also all indices in Figure 5.10 it is observed that the highest value the indices are recorded at line34(25-26).

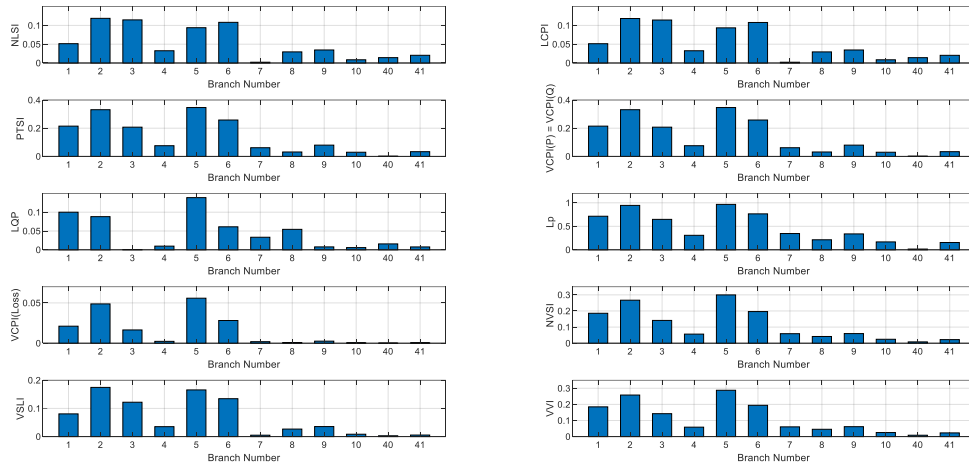


Figure 5.9 VSIs of all 132 kV transmission lines for IEEE 30-bus network under base case condition

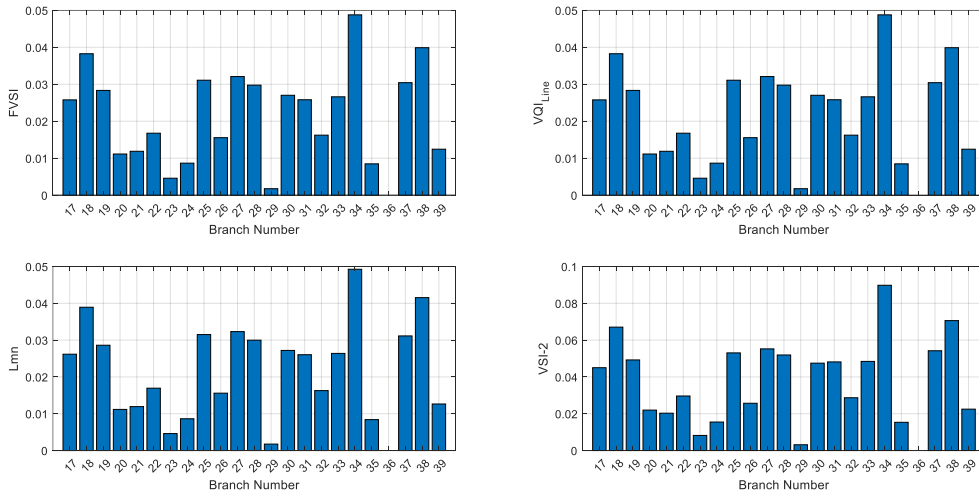


Figure 5.10 VSIs of all 33 kV transmission lines for IEEE 30-bus network under base case condition

In 132kV transmission lines, It is noticeable from the results of the VSIs in Figure 5.9 that the highest value is for line 5 (2-5) for all indices except NLSI, LCPI, and VSLI indices have line 2(1-3) as the highest critical value. We also notice that the fifth line (2-5) has the highest value among the lines for all indices in Figure 5.13 and Figure 5.15. while in Figure 5.11 the line 1 (1-2) is a critical line for all indices

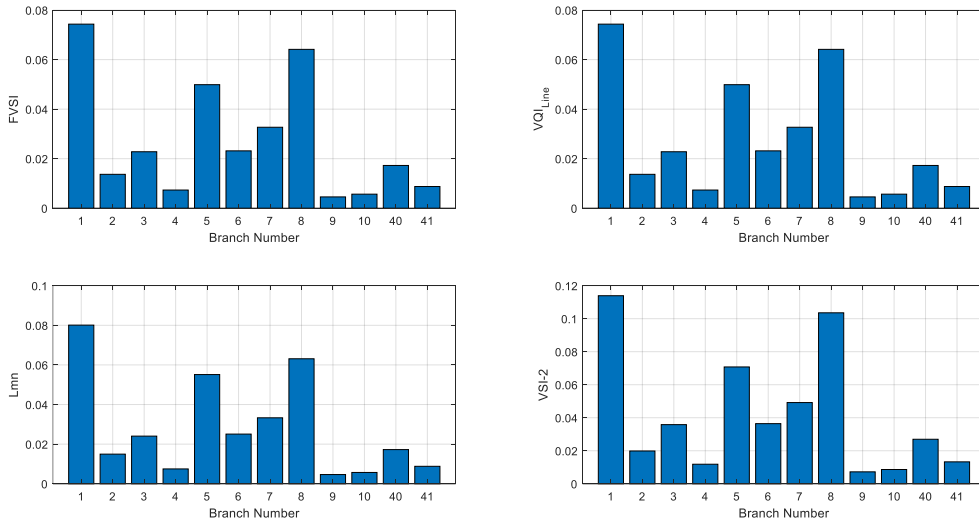


Figure 5.11 VSIs of all 132 kV transmission lines for IEEE 30-bus network under base case condition

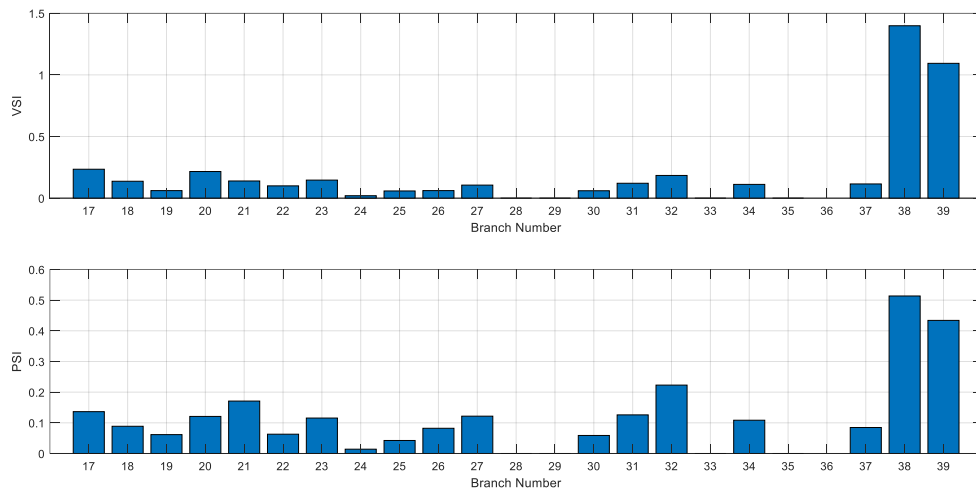


Figure 5.12 VSI & PSI of all 33 kV transmission lines for IEEE 30-bus network under base case condition

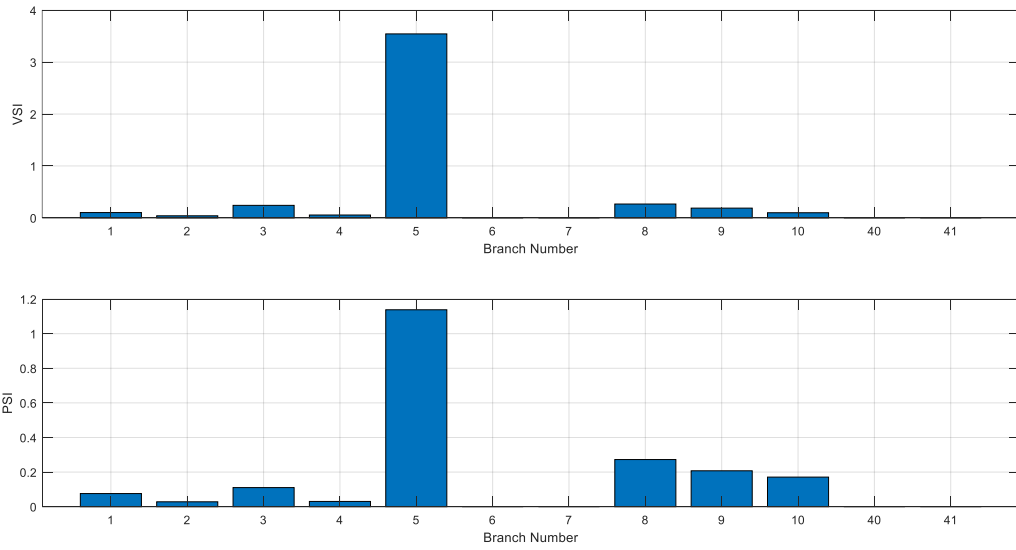


Figure 5.13 VSI & PSI of all 132 kV transmission lines for IEEE 30-bus network under base case condition

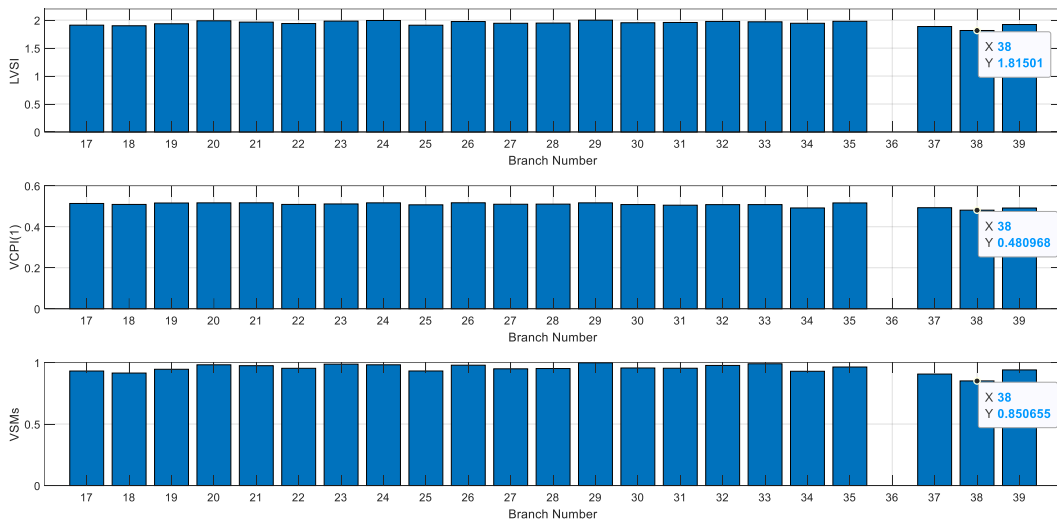


Figure 5.14 LVSI, VCPI(1), and VSMs value of all 33 kV transmission lines for IEEE 30-bus network under base case condition

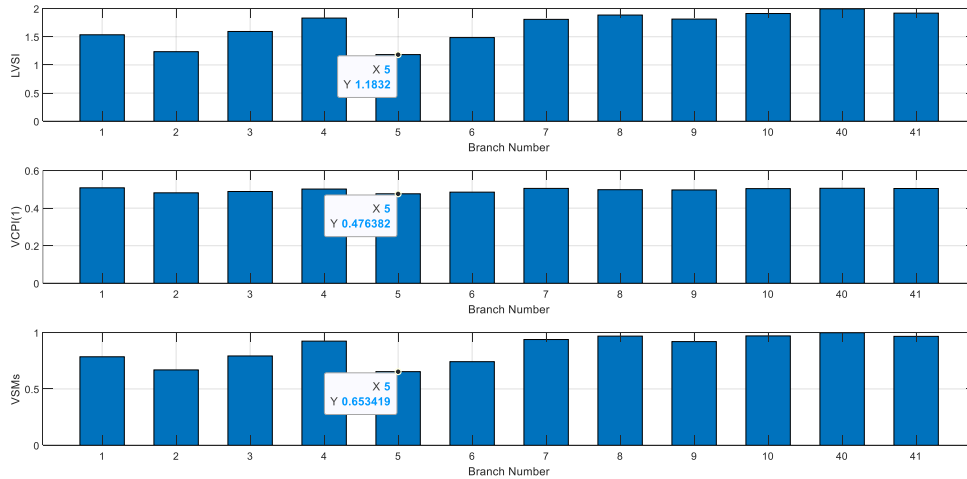


Figure 5.15 LVSI, VCPI (1), and VSMs value of all 132 kV transmission lines for IEEE 30-bus network under base case condition

The voltage stability indices are impacted by factors such as network topology (radial, interconnected, mesh), operating conditions, and the number of inputs for each index. Table 4.1 summarizes the inputs for each index, which in turn influence the value of each indicator. In Table 5.1, the top critical line for each index is summarized under normal loading conditions.

Table 5.1 The top critical line for each voltage stability index (ranking one) for base case loading.

Test system	IEEE 12-bus test system			IEEE 30-bus test system				
	11 kV transmission lines			33 kV transmission lines		132 kV transmission lines		
Critical Line	Line 4 Bus 4 to Bus 5	Line 7 Bus 7 to Bus 8	Line 8 Bus 8 to Bus 9	Line 34 Bus 25 to Bus 26	Line 38 Bus 27 to Bus 30	Line 1 Bus 1 to Bus 2	Line 2 Bus 1 to Bus 3	Line 5 Bus 2 to Bus 5
Index	NLSI	FVSI = VQI_{line}	VSI	FVSI = VQI_{line}	NLSI	FVSI = VQI_{line}	NLSI	PTSI = VCPI(P)
	LCPI	L_{mn}	PSI	L_{mn}	LCPI	L_{mn}	LCPI	LQP
	PTSI = VCPI(P)	VSI_2	VCPI(1)	VSI_2	PTSI = VCPI(P)	VSI_2	VSLI	L_p
	LQP	-	-	LQP	L_p	-	-	VCPI(loss)
	L_p	-	-	-	VCPI(loss)	-	-	NVSI
	VCPI(loss)	-	-	-	NVSI	-	-	VVI
	NVSI	-	-	-	VSLI	-	-	LVSI
	VSLI	-	-	-	VVI	-	-	VSM_s
	VVI	-	-	-	LVSI	-	-	VCPI(1)
	LVSI	-	-	-	VSM_s	-	-	VSI
	VSM_s	-	-	-	L_p	-	-	PSI
	-	-	-	-	VSI	-	-	-
-	-	-	-	PSI	-	-	-	

Second scenario: Second scenario: Simulation test results for assessing voltage stability and voltage stability indices under all buses' heavy active and reactive loading.

This scenario used Continuous Load Flow (CLF) analysis methods to find VSIs for two test systems: P and Q load variation at all buses, keeping PF (Power Factor) constant. In Figure 5.16 and Figure 5.27, the load varies from the base case to the loadability limit for IEEE 12-bus and IEEE 30-bus, respectively. Suppose there are both load buses (buses with load directly connected) and non-load buses (buses without directly connected load). In that case, the "Load Variation" will uniformly vary the loads in load buses, while non-load buses will not be involved in load variation.

Looking at both Figure 5.17 and Figure 5.28, we observe that in both systems, there is a significant decrease in the voltage profile at all buses under the influence of heavy loading. Heavy loading P at all buses causes a decrease in voltage magnitude due to increased line losses. Line losses occur due to resistance in the transmission and distribution lines. As a result, the voltage at the load buses decreases due to the voltage drop across the impedance of the lines.

Whereas heavy loading Q leads to voltage instability. Voltage instability occurs when the voltage magnitude at certain buses drops significantly, leading to a decline in the overall system voltage. This can result from inadequate reactive power support to meet the reactive power demand of the heavily loaded system. Insufficient reactive power can cause voltage instability, resulting in voltage collapse and blackouts.

A. IEEE 12-Bus Test Network

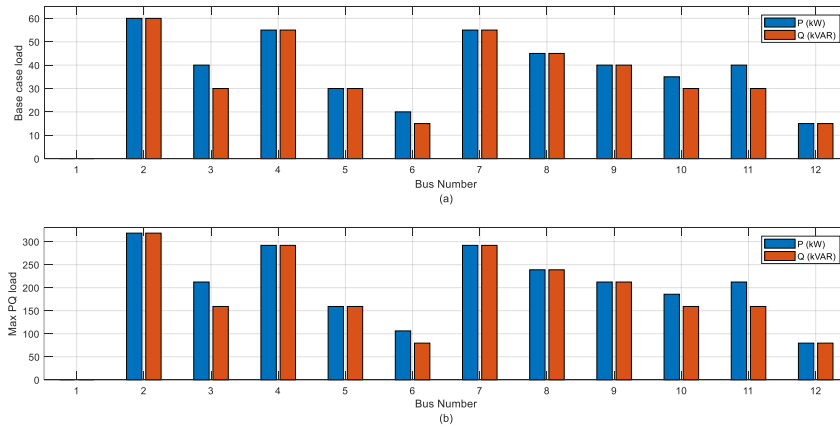


Figure 5.16 Load buses for IEEE 12-bus system (a) under base case condition (b) under heavy PQ loading

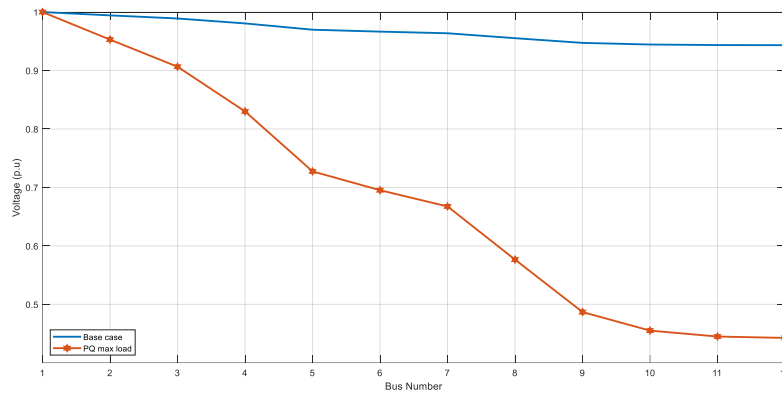


Figure 5.17 Voltage profile for IEEE 12-bus system under heavy PQ loading at all buses

When the system loadings are gradually increased to the maximum at a time by different percentages to determine the voltage stability limit under heavy PQ loading with keep constant power factor. We observe that the values of all voltage stability indices have increased, reaching a stability limit, as shown in Figure 5.18 to Figure 5.21. Furthermore, it is evident that all indices agree that Line 8 (8-9) is the critical line, indicating that Bus 9 is the weakest bus, except for the indices LQP and NVSI, which show that both Line 4 and Line 8 are weaker lines. This is clearly shown in Table 5.2, where these two indices neglect the value of the angle δ in their parameters as shown in Table 4.1.

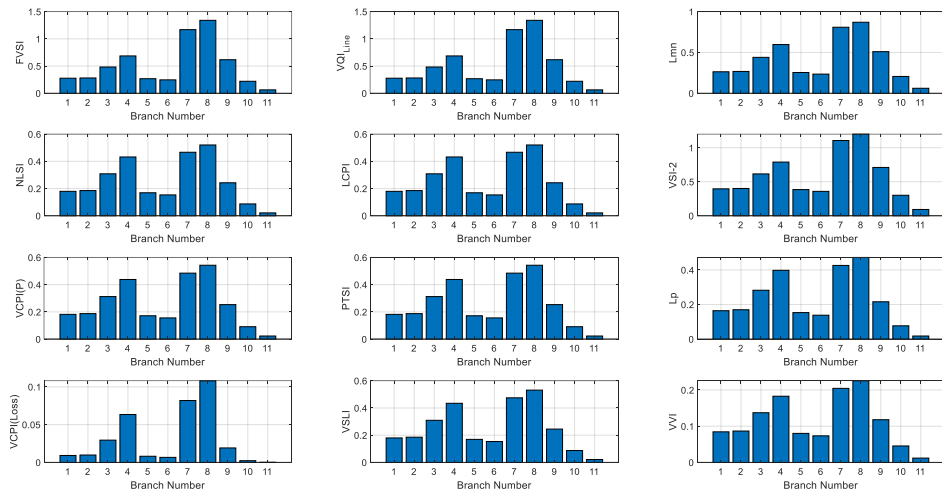


Figure 5.18 VSIs for each line in IEEE 12-bus under heavy PQ loading at all buses

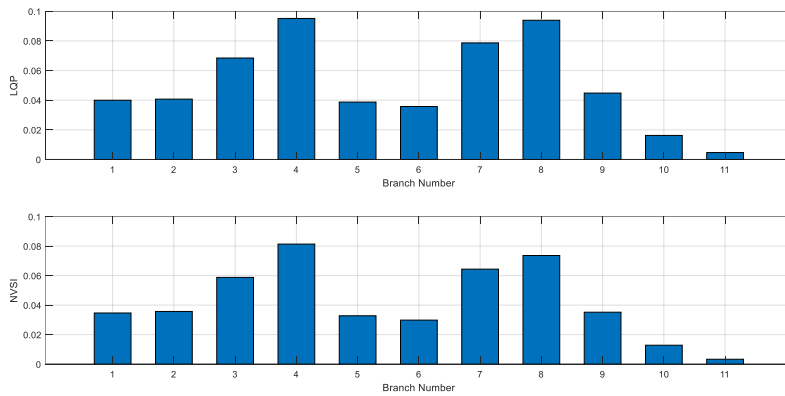


Figure 5.19 LQP & NVSI for each line in IEEE 12-bus under heavy PQ loading at all buses

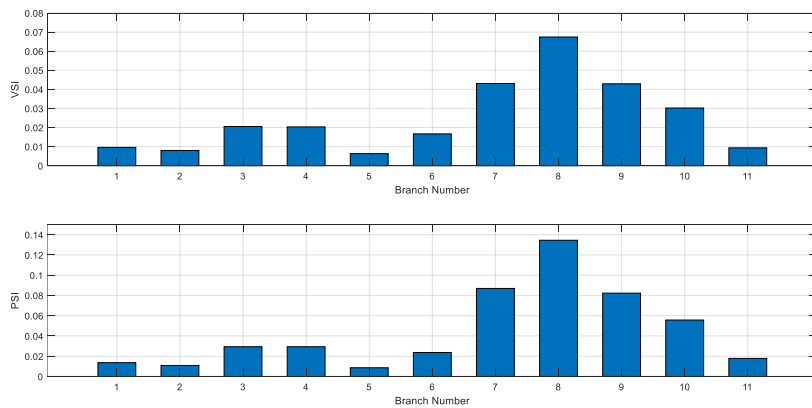


Figure 5.20 VSI & PSI for each line in IEEE 12-bus under heavy PQ loading at all buses

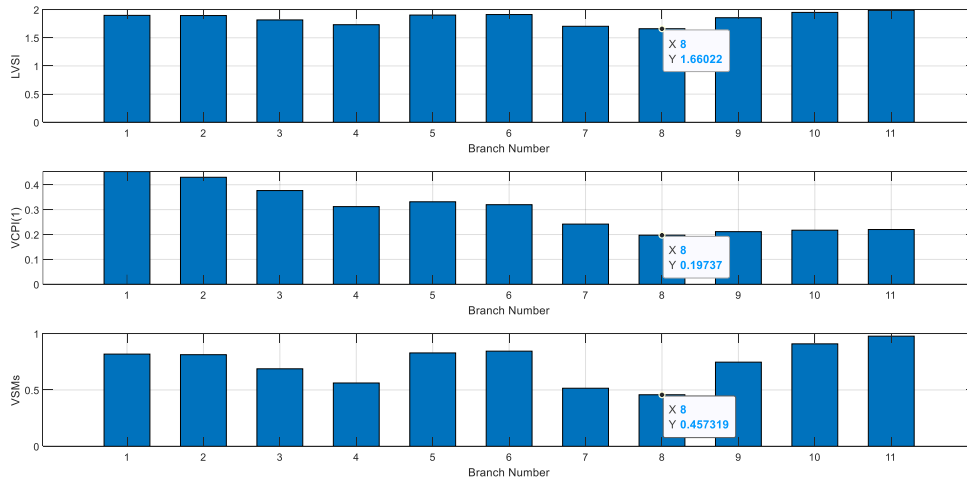


Figure 5.21 LVSI, VCPI(1),and VSMs for each line in IEEE 12-bus under heavy PQ loading at all buses

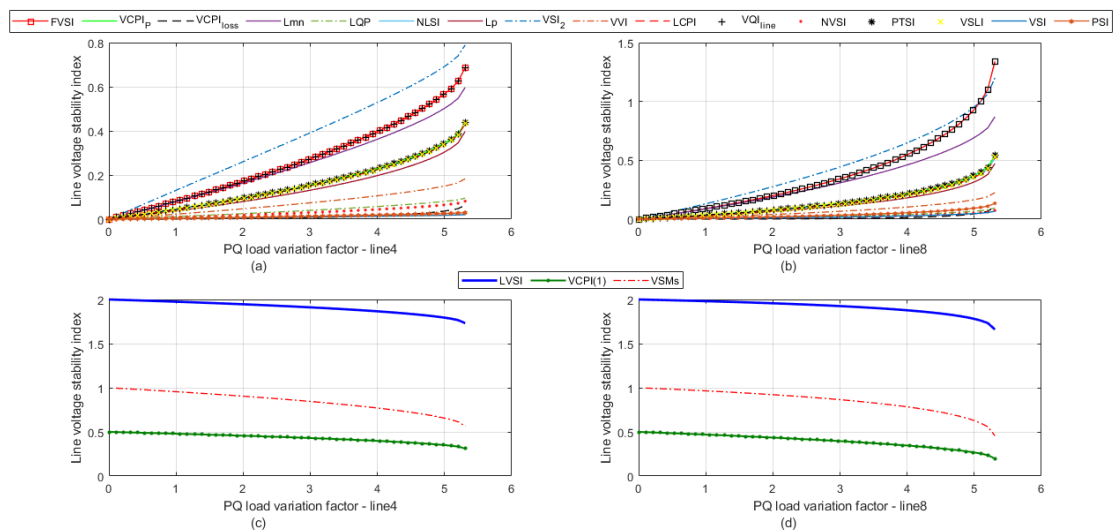


Figure 5.22 The index values for different VSIs with respect to PQ loading in IEEE 12-bus system. (a),(c) Line 4(4-5) - (b),(d) Line 8(8-9)

The indices that depend on reactive power flow Q_j values in their parameters were also noticed to be more sensitive to voltage instability, exceeding the stability threshold of 1, such as the FVSI, L_{mn} , VSI_2 index.

The behavior of all voltage stability indices with varying load, from no-load to maximum loadability, for the critical lines (lines 4 and 8) is presented in Figure 5.22. It was also observed

that the VSI_2 index is the fastest in detecting the weak line.

The behavior of each of the (FVSI, LQP, PSI, and VSM_s) indices for the first three critical lines in the system is depicted in Figures 5.23 to 5.26, based on each index.

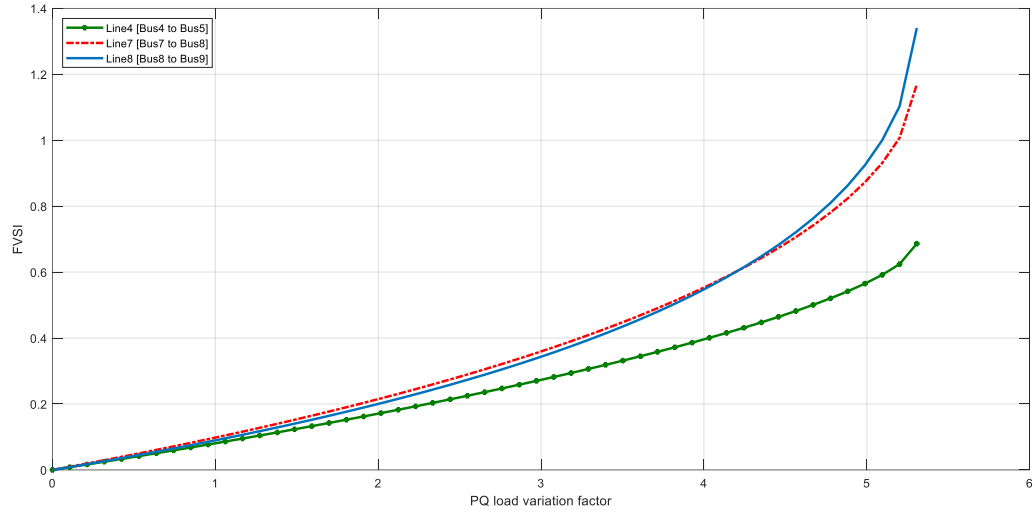


Figure 5.23 FVSI under heavy PQ loading for IEEE 12-bus, top critical lines

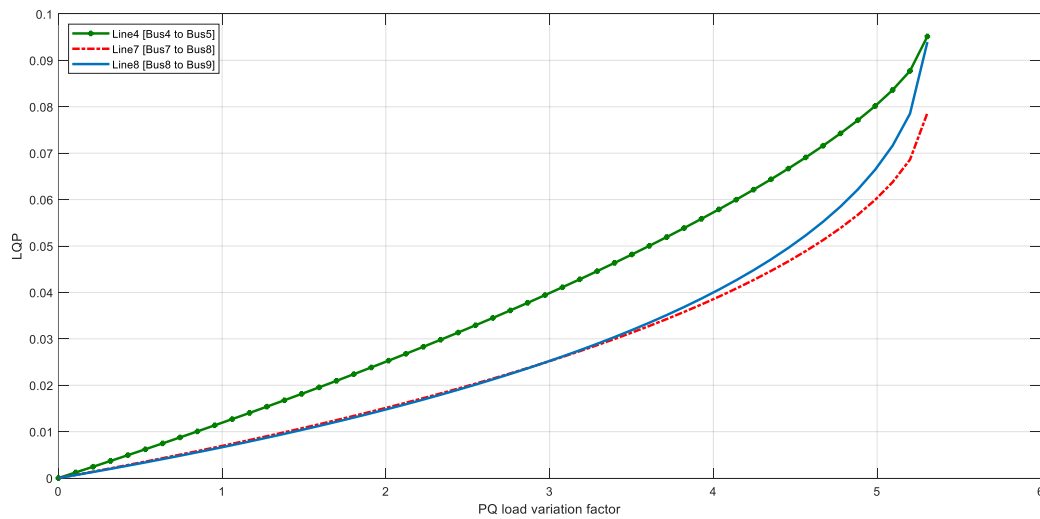


Figure 5.24 LQP under heavy PQ loading for IEEE 12-bus, top critical lines

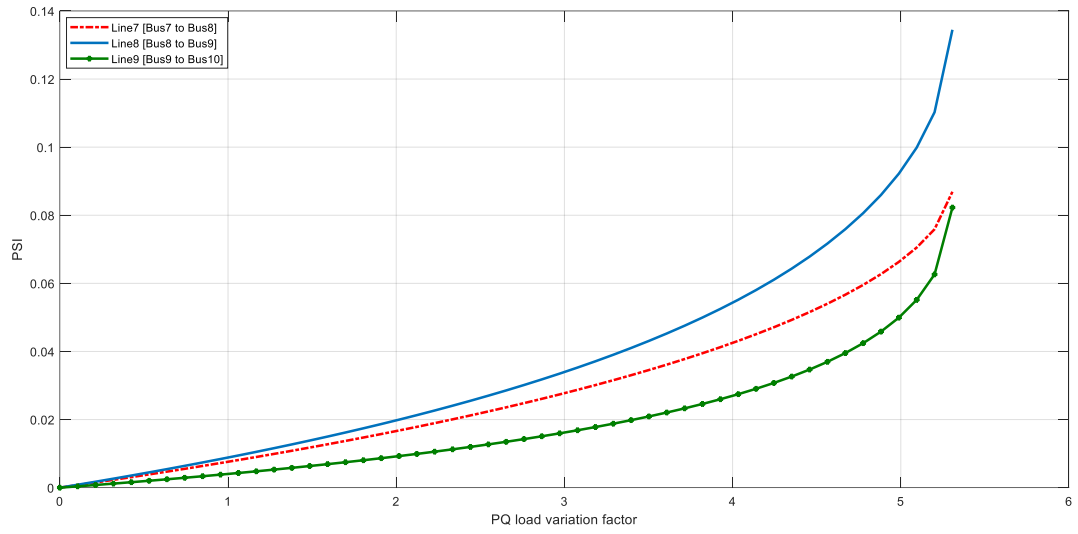


Figure 5.25 PSI under heavy PQ loading for IEEE 12-bus, top critical lines

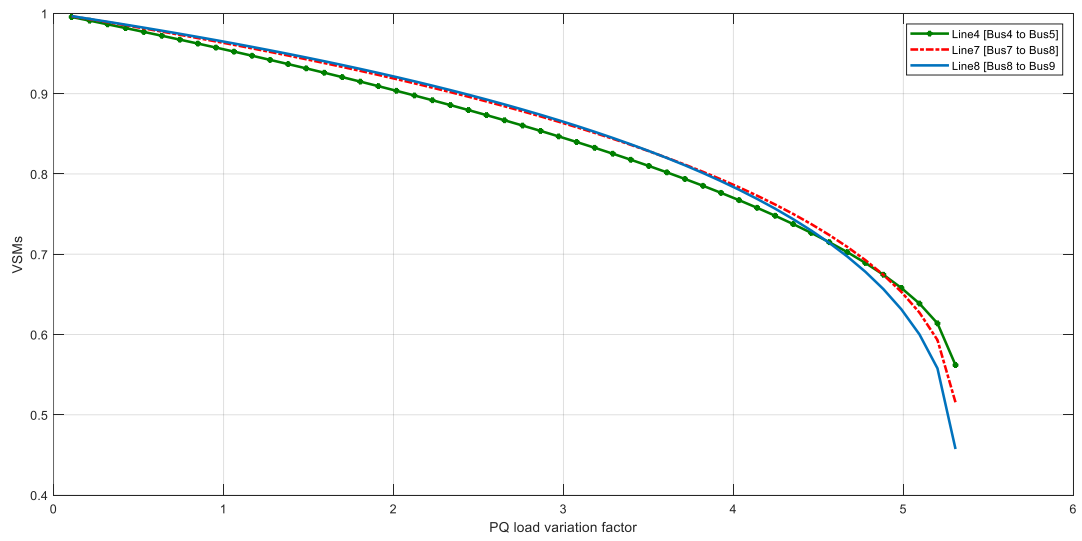


Figure 5.26 VSMs under heavy PQ loading for IEEE 12-bus, top critical lines

B. IEEE 30-Bus Test Network

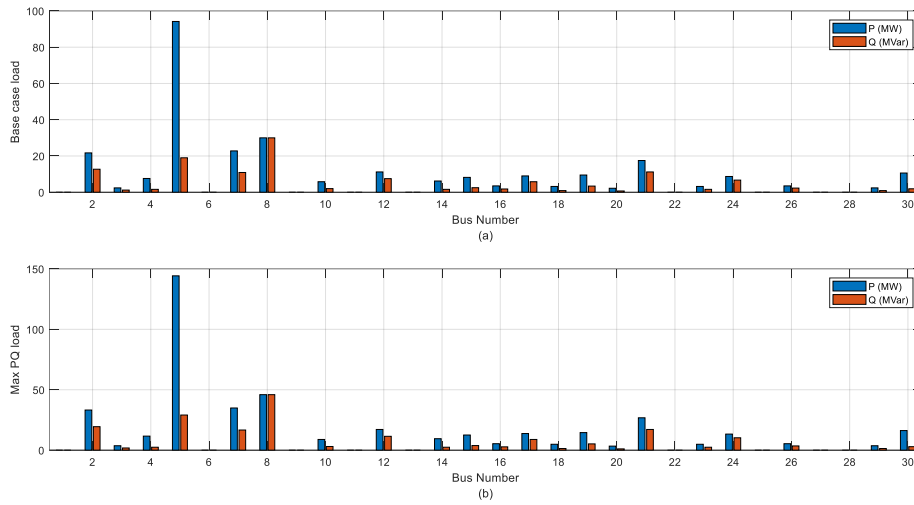


Figure 5.27 Load buses for IEEE 30-bus system (a) under base case condition (b) under heavy PQ loading

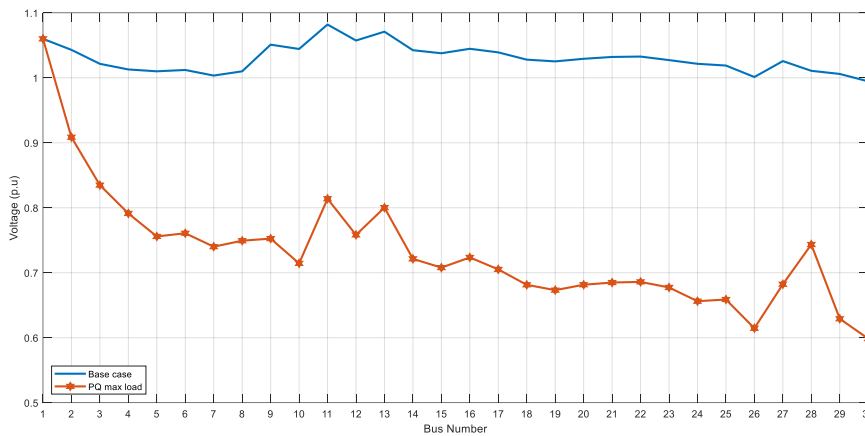


Figure 5.28 Voltage profile for IEEE 30-bus system under heavy PQ loading at all buses

For the IEEE 30-bus system, the VSIs results show for all 33 kV and 132 kV transmission lines under heavy PQ loading. It is observed that the values of all voltage stability indices have increased in all lines, as clear from Figure 5.29 to Figure 5.36.

Furthermore, all indices that consider active power flow have higher values than indices that only consider reactive power flow, the L_p index record the highest value.

Most indices identified bus 30 as the weakest, except for the following indices (FVSI, VQI_{line} ,

VSI₂, and Lmn), which identified bus 26 as the weakest bus of all 33 kV transmission buses, as shown in Table 5.2.

While for of all 132 kV transmission buses, Some indices identified bus 3 as the weakest bus, while others identified bus 5 as the weakest bus, except for the index L_p, which exhibited a distinct behavior compared to the other indices and considered bus 6 as the weakest bus.

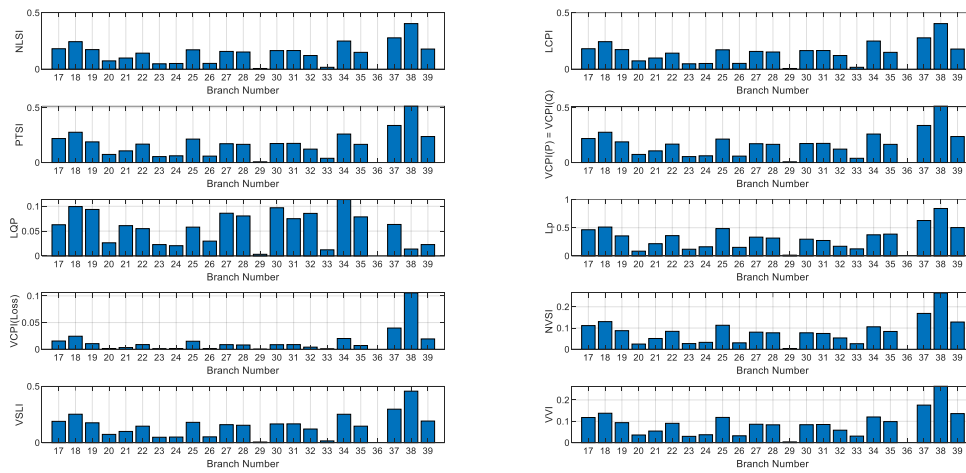


Figure 5.29 VSIs of 33 kV transmission lines for IEEE 30-bus network under heavy PQ loading at all buses

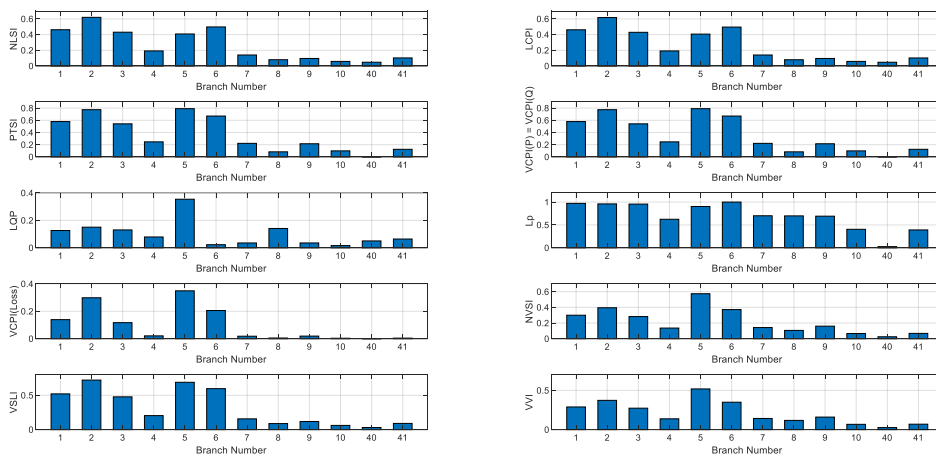


Figure 5.30 VSIs of 132 kV transmission lines for IEEE 30-bus network under heavy PQ loading at all buses

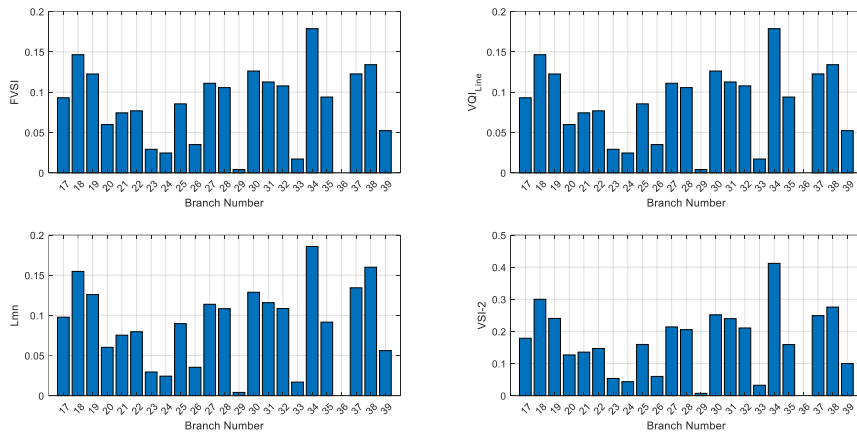


Figure 5.31 VSIs of 33 kV transmission lines for IEEE 30-bus network under heavy PQ loading at all buses

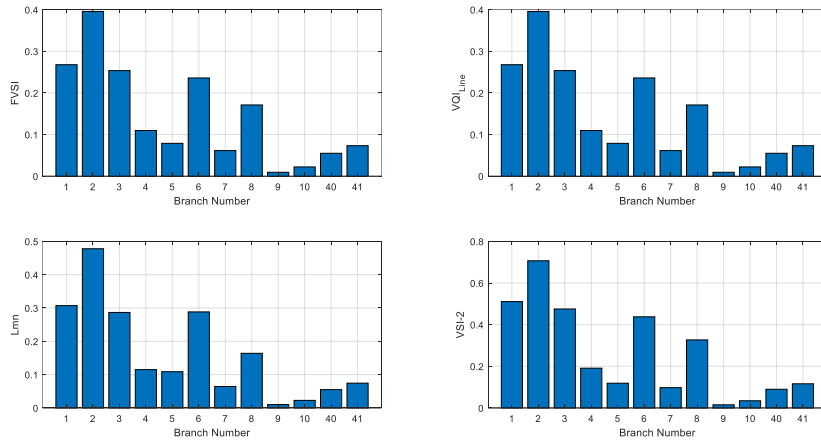


Figure 5.32 VSIs of 132 kV transmission lines for IEEE 30-bus network under heavy PQ loading at all buses

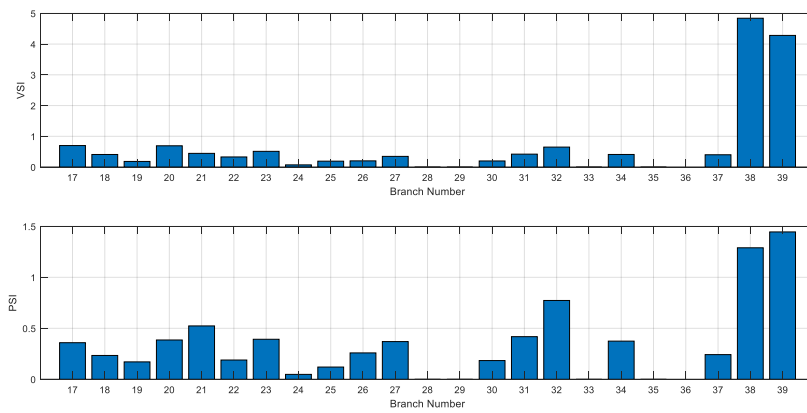


Figure 5.33 VSI and PSI of all 33 kV transmission lines for IEEE 30-bus network under heavy PQ loading

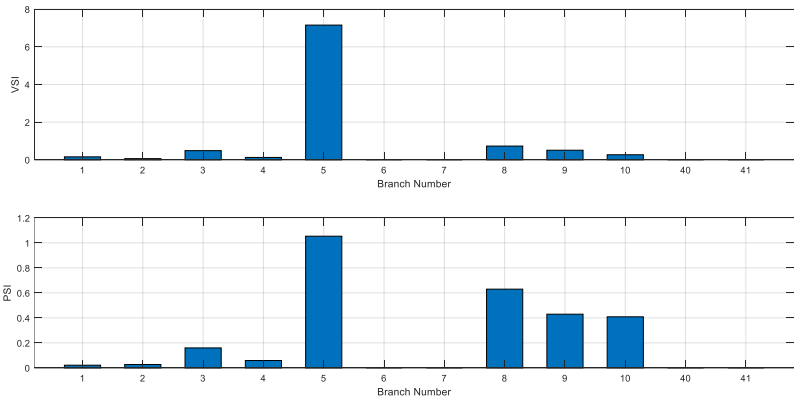


Figure 5.34 VSI and PSI of all 132 kV transmission lines for IEEE 30-bus network under heavy PQ loading

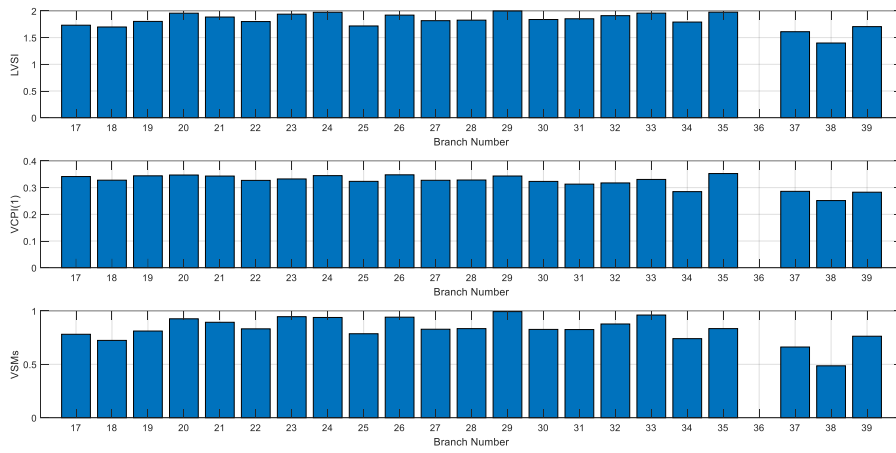


Figure 5.35 LVSI, VCPI(1), and VSMs of all 33 kV transmission lines for IEEE 30-bus under heavy PQ loading

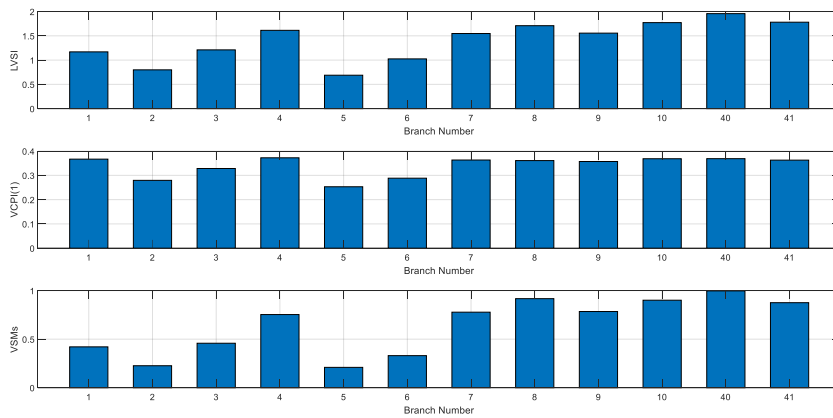


Figure 5.36 LVSI, VCPI(1), and VSMs of all 132 kV transmission lines in IEEE 30-bus under heavy PQ loading

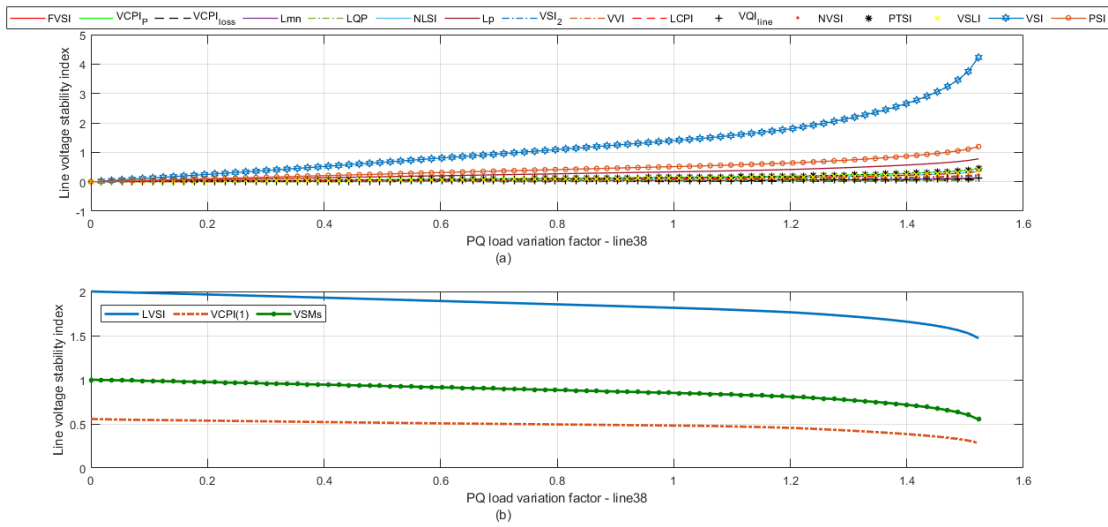


Figure 5.37 Values for different VSIs with respect to PQ loading for line 38 (27-30) in IEEE 30-bus system

The behavior of all voltage stability indices as the load varies from no-load to maximum loadability on critical line 38 is presented in Figure 5.37. It is noticeable that both the VSI and PSI indices are the faster in detecting the weak line, as they depend on both active and reactive load power.

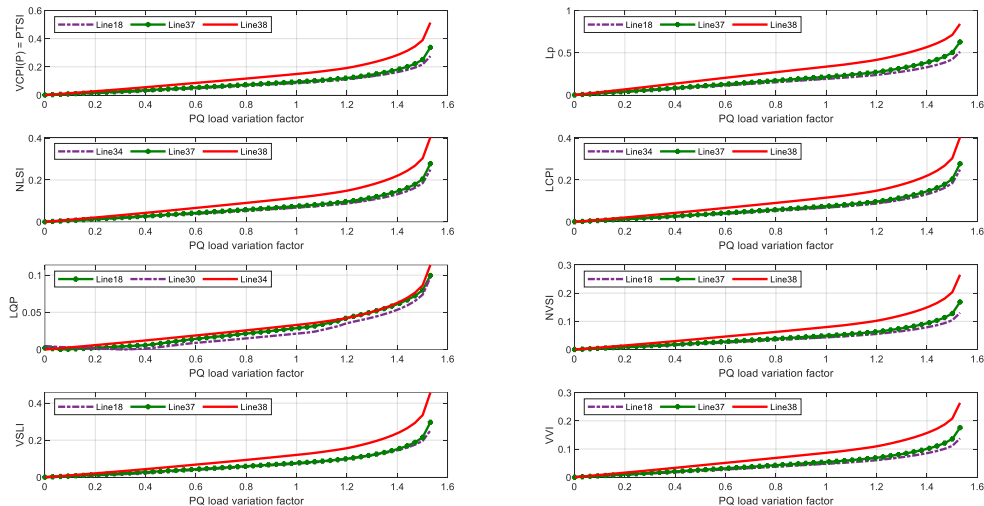


Figure 5.38 VSIs under PQ loading in IEEE 30-bus, top critical lines of all 33 kV transmission lines

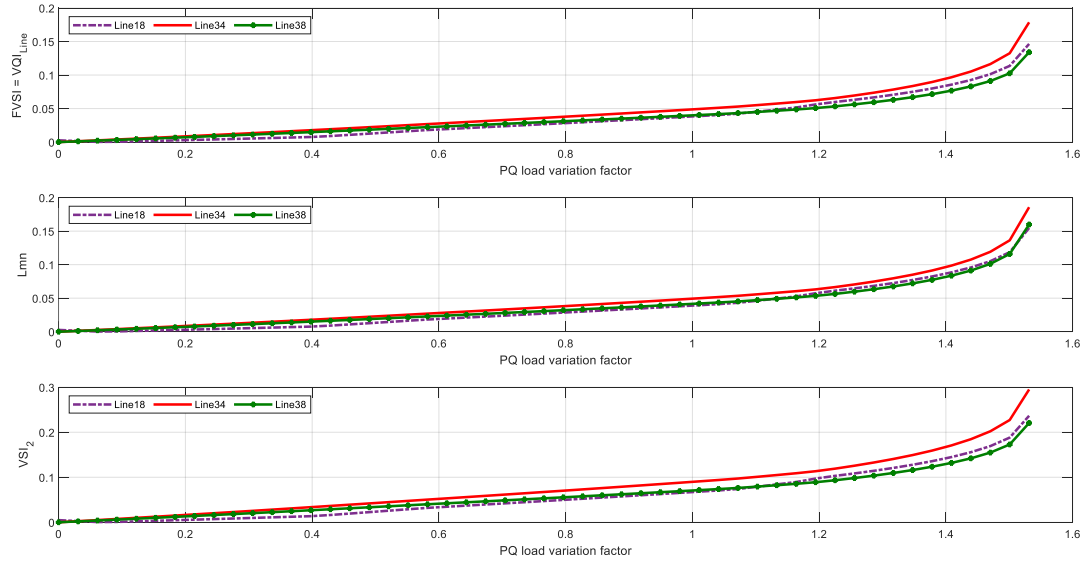


Figure 5.39 VSIs under PQ loading in IEEE 30-bus, top critical lines of all 33 kV transmission lines

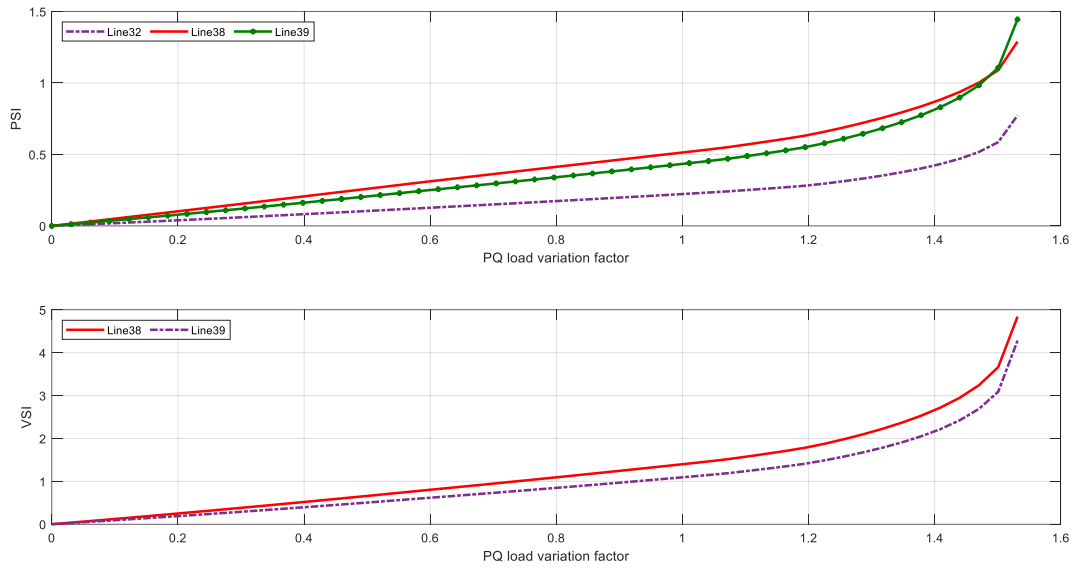


Figure 5.40 PSI & VSI under PQ loading in IEEE 30-bus, top critical lines of all 33 kV transmission lines

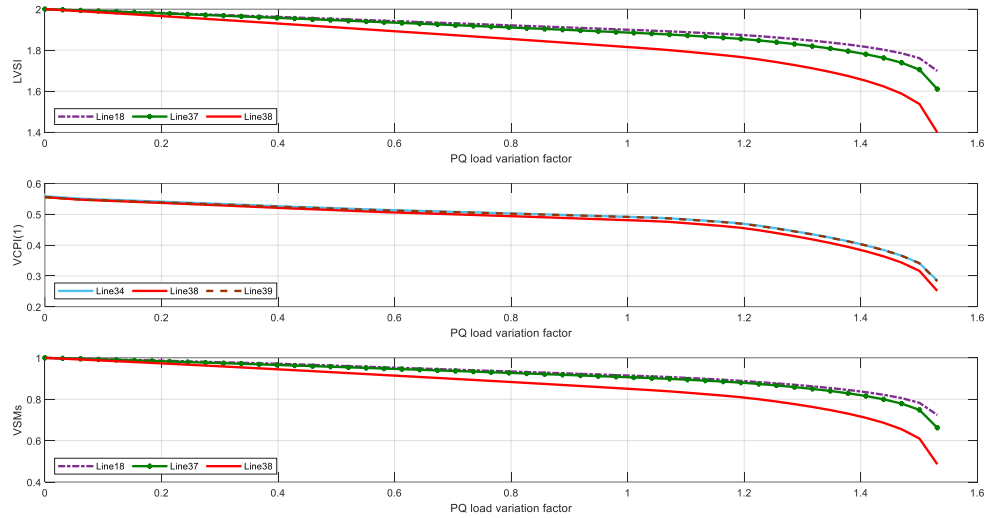


Figure 5.41 LVSI, VCPI(1), and VSMs under PQ loading in IEEE 30-bus, top critical lines of all 33 kV transmission lines

The behavior of each of the indices for the first three critical lines of all 33 kV transmission lines for the IEEE 30 bus system under heavy PQ loading is depicted in Figures 5.38 to 5.41. In Table 5.2, the top critical line for each index is summarized under PQ heavy loading conditions.

Table 5.2 The top critical line for each voltage stability index (ranking one) for PQ incremental loading at all buses.

Test system	IEEE 12-bus test system			IEEE 30-bus test system				
	11 kV transmission lines		33 kV transmission lines			132 kV transmission lines		
Critical Line	Line 4 Bus 4 to Bus 5	Line 8 Bus 8 to Bus 9	Line 34 Bus 25 to Bus 26	Line 38 Bus 27 to Bus 30	Line 39 Bus 29 to Bus 30	Line 2 Bus 1 to Bus 3	Line 5 Bus 2 to Bus 5	Line 6 Bus 2 to Bus 6
Index	LQP	FVSI = VQI_{line}	FVSI = VQI_{line}	NLSI	PSI	NLSI	PTSI = VCPI(P)	Lp
	NVSI	L_{mn}	L_{mn}	LCPI	-	LCPI	LQP	-
	-	VSI_2	VSI_2	PTSI = VCPI(P)	-	VSLI	VCPI(loss)	-
	-	NLSI	LQP	Lp	-	FVSI = VQI_{line}	NVSI	-
	-	PTSI = VCPI(P)	-	VCPI(loss)	-	L_{mn}	VVI	-
	-	Lp	-	NVSI	-	VSI_2	VSI	-
	-	VCPI(loss)	-	VSLI	-	-	PSI	-
	-	LCPI	-	VVI	-	-	LVSI	-
	-	VSLI	-	LVSI	-	-	VSM _s	-
	-	VVI	-	VSM _s	-	-	VCPI(1)	-
	-	LVSI	-	VCPI(1)	-	-	-	-
	-	VSM _s	-	VSI	-	-	-	-
	-	VCPI(1)	-	-	-	-	-	-
	-	VSI	-	-	-	-	-	-
-	PSI	-	-	-	-	-	-	

Through analyzing previous cases in the system networks under study, we observe that there are indices whose values are equal, such as (FVSI, VQI_{line}), and (PTSI, VCPI(P)) and some indicators exhibit similar behaviour. Their values approach each other as (NLSI and LCPI). Moreover, voltage stability indices are affected by various factors and conditions within a power system based on their parameters.

Various factors and conditions within a power system can affect voltage stability indices. Some of the key factors that can influence these indices are Load Conditions, generation capacity, contingency events, and transmission and distribution Network; the characteristics and configuration of the transmission and distribution network can influence voltage stability. Factors include line impedance, the voltage at sending and receiving end, active and reactive power flow, the angle difference between the sending and receiving voltage bus, and load and line angle.

5.6 PV and QV Curve

This section studies P-V and Q-V Analysis for the two test systems using Continuation Load Flow (CLF) analysis methods. Two independent studies are associated with Continuation Load Flow; the result of those studies gives the P-V and Q-V analysis curves. The analysis of the P-V curve is one common application to plot the voltage at a particular bus as the load is varied from the base case to a loadability limit. While the Reactive Power-Voltage (Q-V) curve analysis can define the reactive power margin, the study shows how variations in reactive power affect the voltage in the system.

In this section, The load value (P and Q) will be gradually changed at a step value of 0.01 on all buses while maintaining a constant power factor value, then plot P-V and Q-V curves for all buses. If the system under study has both load buses (buses with load directly connected) and non-load buses (buses without directly connected load). In that case, the “Load Variation” will uniformly vary the loads in load buses, while non-load buses will not be involved in load variation.

A. IEEE 12-Bus Test Network

Figure 5.42 plots the maximum power transfer "Active Power" (P-V) curves for voltage at all buses in the system. The load increases step by step, and after each successful power flow solution, the load is increased by the next increment. If a power flow solution fails, the last successful solution for that scenario is applied, and the process concludes after finding the maximum power transfer or maximum loadability. Figure 5.42 notes that the maximum loadability for bus 5 is 159 kW, bus 8 is 238 kW, and for bus 9 it is 212 kW. The Voltage Stability Margin (VSM) or ΔP values are $\Delta P = 129$ kW, $\Delta P = 193$ kW, and $\Delta P = 172$ kW, respectively. Moreover, the bus that has maximum loadability is bus 2.

Figure 5.43 plots maximum power transfer "Reactive Power" (Q-V) curves for voltage at all

buses in the system. and uses the Continuation Load Flow method to get the V and Q points for V-Q curves.

The part where $Q_{injection} < 0$ represents an increase in MVAR load. The bottom of the curve represents the maximum increase in the load MVAR (MVAR Margin) at this bus.

The process concludes after finding the maximum power transfer. Figure 5.43 shows that the maximum power transfer for bus 5 is 162kVAR, bus 8 is 251 kVAR, and bus 9 is 172 kVAR.

Bus 2 has the maximum kVAR margin.

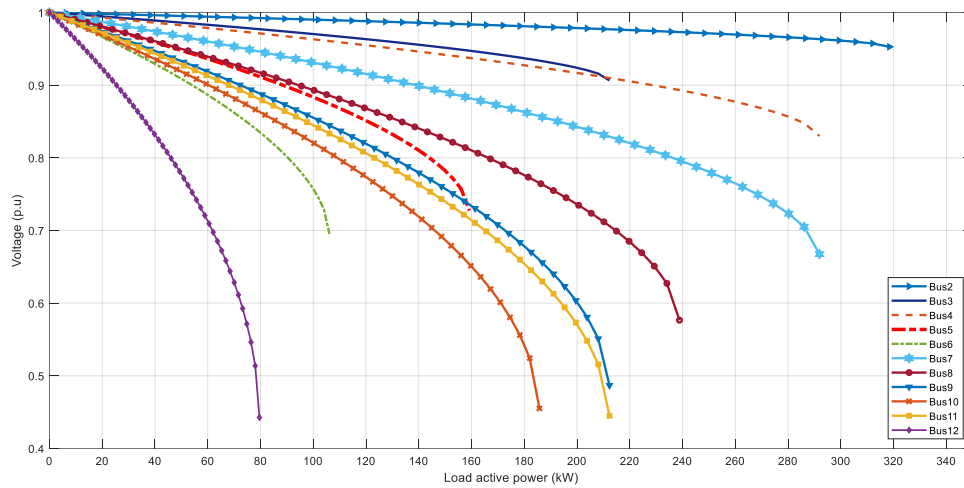


Figure 5.42 P-V curve of a load bus in the IEEE 12-bus

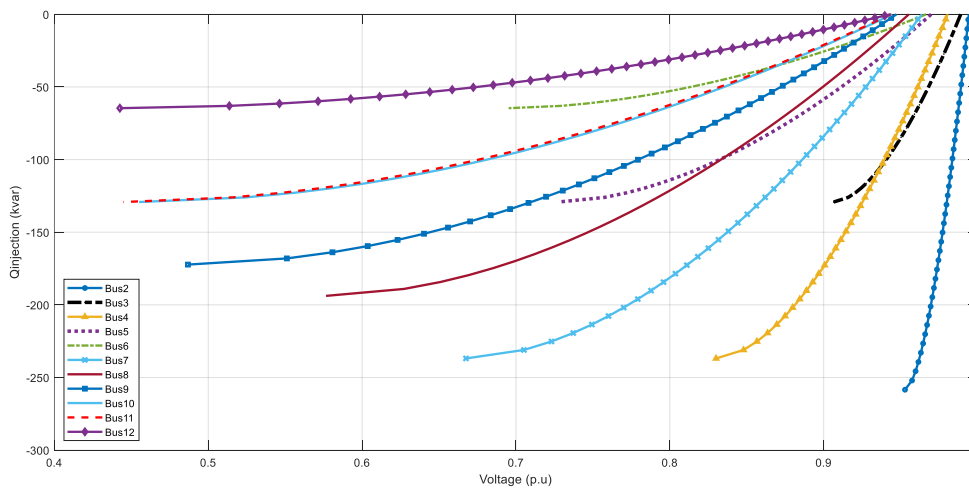


Figure 5.43 Q-V curve of a load bus in the IEEE 12-bus

B. IEEE 30-Bus Test Network

Only the P-V and Q-V analysis results were obtained for all the 33kV and 132kV buses.

During the analysis, it was observed that certain buses in the IEEE 30-bus system were not loaded. Therefore, buses without a directly-connected load will be excluded from the study.

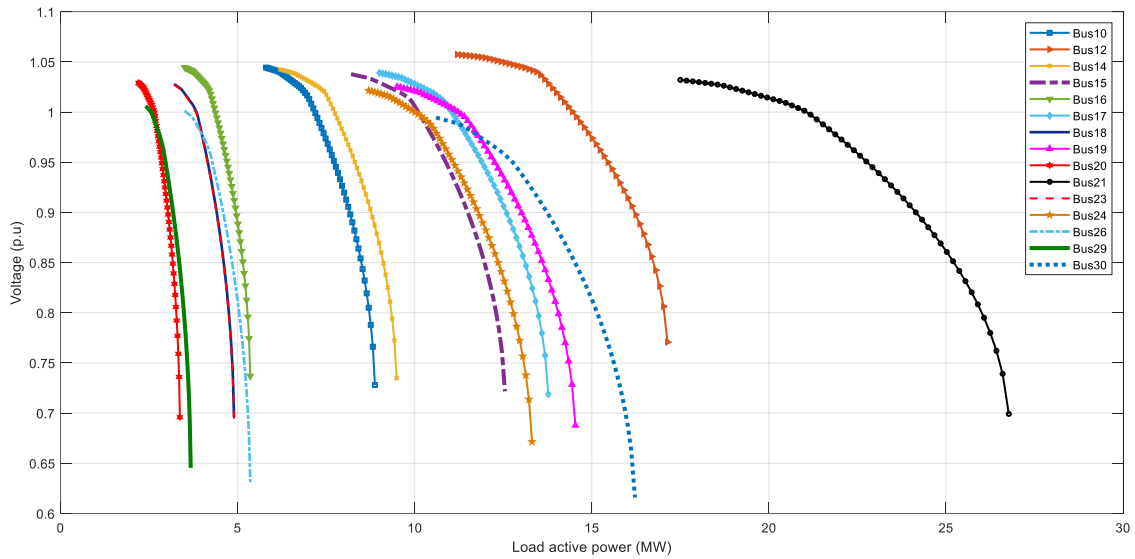


Figure 5.44 P-V curve of all 33 kV buses for IEEE 30-bus.

Figures 5.44 and 5.45 show the P-V and Q-V curves of all 33 kV buses, respectively. Bus 21 has the maximum loadability in terms of both active and reactive power. Figures 5.46 and 5.47 show the P-V and Q-V curves of all 132 kV buses, respectively. These figures show that bus 5 has the maximum active power loadability, while bus 8 has the maximum reactive power loadability.

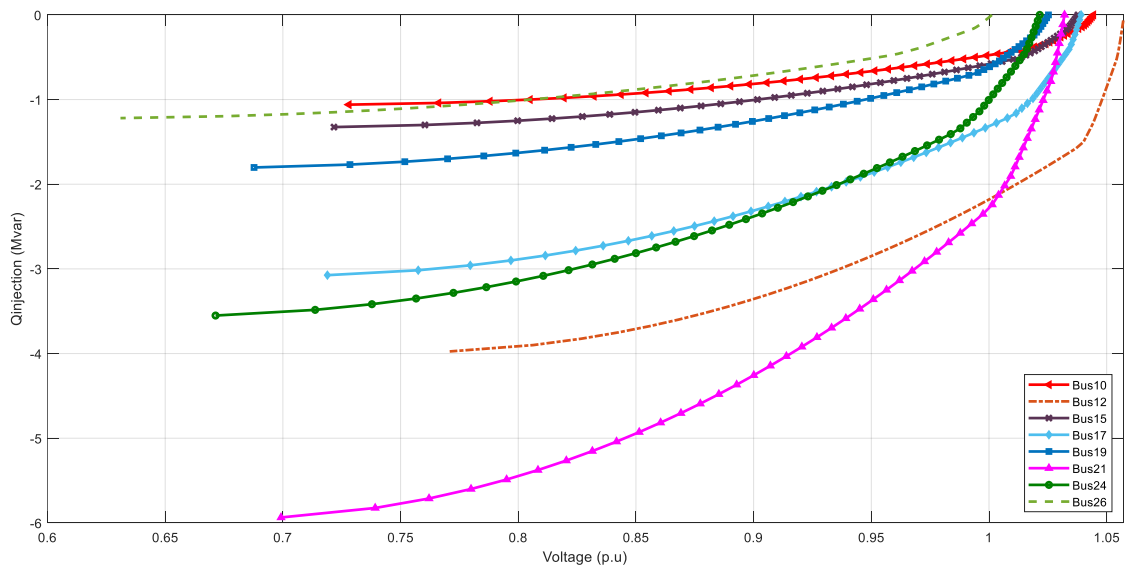
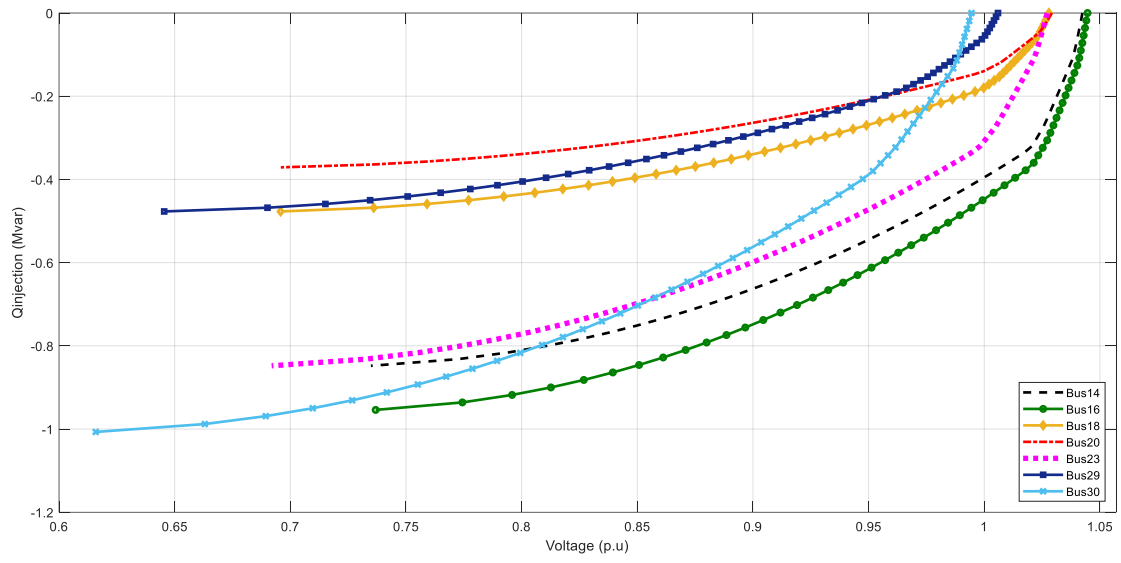


Figure 5.45 Q-V curve of all 33 kV buses for IEEE 30-bus.

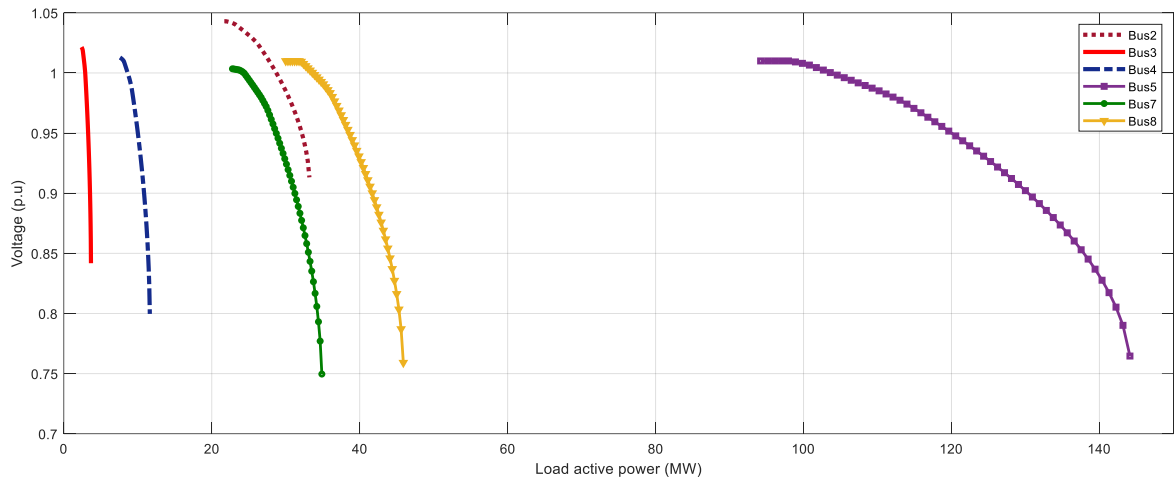


Figure 5.46 P-V curve of all 132 kV buses for IEEE 30-bus.

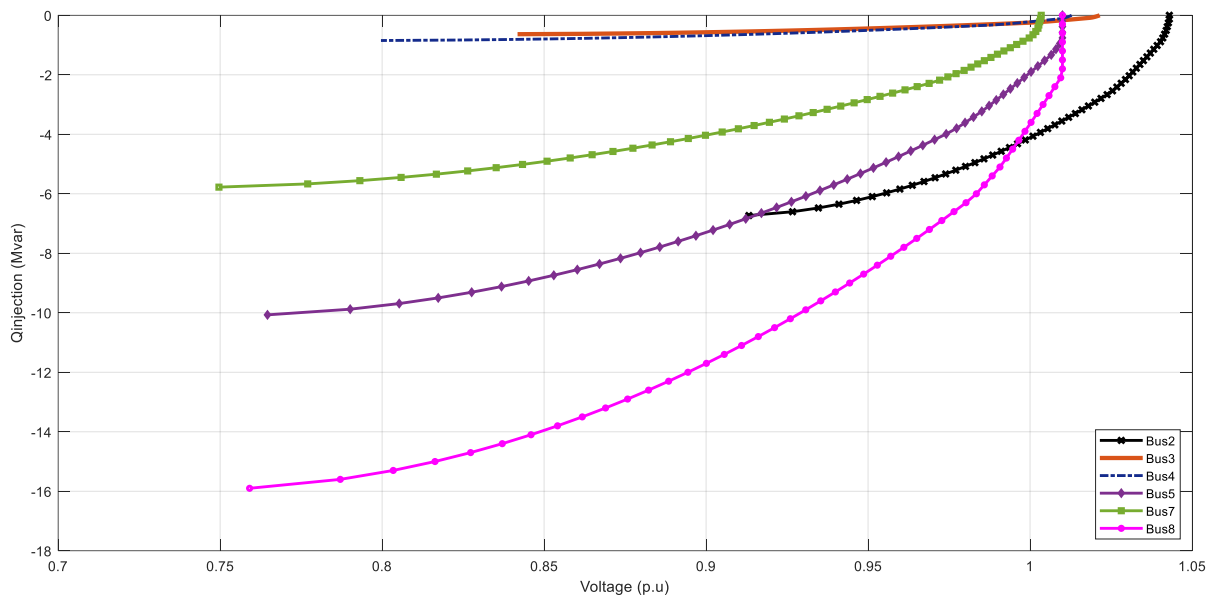


Figure 5.47 Q-V curve of all 132 kV buses for IEEE 30-bus.

CHAPTER 6: Optimal Placement of Distributed Generation (DG) Based on Voltage Stability Indices

6.1 Introduction

In recent years, renewable energy-based Distributed Generation (DG) has rapidly developed worldwide. This is due to the promising potential of renewable energy in reducing the proportion of fossil fuel consumption in electricity production, as well as mitigating power losses and harmful carbon emissions. Integration of DG in the distribution network provides benefits such as relief in transmission and distribution capacity, enhancement in voltage stability, power quality, and system reliability to both electricity end users and providers [87]. The placement of DG plays a crucial role in maximizing the utilization of its generated power. Proper DG placement can improve voltage stability margins, minimize power losses, and enhance voltage profile. The optimal placement of wind DG integration was analyzed from the perspectives of voltage stability, voltage profile, and total system losses [88]. The voltage stability of transmission networks with wind energy source integration is investigated using P-V and P-Q curves [89]. The provision of reactive power support from DG sources exhibits substantial variation depending on the type of DG units, so it can adversely affect the voltage stability of a significant portion of the network. An investigation is presented that examines the selection of the optimal type of DG unit from various types and its ideal placement, which can promote voltage stability in the distribution network while concurrently improving the voltage profile [90]. Several studies have been carried out to achieve an optimum location and size of DG; some of the studies depended on VSIs in DG placement and sizing problems. The efficacy of various voltage stability indices was assessed in the optimal utilization of DG units within specified limitations and constraints [91].

A novel index-based algorithm was presented for determining the placement and sizing of DG in distribution systems [78][79].

This chapter discusses the use of Voltage Stability Indices (VSIs) proposed in the literature for voltage stability assessment, placement and sizing of Distributed Generation (DG), detecting weak lines and buses, and triggering countermeasures against voltage instability.

6.2 Types and Sizing of DG

DG can be categorized into four main categories based on their terminal characteristics regarding their ability to deliver real and reactive power, which are as follows [91], [92] :

- 1) Type 1: DG capable of injecting both P and Q.
- 2) Type 2: DG capable of injecting P but consuming Q.
- 3) Type 3: DG capable of injecting P only.
- 4) Type 4: DG capable of injecting Q only.

DG units based on synchronous machines fall in Type 1. Type 2 mainly consists of induction generators commonly used in wind farms. Photovoltaic, microturbines, and fuel cells, integrated into the main grid with the help of converters/inverters, are good examples of Type 3; synchronous compensators serve as prime examples of Type 4.

This thesis has considered and analyzed the four main types comprehensively.

The reactive power output of DG can be represented in (6.1), as given.

$$a = (\text{sign}) \tan(\cos^{-1}(PF_{DGi}))$$

$$Q_{DGi} = a P_{DGi} \tag{6.1}$$

In which,

sign = +1: DG injecting reactive power.

sign = -1: DG consuming reactive power.

PF_{DG} is the power factor of DG.

At bus i , where the DG is located, the active and reactive power injections are quantified by equations (6.2) and (6.3), respectively [92], [93].

$$P_i = P_{DG_i} - P_{Di} \quad (6.2)$$

$$Q_i = Q_{DG_i} - Q_{Di} = aP_{DG_i} - Q_{Di} \quad (6.3)$$

The power factor of a Distributed Generator (DG) is affected by both its operating conditions and type. the PF_{DG} and the (a) Parameters for the major Types of DG can be found in the following way:

- 1) *Type 1*: $0 < PF_{DG} < 1$, **sign** = +1 and "**a**" is a constant,
- 2) *Type 2*: $0 < PF_{DG} < 1$, **sign** = -1 and "**a**" is a constant,
- 3) *Type 3*: power factor is at unity, **PF_{DG}** = 1, **a** = 0.
- 4) *Type 4*: **PF_{DG}** = 0 and **a** = ∞ .

optimal power factor:

To minimize the total power losses, the operating power factor of the distributed generator DG (PF_{DG}) should be equivalent to the power factor of the collective load (PF_D) on the feeder [94]. This ensures maximum efficiency and reduces the power lost in the transmission process.

$$PF_D = P_D/S_D \quad (6.4)$$

$$PF_{DG} = PF_D \quad (6.5)$$

sizing and limits of DG:

The optimal location and sizing of Distributed Generators (DGs) can enhance the voltage profile and minimize power losses in an electrical network. A Penetration Level (PL) parameter has been established to examine the impact of DG capacity on the system performance, a Penetration Level (PL) parameter has been established. This parameter is defined as the ratio of the total complex power generated from DGs (S_{DG}) to the complex power peak load demand (S_{load}) and can be calculated as follows [93]:

$$PL = \frac{\sum S_{DG}}{\sum S_{Load}} * 100\% \quad (6.6)$$

In this thesis, the capacity of DG units is changed to provide different penetration levels. The results are evaluated based on the best penetration level that reduces active power loss and enhances the voltage profile..

Bus voltage constraints at each Bus:

When injecting Distributed Generators (DGs) into the system, it is crucial to ensure that the voltage level remains within the acceptable upper and lower limit range:

$$|V_{i,min}| \leq |V_i| \leq |V_{i,max}| \quad (6.7)$$

$$0.95 \text{ p.u} \leq |V_i| \leq 1.05 \text{ p.u}$$

DG power generation constraints:

$$0 \leq S_{DG,i} \leq \sum S_{Load} \quad (6.8)$$

where, $S_{DG,i}$ is the apparent power generation and $\sum S_{Load}$ is apparent power load connected to the system.

In addition to reducing power losses and improving voltage profiles, Integrating DG units into the power systems has many benefits improving load factors, grid reinforcement, deferring or eliminating system upgrades, reducing on-peak operating costs, and improving system integrity, reliability, and efficiency [95].

6.3 VSIs in DG Placement

In the initial stage of the process, the potential sites for deploying DG units are selected based on Voltage Stability Indices (VSIs). A majority of VSIs, capable of identifying weak buses and lines, can be utilized in this step. The optimal placement of DG units is then determined in the subsequent stage by solving an optimization problem that aims to minimize power losses, improve voltage profile, and maximize Voltage Stability Margin (VSM). Using more accurate

VSI values can lead to better locations for DG units. However, it should be noted that utilizing complex VSIs increases the computational time of the optimization problem, especially in large power systems. Therefore, an accurate and simple VSI must be used in DG placement and sizing problems.

6.4 Simulation Results and Evaluation

Based on the Voltage Stability Indices (VSIs) studied in chapter four and the results obtained from the first scenario in chapter five, the top three critical lines were identified in each network in Table 5.1. Identifying these critical lines is the first step to determining the location for the penetration of DG units.

Voltage Stability Indices (VSIs) values are calculated for each line in the network and sorted in descending order. The DG unit should be placed on the j-bus of line i-j, which has the highest Voltage Stability Index (VSI) value. For multiple DG unit placements, the placement of the second DG unit is determined based on the impact of the first DG unit on the VSIs. The VSI values for each line are then re-calculated and re-sorted in the same manner, from the highest to the lowest value. The location for the second DG unit will be placed at the end of the line having the highest value of VSIs.

6.4.1 IEEE 12-Bus Test Network

A. Optimal Placement and Sizing of DG Based on VSIs and Total Active Power Losses.

According to the proposed Voltage Stability Index (VSI) approach, the base case IEEE 12-bus system analysis reveals that the top three critical lines are line 4, line 7, and line 8. In order to address these critical areas, the DG types, respectively, are placed on bus 5, bus 8, and bus 9. By gradually changing the sizes of the DG in small steps, the apparent power produced by the DG can vary from 0% to 100% of the total apparent power load. During this process, it is

essential to consider the limitations related to generation and voltage, as indicated in equations (6.7) and (6.8).

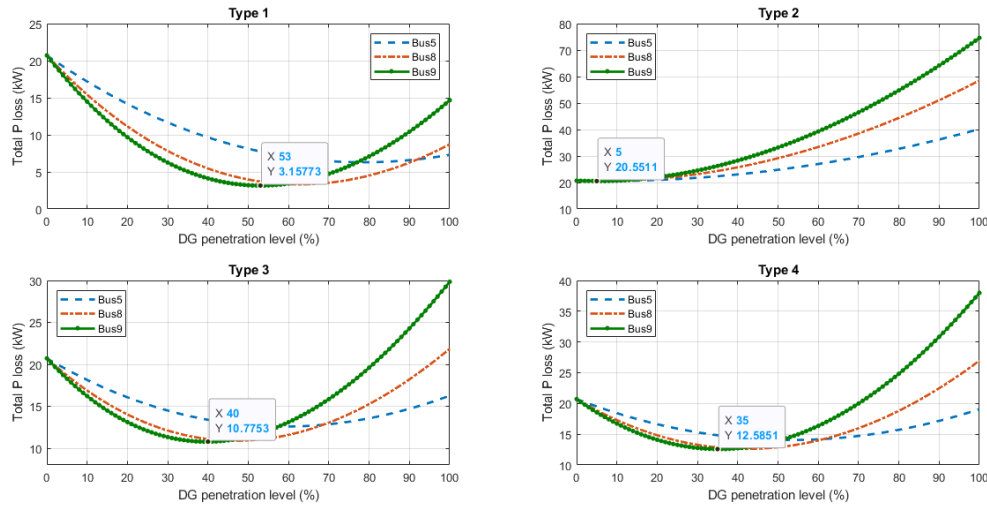


Figure 6.1 Active power losses vs. PL for different DG types

The empirical relationship between the size of a DG unit and the resultant losses exhibits a parabolic curve, characterized by decreases at first and then start increases. The DG size estimate's accuracy depends upon the selected step size. The current study maintains a step size of 1% of the total load demand. However, decreasing step size may improve precision and substantially increase computational time.

Determine the optimal location and size of DG to achieve minimum network losses.

The base kVA and kV of the IEEE 12-bus test system are: $(\text{kVA})_{\text{Base}} = 1 \text{ kVA}$, $(\text{kV})_{\text{Base}} = 11 \text{ kV}$. For 12 bus systems without installation of DG, active and reactive power losses are 20.71353 kW and 8.041039 kVAR, respectively. Real and reactive power from the substation is 455.7135 kW and 413.041 kVAR, respectively.

Following the installation of various types of DG, it was observed that bus 9, where a type 1 DG capable of injecting both real and reactive power was utilized, exhibited the lowest active power loss. This finding is depicted in Figure 6.1.

Where the total active power loss is obtained minimum at bus 9 with injection type1 DG with penetration level 53% (230.55 kW and 214.65 kVAR at 0.732 lagging power factor), the active and reactive power losses are 3.158 kW and 1.11 kVAR, respectively. Also, real and reactive power delivered from the substation reduces to 207.61 kW and 191.46 kVAR.

DG units injecting active power and reactive power injection at bus 9 can reduce power losses in the distribution system. By supplying local loads with active power, the DG units decrease the amount of power that needs to flow through the main grid and distribution lines. The power from the substation reduces to 207.61kW. This reduction in power flow leads to lower resistive losses in the lines, resulting in reduced overall power losses, where the active power losses decrease to 3.158 kW. Reactive power Injection can also help reduce power losses. Reactive power injection reduces the amount of reactive power that needs to be supplied by the main grid and decreases the reactive power flow in the distribution lines; reactive power delivered from the substation reduces 191.46 kVAR. As a result, the reactive power losses in the lines are reduced, leading to a decrease in overall power losses, where the reactive power losses decrease to 1.11 kVAR.

Moreover, when DG units inject active and reactive power, they can improve the power factor at bus 9. The power factor is “the ratio of active power to apparent power” and represents the efficiency of power utilization. By injecting reactive power, the DG units compensate for the reactive power demand of the load, which improves the power factor. This results in a higher power factor, which reduces losses and improves the system's overall efficiency.

B. Effect of DG on Voltage Profile

The injection of active and reactive power by DG units affects the voltage profile, which, in turn, influences the power losses. When DG units inject power, they can help maintain the voltage magnitude at the bus closer to its nominal value. This reduces the voltage drop along the distribution lines, subsequently reducing resistive losses and improving the system's overall efficiency.

The V_{\min} of 0.943p.u for the base case was obtained at bus 12. The data depicted in Figure 6.2 reveals enhancement in the voltage profile for all three buses with the integration of Type I DG. However, comparative analysis indicates that the injection of DG at buses 8 and 9 results in a more substantial improvement in voltage than bus 5. The minimum bus voltage is increased from 0.943p.u. to 0.974531873p.u., 0.988574989p.u., and 0.995516652p.u. with the installation of type 1 DG at the 5th, 8th, and 9th bus respectively, as shown in Table 6.2 the minimum voltage occurs at bus 7 with value 0.991p.u when injecting DG Type I at bus 9.

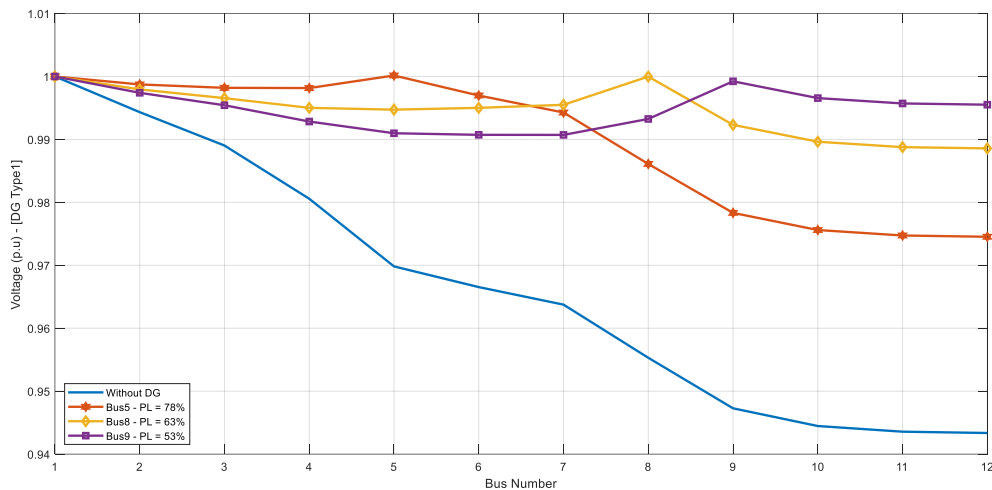


Figure 6.2 Voltage profile of each bus in the IEEE 12-bus system – (Type I DG injection at bus 5,8,9).

Figure 6.3 shows the voltage profile of various Distributed Generation (DG) types injected at bus 9, with the optimum size for each type. The findings show that all DG types improve the

voltage profile. However, DG types 1 and 3 exhibit more voltage enhancement than the other two types. Figure 6.4 clearly illustrates the positive impact of DG integration on the voltage profile for all DG types at different Penetration Levels (PL). Type 1 and type 3 DGs outperform the other types in terms of voltage improvement. Additionally, Figure 6.4 shows that an increase in DG penetration levels leads to greater voltage profile enhancement.

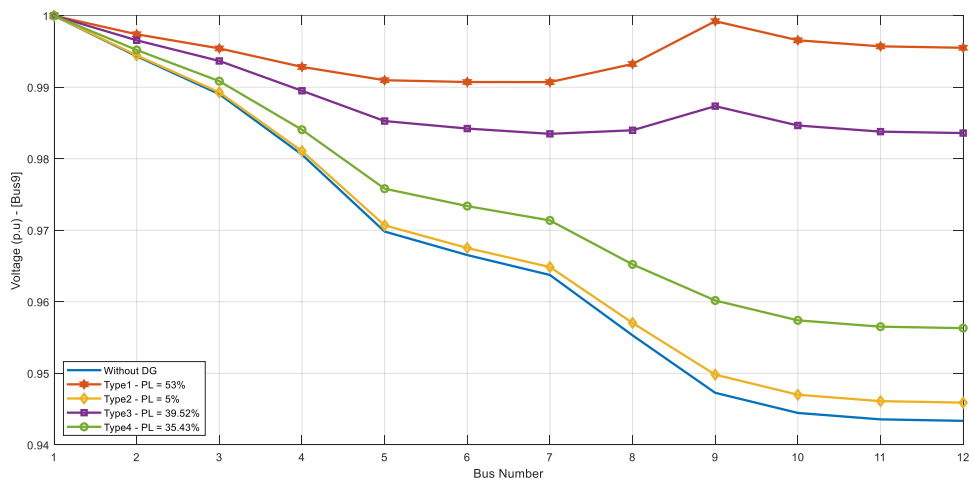


Figure 6.3 Voltage profile of each bus in the IEEE 12-bus system – (optimum PL% for each Type of DG at 9)

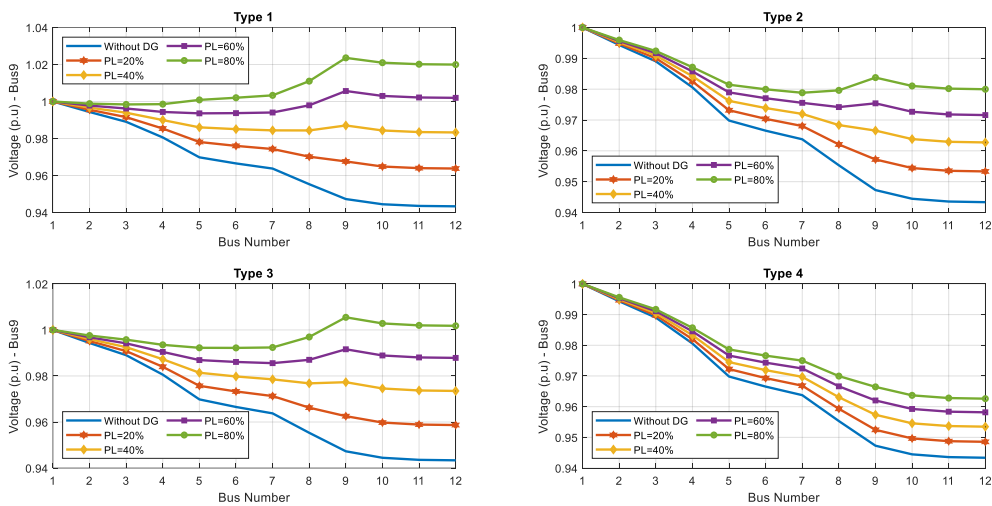


Figure 6.4 Voltage profile of each bus in the IEEE 12-bus - (different DG types vs. different penetration levels)

Table 6.1 summarizes the results of integrating different types of distributed generators (DGs) at bus 9, while Table 6.2 summarizes the results of the penetration of type 1 distributed generators at different buses (buses 5, 8, and 9).

Table 6.1 Results of IEEE 12-Bus System.

	Without DG	With Type I DG (kVA) at 0.732 PF lag & PL = 53%	With Type II DG (kVA) at -0.999 PF lead & PL = 73%	With Type III DG (kW) & PL = 39.5%	With Type IV DG (kVAR) & PL = 35.43%
DG location	-	9	9	9	9
DG size	-	315	435	234.89	210.58
TLP (kW)	20.714	3.158	17.2352	10.774	12.584
TLQ (kVAR)	8.04	1.11	6.02	4.13	4.82
V_{min}	0.943 @ bus 12	0.991 @ bus 7	0.996 @ bus 4	0.983 @ bus 7	0.956 @ bus 12

Table 6.2 Comparison of results with Type I DG injection at different buses.

	With Type I DG (kVA) at 0.732 PF & PL = 78%	With Type I DG (kVA) at 0.732 PF & PL = 63%	With Type I DG (kVA) at 0.732 PF & PL = 53%
DG location	5	8	9
DG size	463.6	374.4	315
TLP (kW)	6.301	3.318	3.158
TLQ (kVAR)	2.07	1.04	1.11
V_{min}	0.975 @ bus 12	0.989 @ bus 12	0.991 @ bus 7

C. Impact of DG on Voltage Stability Margin (VSM)

The impact of different Distributed Generation (DG) types and their varying penetration levels on Voltage Stability Margin (VSM) at bus 9 was studied by performing power flow analysis on test distribution networks. The P-V and Q-V curves for the DG types were plotted and analyzed to determine the effect of DG installation on VSM.

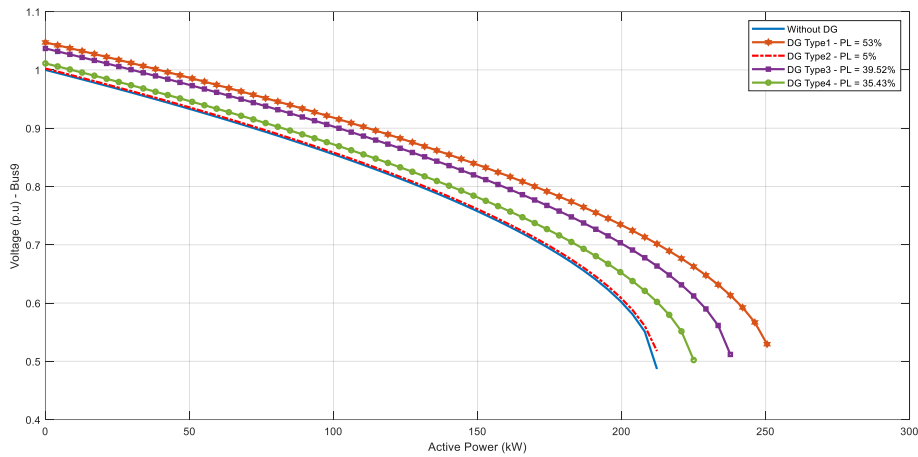


Figure 6.5 P-V curves at bus 9 for different DG types vs. optimum (PL%) for each type

Figures 6.5 and 6.6 show the P-V and Q-V curves for the four types of Distributed Generators (DGs). These curves illustrate the improvement in Voltage Stability Margin (VSM) achieved after DG installation for all types considered in this study. DG types 1 and 3 exhibit more VSM enhancement than the other two types.

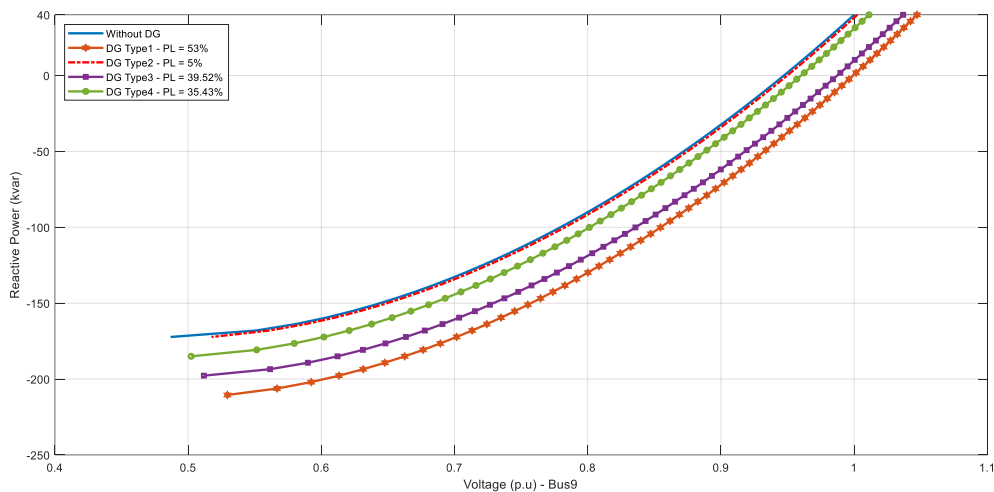


Figure 6.6 Q-V curves at bus 9 for different DG types vs. optimum (PL%) for each type

To further examine the influence of DG penetration level on the P-V and Q-V curves, type 1 DG was plotted at various penetration levels and presented in Figures 6.7 to 6.8. The results show a direct correlation between DG penetration level and VSM improvement. In other words,

as the DG penetration level increases, the VSM improvement also increases correspondingly. Installing DGs at optimal locations and sizes effectively increases the system capacity and loadability, thereby ensuring the stability and security of power system operations.

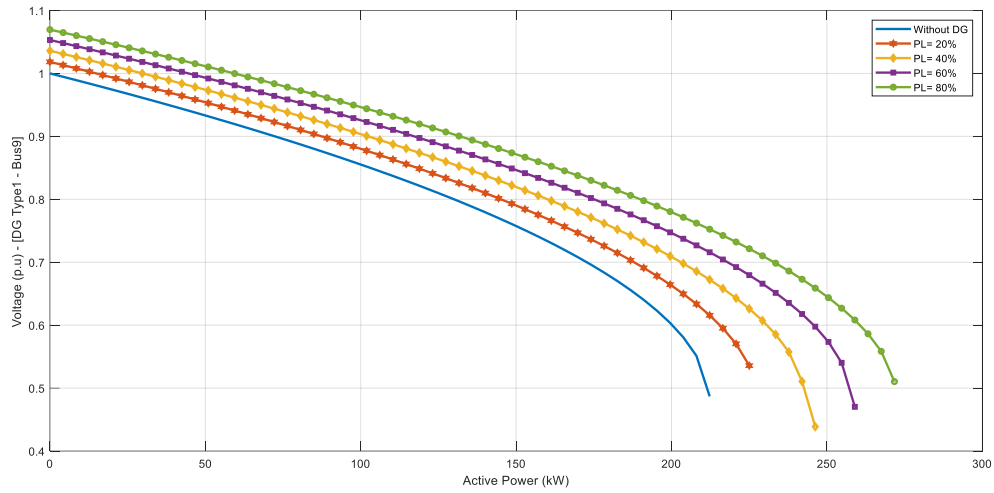


Figure 6.7 P-V curves at bus 9 for different penetration level-type 1 DG

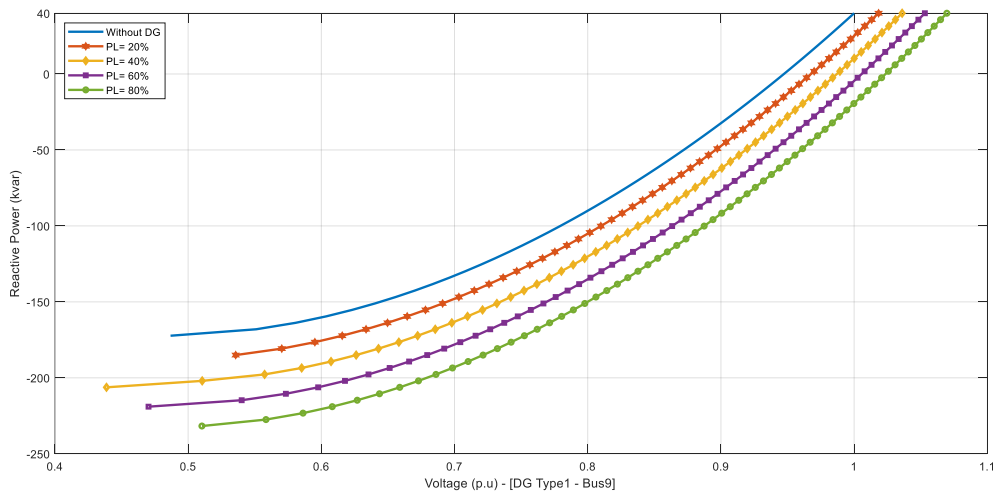


Figure 6.8 Q-V curves at bus 9 for different penetration level- type 1 DG

D. Impact of DG on Voltage Stability Indices (VSIs)

The voltage stability indices values exhibited an apparent decrement across all lines values upon the injection of distributed generation at bus 9. as clear from Figure 6.9 and Figure 6.11, and indices in Figure 6.10 exhibited increment across all lines values trending towards stability values. However, in the context of voltage stability analysis, a lower value of voltage stability indices and its deviation from critical values typically indicates a more stable system.

Where the DG penetration can also have a positive impact on voltage stability indices, when properly integrated and controlled, DGs can provide local voltage support, enhance voltage regulation, and improve system stability.

Therefore, the observed decrease in voltage stability indices values after the injection of Type 1 of DG at bus 9 is a positive outcome as it indicates an improvement in the voltage stability of the network. This is due to the added reactive power support and improved voltage regulation provided by the DG system, which enhances the overall voltage stability of the network.

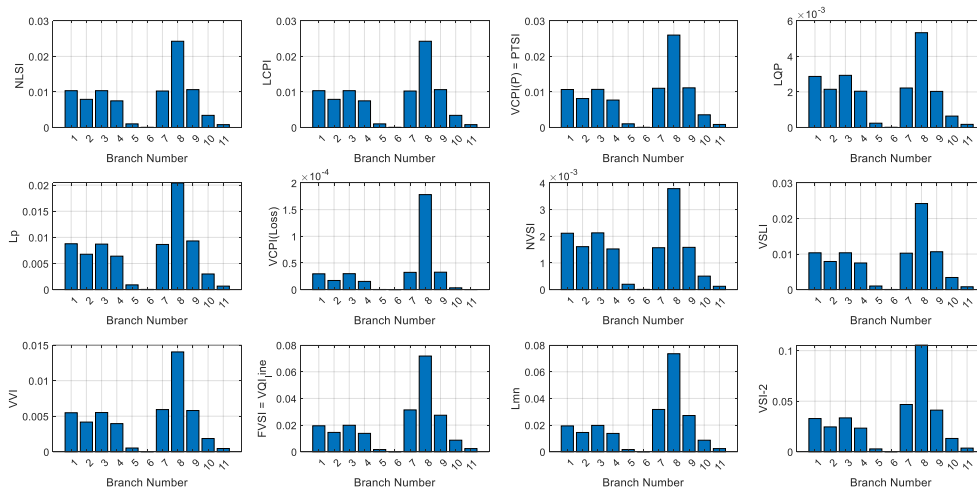


Figure 6.9 VSIs of each lines for IEEE 12-bus under injection DG(Type1at bus 9, size = 230.55 + j214.65 kVA)

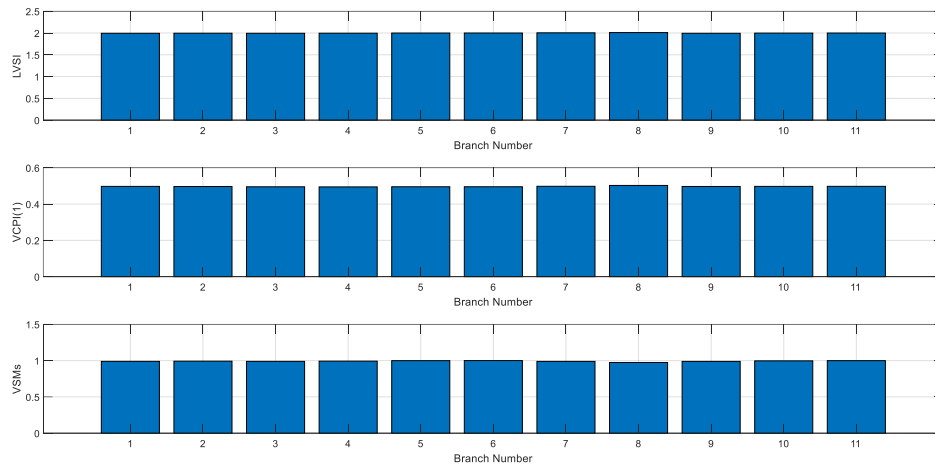


Figure 6.10 LVSI, VCPI(1),and VSMs of each lines for IEEE 12-bus under injection DG (Type 1 at bus 9, size = 230.55 + j214.65 KVA)

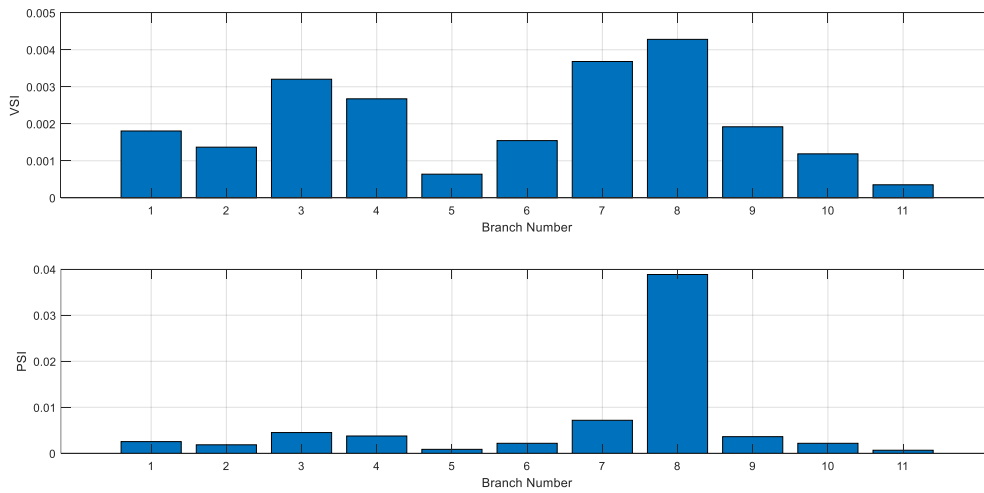


Figure 6.11 VSI and PSI of each lines for IEEE 12-bus under injection DG (Type 1 at bus 9, size = 230.55 + j214.65 KVA)

6.4.2 IEEE 33-Bus Test Network

A. Optimal Placement and Sizing of DG Based on VSIs and Total Active Power Losses.

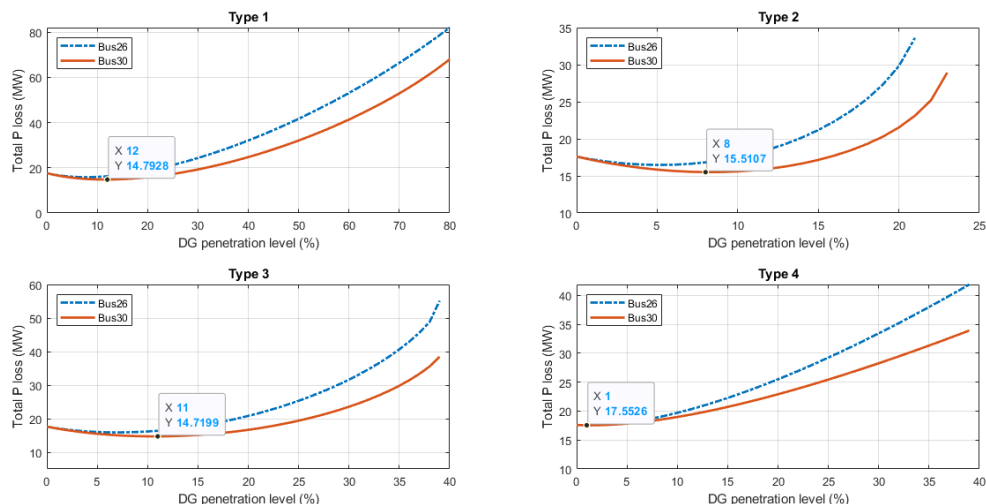


Figure 6.12 Active power losses vs. PL for different DG types of 33kV buses

The normal operating condition of the IEEE 30-bus test system, which was designed using specific parameters, is utilized and examined. Using the voltage stability indices and the maximum loadability limit (VSM) obtained from the previous chapter for all buses connected to the 33kV transmission line, the weak bus is identified. In this scenario, distributed generation (DG) is deployed at potential buses, and the optimal location of the DG is determined based on the Voltage Stability Indices (VSIs).

In this case, two weak buses were selected based on their VSIs values, as shown in Table 5.1. These buses were injected with different types of Distributed Generation (DG), and the system's behavior was observed. To determine the optimal location of the DG, the size of the DG was gradually increased in steps. The amount of apparent power from the DG changed from 0% to 100% of the total apparent power load. The current study maintained a step size of 1% of the total load demand, while considering the constraints of generation and voltage given in equations (6.7) and (6.8).

To determine the best location for Distributed Generation (DG) penetration into a network system, DG units were injected into different locations in the system to compare the power losses under the different locations. Two different locations were selected based on their Voltage Stability Index (VSI) values, as shown in Table 5.1. The buses 26 and 30 were selected, which means they are the weakest buses in the system. The power losses and the voltage profile in the overall network system were monitored to determine the best location for DG penetration.

The base MVA and kV of the IEEE 30 bus-test system are $(MVA)_{Base} = 100$ MVA, which operate at four different voltage levels: 132 kV, 33 kV, 11 kV, and 1 kV. For the system without installation of DG, active and reactive power losses are 17.599 MW and 22.24 MVAR, respectively, and the real power delivery from the substation is (261 MW) and absorbs reactive power (-17.02 MVAR).

Table 6.3 Results of IEEE 30-Bus System for bus 26.

	Base Case	With Type I DG (kVA) at 0.914 PF lag & PL = 8%	With Type II DG (kVA) at 0.914 PF lead & PL = 5%	With Type III DG (kW) & PL = 7%	With Type IV DG (kVAR) & PL = 1%
DG location	-	26	26	26	26
DG size	-	24.81	15.5	21.72	3.1
Gen. P (MW)	261	236.57	245.71	237.59	260.94
Gen. Q (MW)	-17.02	-13.96	-14.50	-13.60	-17.18
TLP (MW)	17.599	15.845	16.479	15.901	17.542
TLQ (MVAR)	22.24	11.29	15.82	12.09	21.96
V_{min}	0.995 @ bus 30	1.005 @ bus 7	0.985 @ bus 30	1.003 @ bus30	1.002 @ bus 30

When there is an excess of reactive power in a power system (-17.02 MVAR), the reactive power supplied by generators or capacitive elements and synchronous condensers is higher than the reactive power consumed by inductive loads. In other words, the system has more capacitive elements, generators, or synchronous condensers generating reactive power than the inductive elements. In the system, the reactive power provided by the generator, synchronous condensers, and the capacitive bank is (165.46 MVAR), While loads plus the loss in the system

consume only (148.44 MVAR); this leads to an excess in the reactive power of the system (-17.02 MVAR). Figure 6.12 and Tables 6.3 and 6.4 show that the minimum power losses occur when DG of types 1 and 3 is injected at bus 30.

Table 6.4 Results of IEEE 30-Bus System for bus 30.

	Base Case	With Type I DG (kVA) at 0.914 PF lag & PL = 12%	With Type II DG (kVA) at 0.914 PF lead & PL = 8%	With Type III DG (kW) & PL = 11%	With Type IV DG (kVAR) & PL = 1%
DG location	-	30	30	30	30
DG size	-	37.2	24.8	34.13	3.1
Gen. P (MW)	261	224.18	236.24	223.99	260.95
Gen. Q (MW)	-17.02	-12.08	-12.77	-11.29	-17.18
TLP (MW)	17.599	14.793	15.511	14.720	17.553
TLQ (MVAR)	22.24	7.57	12.51	7.87	21.98
V_{min}	0.995 @ bus 30	1.006 @ bus 7	0.981 @ bus 30	1.005 @ bus 7	1.004 @ bus 7

B. Effect of DG on Voltage Profile

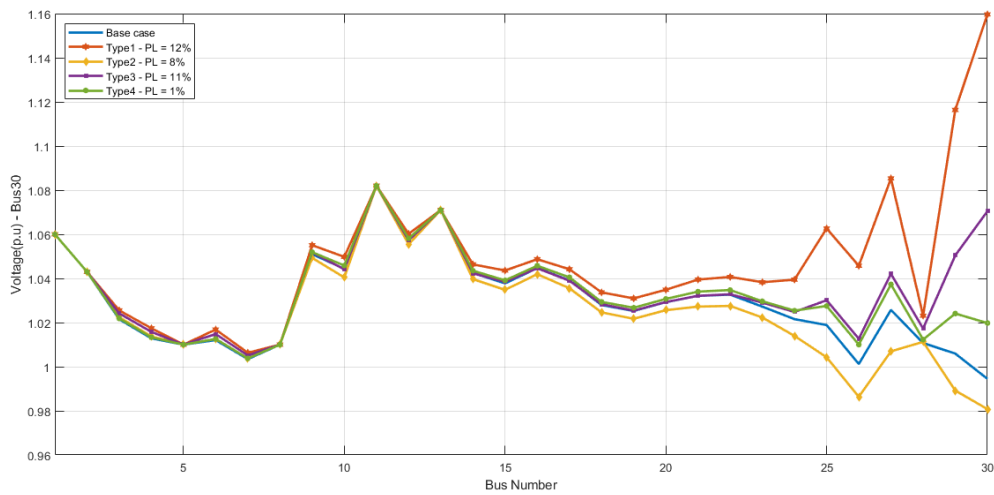


Figure 6.13 Voltage profile of each bus in the IEEE 30-bus – (optimum PL% for each Type of DG at bus 30)

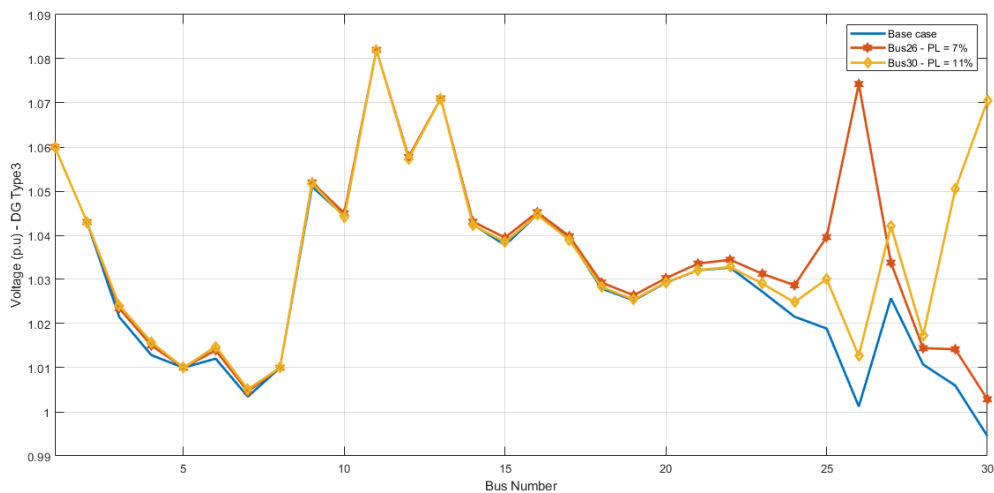


Figure 6.14 Voltage profile of each bus in the IEEE 30-bus system – (Type3 DG injection at bus 26,30)

The voltage profile is an important factor to consider when integrating DG into a power system. The voltage profile is the distribution of voltage levels throughout the system, and it is important to ensure that the voltage remains within acceptable limits .

Integrating DGs into a power system requires careful consideration of the voltage profile. During the planning phase, the system's voltage profile is thoroughly analyzed to ensure that the installation and connection of DGs maintain acceptable voltage levels and avoid voltage stability problems. As shown in Figure 6.14, the presence of DGs in the system, specifically when employing injection type 3 of DGs at bus 26 and 30 with optimal penetration levels, leads to noticeable enhancements in the voltage profile.

Figure 6.13 shows that injecting DG of types 3 and 4 with the optimal size improves the voltage within acceptable limits more than the other two types .

When DG of type 1 injects active and reactive power into bus No. 30, as shown in Figure 6.13: when DG injects active power (real power) into the system at bus No. 30, it acts as a generation source, increasing the total active power supply in the system. This increase in active power helps to meet the local demand and reduce the burden on other generators in the system. Consequently, the voltage at bus No. 30 and surrounding buses may rise slightly, but not excessively, assuming the system has sufficient reactive power support.

By injecting reactive power into the grid, the DG supplies additional reactive power that supports the voltage level. This tends to increase the voltage at bus No. 30 and helps to compensate for voltage drops caused by reactive power consumption in other parts of the system. However, if there is already sufficient reactive power support in the system, injecting more reactive power at bus No. 30 may lead to an exaggerated increase in voltage, as the system may become overvolted. Therefore, when a DG source injects active and reactive power into bus No. 30 of the IEEE 30 bus test system, it will cause a voltage rise at that bus.

On the other hand, when a DG source injects active power and consumes reactive power like type 2 of DG into bus No. 30 of the IEEE 30 bus test system, it will cause a voltage drop at that bus. The voltage drop will be more noticeable if the DG source consumes a large amount of reactive power; when the DG at bus No. 30 consumes reactive power (instead of injecting it), it acts as a reactive power load. This tends to reduce the voltage at bus No. 30 and surrounding buses since it creates a local demand for reactive power. Insufficient reactive power support from other sources in the system can lead to a significant voltage drop at bus No. 30.

Figure 6.15 shows how different types of DG affect the voltage profile of the network, which is an essential indicator of power quality and reliability. The voltage profile is the variation of the voltage magnitude along the network, and it should be maintained within acceptable limits.

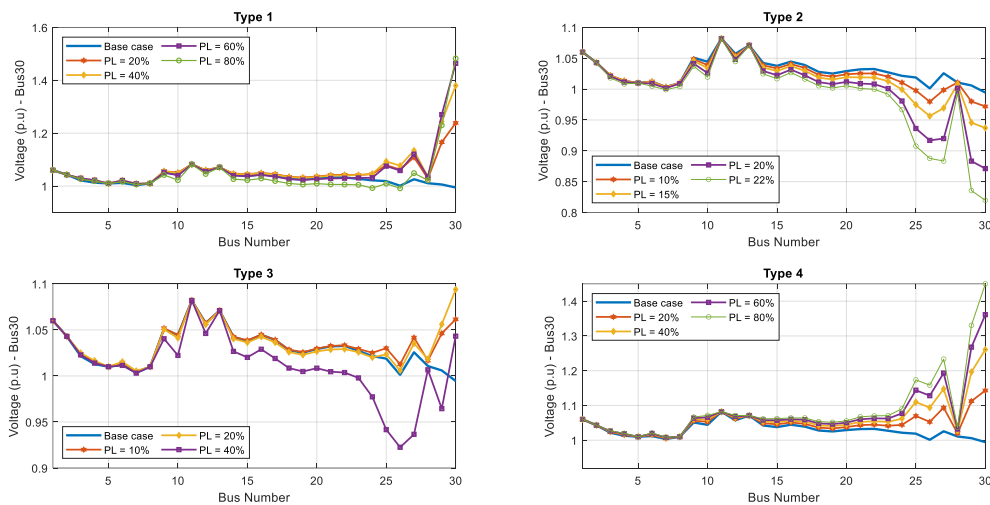


Figure 6.15 Voltage profile of each bus in the IEEE 30-bus - (different DG types vs. different penetration levels)

The study results show in Figure 6.15 that DGs' impact on the voltage profile depends on the type of DG and the penetration level.

The results show that when a Type 1 DG that injects both active and reactive power is connected to bus 30, it improves the voltage profile of the system, especially at bus 30, where

the voltage magnitude increases. This is because the DG provides both real and reactive power to support the load demand and reduce the line losses. However, if the penetration level (the ratio of DG capacity to system capacity) is too high, the voltage magnitude may exceed the acceptable limits and cause overvoltage problems.

The results also show that when a DG that injects active power and absorbs reactive power is connected to bus 30, it worsens the voltage profile of the system, especially at bus 30, where the voltage magnitude decreases. This is because the DG consumes reactive power from the system and increases the line losses. If the penetration level is too high, the voltage magnitude may fall below the acceptable limits and cause undervoltage problems.

The results further show that when a DG that injects only active power is connected to bus 30, it has a mixed effect on the voltage profile of the system. At low penetration levels, it improves the voltage profile by providing real power to support the load demand and reduce line losses. However, high penetration levels worsen the voltage profile by creating a mismatch between active and reactive power in the system and increasing the line losses.

Finally, the results show that when a DG that injects only reactive power is connected to bus 30, it improves the voltage profile of the system by providing reactive power to maintain the voltage level and reduce the line losses. However, if the penetration level is too high, it may cause overvoltage problems by injecting too much reactive power into the system.

C. Impact of DG on Voltage Stability Margin (VSM)

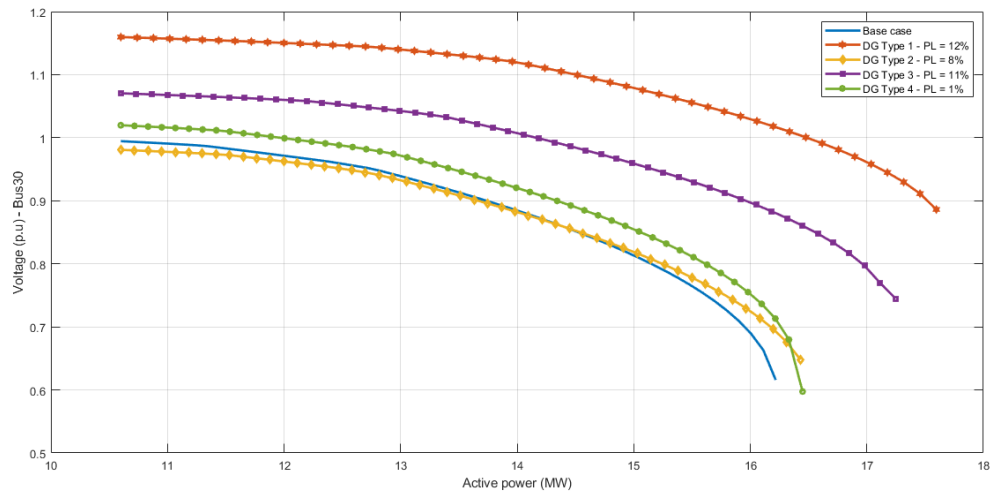


Figure 6.16 P-V curves at bus 30 (33kV buses) - (different DG types vs. PL%)

The effect of different types of distributed generation (DG) connected to bus 30 and their different penetration levels on voltage stability margin (VSM) and increased maximum loadability was studied by performing continuous power flow analysis on a test distribution network. Then P-V and Q-V curves for each DG type were plotted and analyzed to determine the impact of DG installation on VSM.

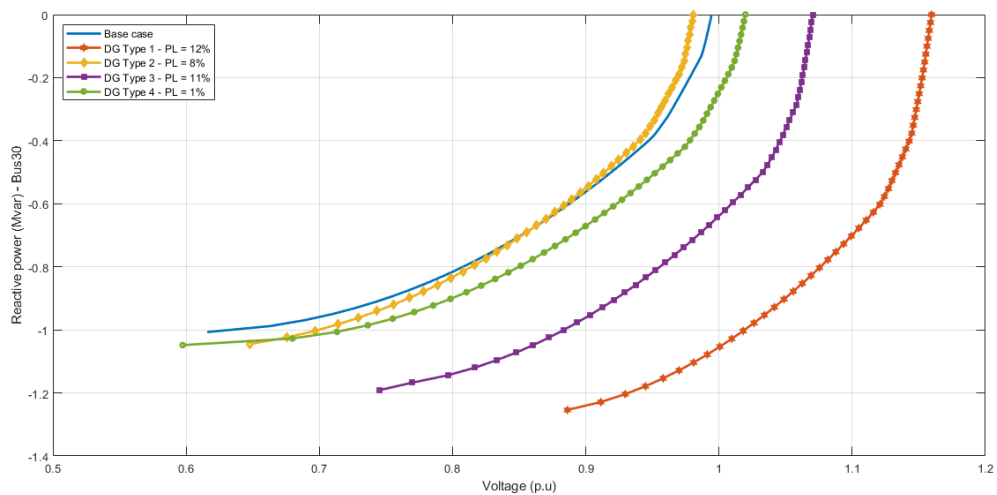


Figure 6.17 Q-V curves at bus 30 (33kV buses) - (different DG types vs. PL%)

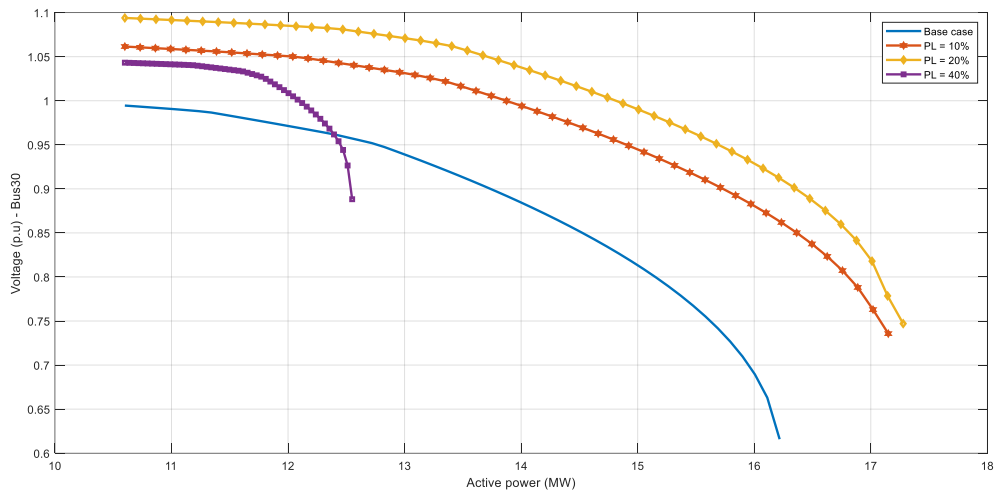


Figure 6.18 P-V curves at bus 30 (33kV buses) – (type 3 DG vs. different PL%)

Figures 6.16 and 6.17 show the P-V and Q-V curves for the four different DG types. The curves illustrate the improvement in VSM after DG installation, with DG types 1 and 3 demonstrating more remarkable VSM improvement than the other two types.

To investigate the impact of DG penetration level on voltage stability margin (VSM), P-V and Q-V curves were plotted for type 3 DG injection at bus 30 with different penetration levels and presented in Figures 6.18 - 6.19, respectively. The results show that an increase in DG penetration level leads to a corresponding increase in VSM improvement up to a certain point. Where continued DG integration can have implications for the margin of voltage stability and maximum loadability for the bus. This means that the bus may not be able to accommodate as much additional load without exceeding the operational limits, as shown in Figures 6.18 and 6.19 for a 40% penetration level for type 3 of DG at bus 30.

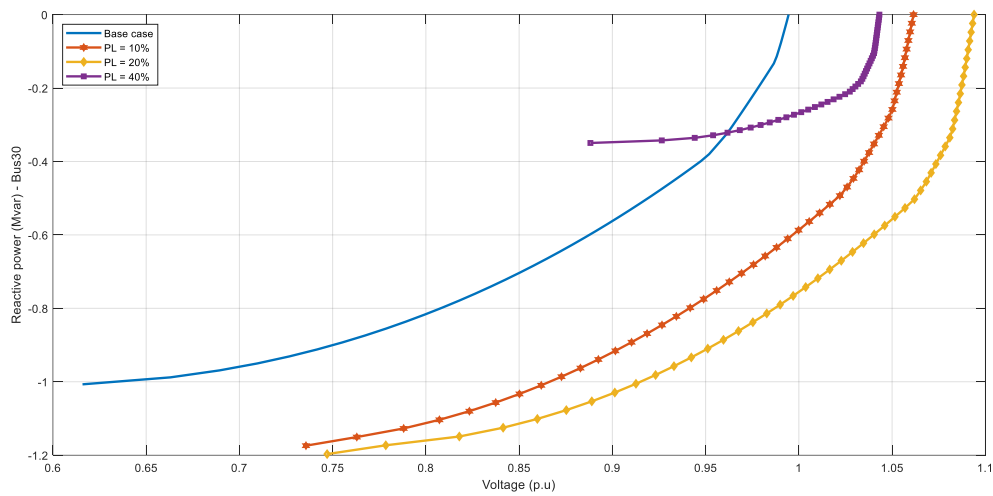


Figure 6.19 Q-V curves at bus 30 (at 33kV buses) – (type 3 DG vs. different PL%)

Finally, integrating DG units into a power system has significant implications on multiple aspects, including the voltage profile, system power loss, Voltage Stability Margin (VSM), and loadability. By introducing DG units, the VSM can be improved, and the system's loadability can be increased through the provision of additional sources of active and reactive power. However, the effect of DG units on voltage stability is influenced by various factors, such as their location, size, control mode, and penetration level.

Overall, the integration of DG units can significantly impact a power system's voltage stability. It is important to carefully consider the location, size, and penetration level of DG units to minimize their impact on voltage stability.

D. Impact of DG on Voltage Stability Indices (VSIs)

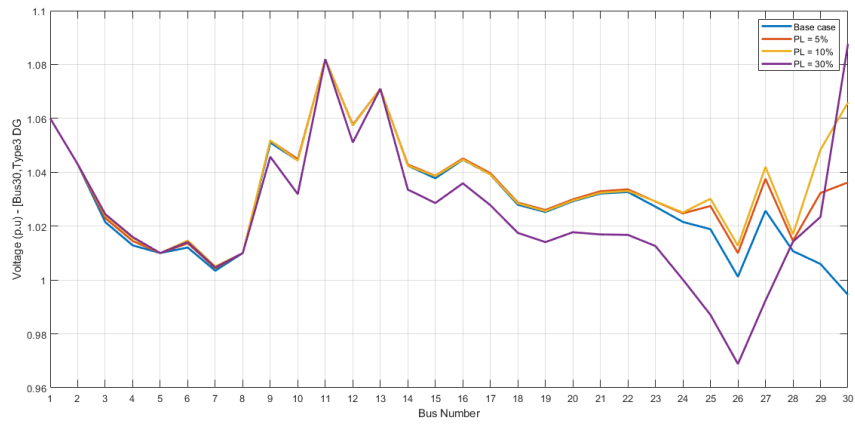


Figure 6.20 Voltage profile vs. different PL% at bus 30, type3 DG



Figure 6.21 VSIs of all 33 kV transmission lines, Base case



Figure 6.22 VSIs of all 33 kV transmission lines, PL = 5%, type3 DG.

With the injection of distributed generator type 3 (real power inject) into bus 30, we observe from Figure 6.20 that the voltage profile improves with the injection of the distributed generator at penetration levels (PL = 5%, PL = 10%). Where the results show that injecting DG at bus 30 improves the voltage profile of the system, especially at bus 30 itself. This is because DG reduces the power flow and losses in the transmission lines and increases the voltage at the injection point. However, the improvement is not uniform across all buses. The buses closer to bus 30 experience a higher voltage increase than those farther away from bus 30. This is

because the voltage drop along the transmission lines depends on the distance and impedance of the lines.

The results also show that increasing the penetration level of DG increases the voltage profile of the system, but only up to a specific limit. When the penetration level is 5%, the voltage profile is within the allowable limits. When the penetration level is 10%, the voltage profile rises more but remains within the limits. However, when the penetration level is 30%, the voltage profile exceeds the limits at bus 30, where a sudden and excessive increase occurs. This is because injecting too much power from DG can cause overvoltage and instability in the system.

As shown in Figure 6.22, with an increase in the penetration level (PL = 5%), the values of voltage stability indices significantly decrease. Notably, indices that include real power in their calculations experience a noticeable decline in values of VSIs such as NLSI, LQP, L_p , and NVSI. On the other hand, indices that do not contain the parameter (P) do not exhibit a significant change in their values as FVSI, VQI_{Line} , and L_{mn} .

As the injection of real power continues, the values of the indicators start to rise, as observed in Figures 6.23 and 6.24. This indicates voltage instability, which is also evident in the voltage profile in Figure 6.20.



Figure 6.23 VSIs of all 33 kV transmission lines, PL = 10%, type3 DG

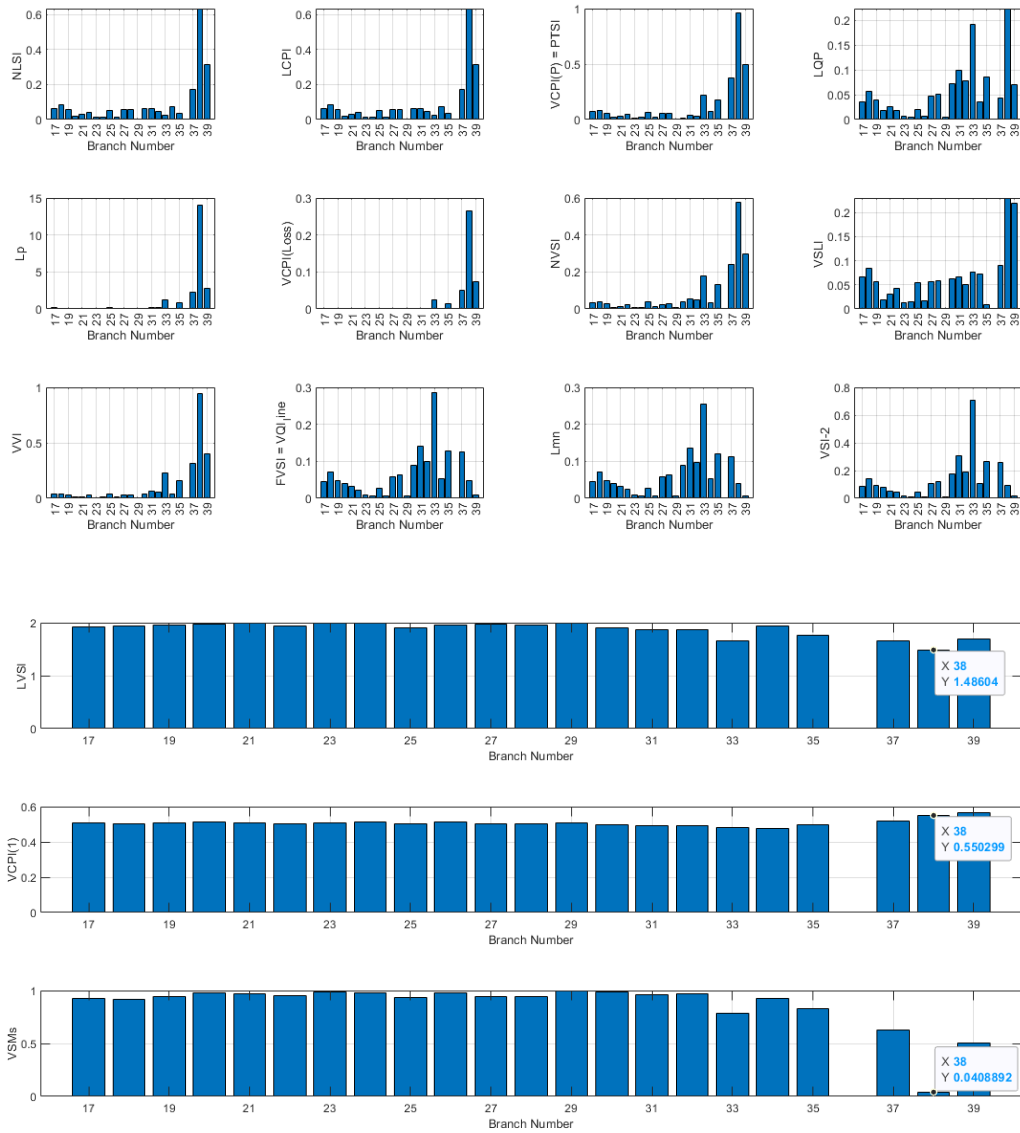


Figure 6.24 VSIs of all 33 kV transmission lines, PL = 30%, type3 DG

The magnitude of real power flow in the lines near the DG unit changes with the amount of real power injected by the DG unit. This also causes the angular difference between the sending and receiving terminal voltages (δ) to increase proportionally, especially at the bus where the DG unit is located.

It is noted that the indices that consider the effect of real power, line resistance, and δ in their formulation, such as L_p , provide a more accurate measure of voltage stability than other VSIs.

Furthermore, Voltage Stability Indices (VSIs) such as FVSI, VSI₂, and VCPI(1) that do not consider the angular difference between the sending and receiving end voltage, represented by δ , yield inaccurate results.

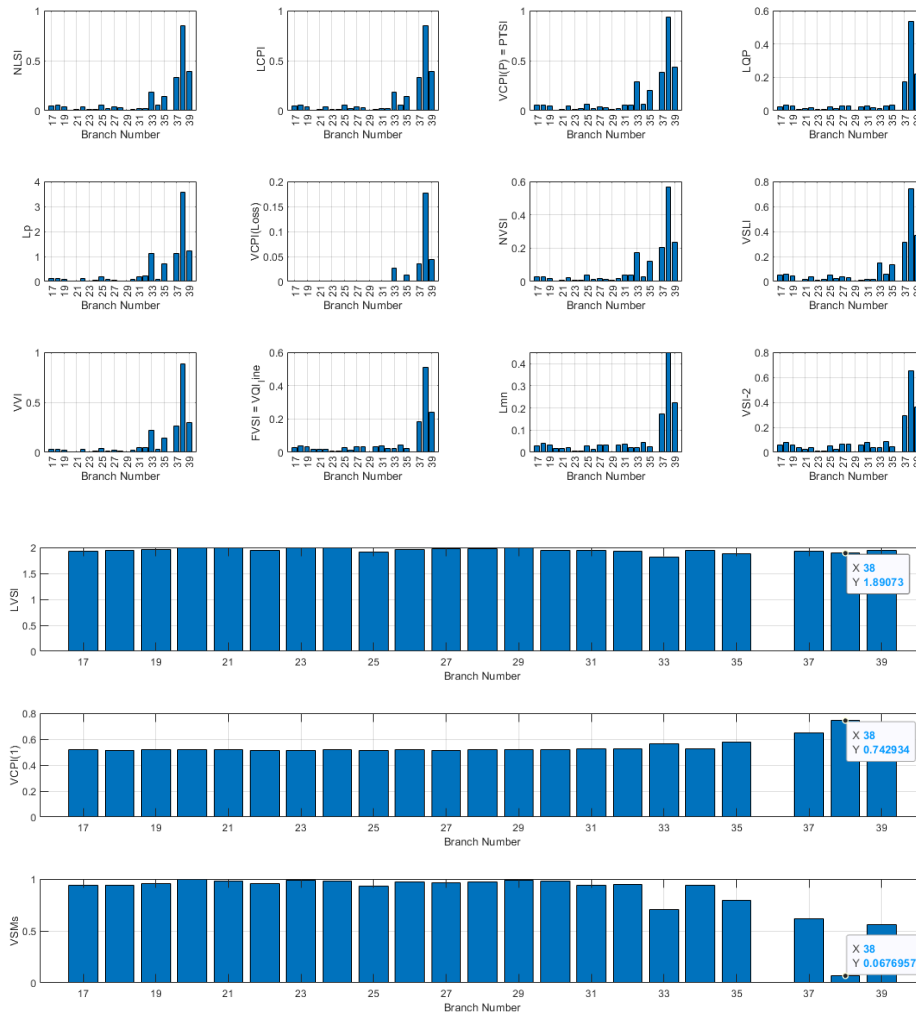


Figure 6.25 VSIs of all 33 kV transmission lines, PL = 30%, type1 DG

When introducing reactive power (Q) through injection, as observed in type 1 and type 4 DG systems, or consuming it, as seen in type 2 systems, a high penetration level (PL) of reactive power results in an enhancement of the voltage profile in buses near the injection point. The maximum distributed generator penetration refers to the highest level of DG capacity that can be injected into the electrical grid without causing power flow failures or (non-convergence) issues in the system.

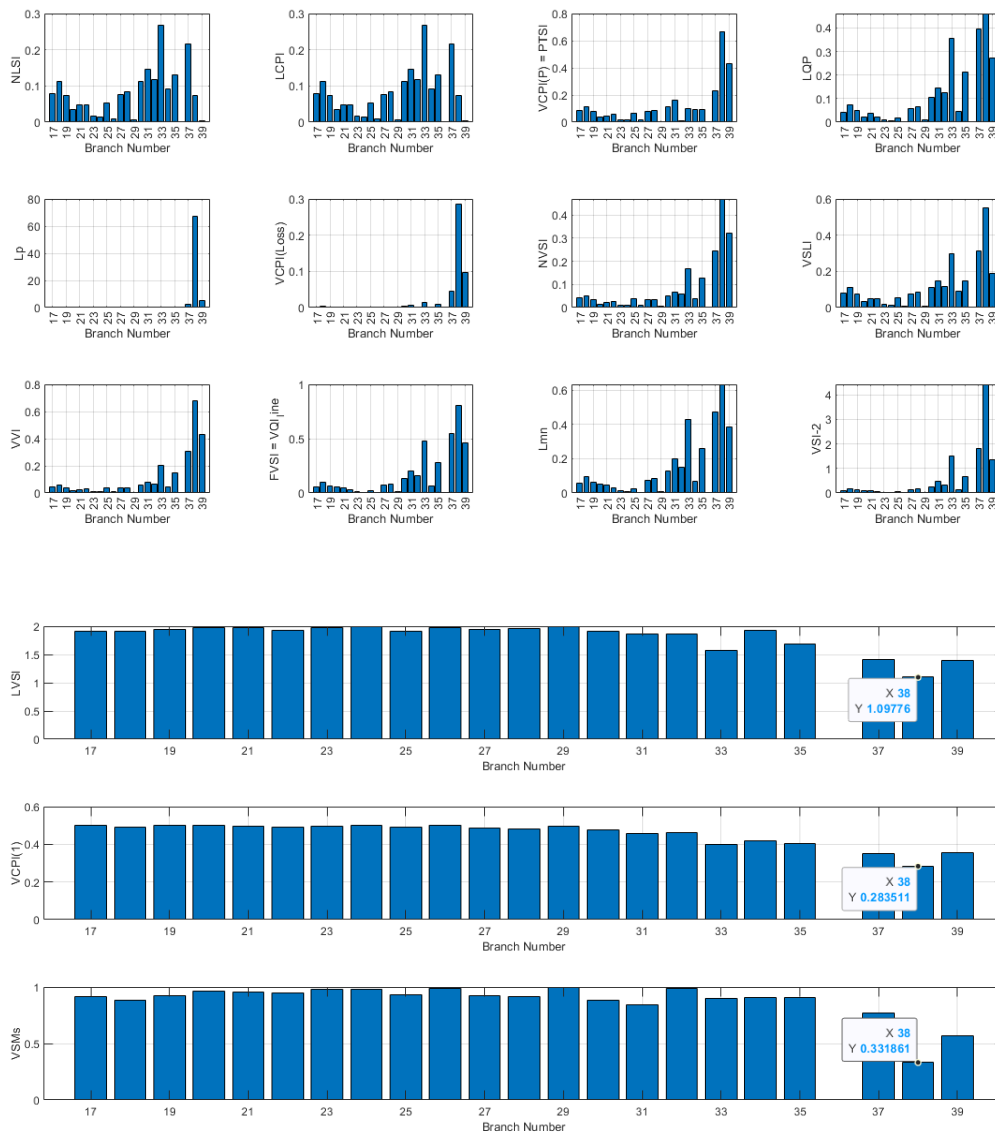


Figure 6.26 VSIs of all 33 kV transmission lines, PL = 23%, type2 DG

As seen in DG of type 1 and type 4, the injected bus experiences overvoltage (bus 30), as illustrated in Figure 6.15. On the other hand, in type 2 of DG, there is a sharp decline in the voltage profile when the DG consumes reactive power from the grid. Including reactive power parameters significantly impacts various indices, such as FVSI, L_{mn} , VQI_{line} , and VSI_2 . Of these indices, VSI_2 stands out by recording the highest value, clearly indicating its sensitivity to changes in reactive power within the system. This is evident in Figures 6.25 to 6.27. Indices that approach their critical values are indicative of potential system instability.

The results obtained from these cases demonstrate that integrating a DG unit enhances the voltage stability of the overall system. Nevertheless, reaping benefits such as power loss reduction, voltage profile improvement, and enhanced voltage stability requires careful consideration of the appropriate size and location of the DG unit.

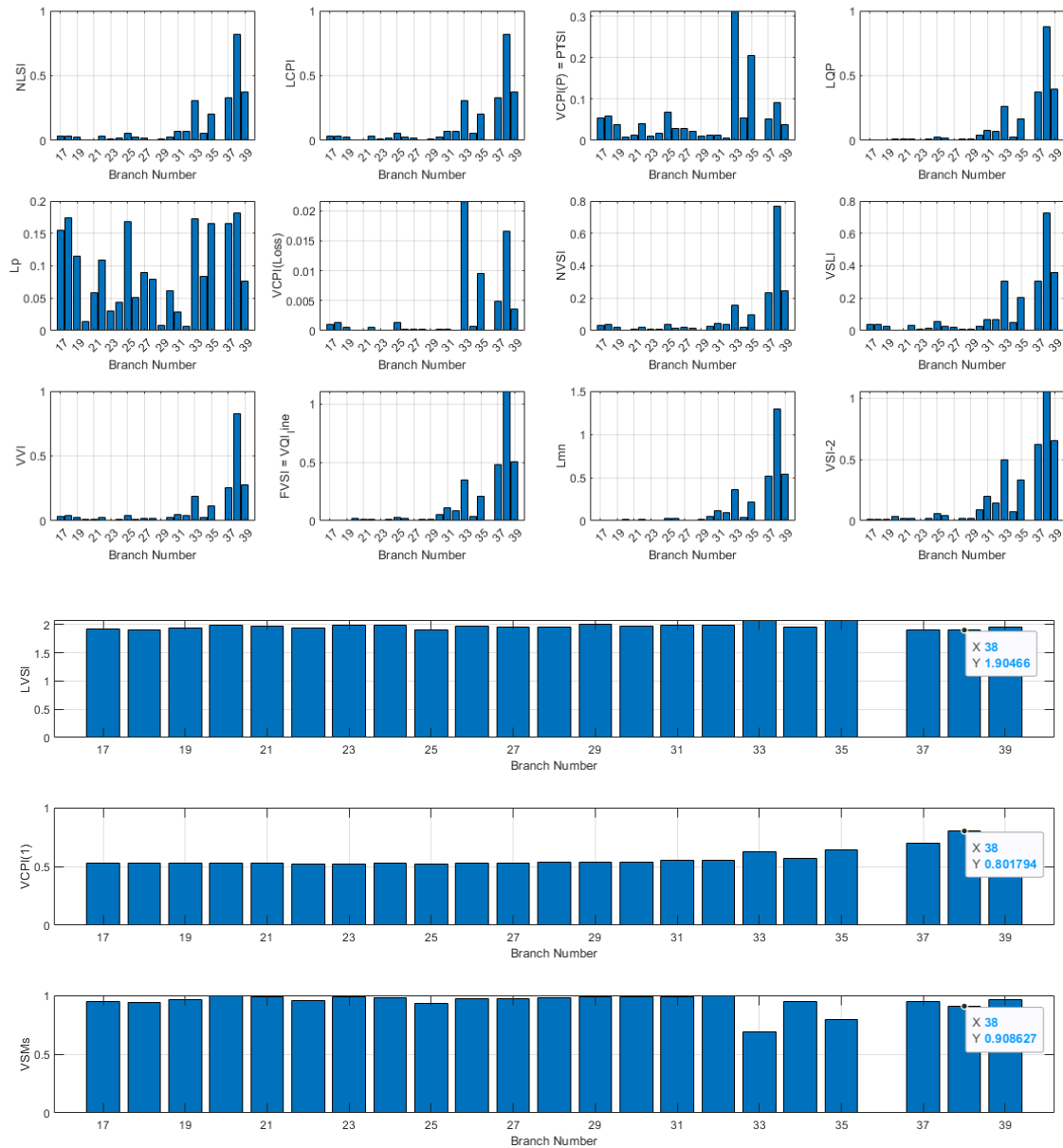


Figure 6.27 VSIs of all 33 kV transmission lines, PL = 30%, type 4 DG

CHAPTER 7: Conclusions and Recommendations for Future Work

7.1 Conclusions

This thesis investigates voltage stability issues, which are crucial concerns in power systems. Enhancing voltage stability is essential to prevent the occurrence of cascading failures. The thesis focuses on the indices derived from system variables-based approaches using a two-bus power system model and examines and presents the specifications of 19 different voltage stability indices.

A comprehensive comparative analysis is conducted among various voltage stability indices to highlight their foundational principles, performance, abbreviations, calculation methods, underlying assumptions, main concepts, stable conditions, critical values, unstable conditions, and overall behaviors. The evaluation uses several IEEE benchmark test systems, including 12-bus and 30-bus distribution systems. Additionally, traditional analysis techniques such as P-V and Q-V curves are discussed.

Furthermore, the sensitivity of these indices to changes in base case loading and under heavy PQ loading at all buses is examined. The impact of integrating different penetration levels of DG is also validated to determine the consequences of neglecting certain variables, such as active power, reactive power, the angular difference between sending and receiving bus voltages, line impedance, and shunt admittance, in the formulation of voltage stability indices. Under normal load conditions, the voltage stability indices exhibited values far from their critical thresholds. However, under heavy PQ loads, the indices approached their critical values.

It is important to note that voltage stability indices do not exhibit the same behaviour due to

the various considerations taken during their formulation. Each index is based on a different set of parameters. For instance, some indices neglect the effect of active power, while others ignore reactive power, voltage angle differences (δ), line impedance, or shunt admittance.

Conditions highlighted are taken for assessment of VSIs as follows:

- Indices that exclude the effect of real power, voltage angle differences between the sending and receiving end voltages (δ), and line resistance may not be suitable for analyzing issues related to changes in real power, such as both P and PQ loading events.
- Ignoring voltage angle differences can lead to erroneous collapse predictions, mainly when dealing with heavily loaded lines in a radial network. In such cases, which provides a predicted value higher than the actual value.
- Indices that exclude line resistance may produce inaccurate results, as in the case of the LQP index. Assuming zero-line resistance may not be viable for radial distribution networks due to the high R/X ratio at the distribution level.
- Indices that include reactive power and bus voltage in their formulation are suitable for analyzing problems related to reactive power, like Q loading and reactive power dispatch.
- Some indices consider the directions and magnitudes of real and reactive power flow to assess the voltage stability status of the system. These indices can provide more accurate results than others.
- The location of buses plays a role, as buses far from the main power source are more likely to exhibit higher VSIs values in the line.
- Lines connected to buses that have large loads are also prone to higher values of the VSIs in line.
- Lines connecting to substations carry significant amounts of real and reactive power

flow, which can contribute to higher values of the voltage stability indices.

Through different VSIs has been determined the critical lines; thus, the weak buses have been determined; identification of critical lines and the weak bus is essential and plays a key role in the optimal placement of DG resources. This thesis analyzes the performance of different voltage stability indices and their enhancement by placing the optimal location of different types of DG and finding the optimal size and power factor of DG units to minimization of the total active power losses and bus voltage deviation to enhance voltage profile, as well as the maximization of the voltage stability margins.

In IEEE 12-bus system at normal loading, the DG of type 1 with a penetration level of 53% has the highest bus voltage values and the lowest total active and reactive power losses. Where enhance the active and reactive power supplied locally by the DG units lead to decreased active and reactive power flow through the electrical lines, improved bus voltage profile and lower total active and reactive power losses.

For a network IEEE 30-bus at base case loading, it is noticed that the minimum power losses occur when DG of types 1 and 3 are injections at bus 30, and the best-enhanced voltage profile within voltage limits occurs when DG of types 3 at bus 30.

It is important to note that the optimal placement and size of DG systems will vary depending on the specific characteristics and requirements of the distribution network. In conclusion, DG helps reduce losses by minimizing transmission and distribution losses through localized generation near the point of consumption. Voltage enhancement can also reduce loss by compensating for voltage drop issues and reducing resistive losses.

7.2 Recommendations for Future Work

Based on this thesis, the following recommendations can be made for future work:

- 1- Further Investigation of Voltage Stability Indices: The thesis analyzed and compared 19 voltage stability indices. However, there are additional indices that could be explored. Future research could focus on studying other indices and developing new indices or refining existing ones to improve their accuracy and applicability in different power system scenarios.
- 2- A more comprehensive classification of voltage stability indices.
- 3- Validation and application of VSIs within a power system network locally through field testing and validation.
- 4- The thesis analyzed the performance of different voltage stability indices with the placement of DG units. Future work could expand on this aspect by merging algorithms with VSIs or developing optimization algorithms or techniques to determine the optimal placement and sizing of DG systems in distribution networks.
- 5- Future work could incorporate a cost-benefit analysis to assess the economic feasibility of implementing the recommended strategies for voltage stability enhancement.

Addressing these areas of future work can advance the understanding of voltage stability issues and contribute to developing effective strategies for enhancing power system stability.

APPENDIX A.

a. IEEE 12-Bus Test System: Bus and Line Data

Table A.1 Bus data for IEEE 12-bus system.

Node no.	P_L (kW)	Q_L (kVAr)
1	0	0
2	60	60
3	40	30
4	55	55
5	30	30
6	20	15
7	55	55
8	45	45
9	40	40
10	35	30
11	40	30
12	15	15

Table A.2 Line data for IEEE 12-bus system.

Branch no.	Sending end	Receiving end	R (ohms)	X (ohms)
1	1	2	1.093	0.455
2	2	3	1.184	0.494
3	3	4	2.095	0.873
4	4	5	3.188	1.329
5	5	6	1.093	0.455
6	6	7	1.002	0.417
7	7	8	4.403	1.215
8	8	9	5.642	1.597
9	9	10	2.89	0.818
10	10	11	1.514	0.428
11	11	12	1.238	0.351

$S_{base} = 100$ and $V_{base} = 11$ kV

b. IEEE 30-Bus Test System: Bus and Line Data

Table A.3 Bus data for IEEE 30-bus system.

Bus no.	Bus code	Voltage Mag.	Angle Degree	Load		Generator				Injected Mvar
				MW	Mvar	MW	Mvar	Qmin	Qmax	
1	1	1.06	0	0	0	0	0	0	0	0
2	2	1.043	0	21.7	12.7	40	0	-40	50	0
3	0	1	0	2.4	1.2	0	0	0	0	0
4	0	1.06	0	7.6	1.6	0	0	0	0	0
5	2	1.01	0	94.2	19	0	0	-40	40	0
6	0	1.0	0	0.0	0.0	0	0	0	0	0
7	0	1.0	0	22.8	10.9	0	0	0	0	0
8	2	1.01	0	30.0	30.0	0	0	-10	40	0
9	0	1.0	0	0	0	0	0	0	0	0
10	0	1.0	0	5.8	2.0	0	0	-6	24	19
11	2	1.082	0	0	0	0	0	0	0	0
12	0	1.0	0	11.2	7.5	0	0	0	0	0
13	2	1.071	0	0	0	0	0	-6	24	0
14	0	1	0	6.2	1.6	0	0	0	0	0
15	0	1	0	8.2	2.5	0	0	0	0	0
16	0	1	0	3.5	1.8	0	0	0	0	0
17	0	1	0	9.0	5.8	0	0	0	0	0
18	0	1	0	3.2	0.9	0	0	0	0	0
19	0	1	0	9.5	3.4	0	0	0	0	0
20	0	1	0	2.2	0.7	0	0	0	0	0
21	0	1	0	17.5	11.2	0	0	0	0	0
22	0	1	0	0	0	0	0	0	0	0
23	0	1	0	3.2	1.6	0	0	0	0	0
24	0	1	0	8.7	6.7	0	0	0	0	4.3
25	0	1	0	0.0	0.0	0	0	0	0	0
26	0	1	0	3.5	2.3	0	0	0	0	0
27	0	1	0	0	0	0	0	0	0	0
28	0	1	0	0	0	0	0	0	0	0
29	0	1	0	2.4	0.9	0	0	0	0	0
30	0	1	0	10.6	1.9	0	0	0	0	0

Table A.4 Line data for IEEE 30-bus system.

Branch no.	Sending end	Receiving end	R (p.u)	X (p.u)	1/2 B (p.u)	= 1 for lines > 1 or < 1 Transformer Tap
1	1	2	0.0192	0.0575	0.02640	1
2	1	3	0.0452	0.1852	0.02040	1
3	2	4	0.0570	0.1737	0.01840	1
4	3	4	0.0132	0.0379	0.00420	1
5	2	5	0.0472	0.1983	0.02090	1
6	2	6	0.0581	0.1763	0.01870	1
7	4	6	0.0119	0.0414	0.00450	1
8	5	7	0.0460	0.1160	0.01020	1
9	6	7	0.0267	0.0820	0.00850	1
10	6	8	0.0120	0.0420	0.00450	1
11	6	9	0	0.2080	0	0.978
12	6	10	0	0.5560	0	0.969
13	9	11	0	0.2080	0	1
14	9	10	0	0.1100	0	1
15	4	12	0	0.2560	0	0.932
16	12	13	0	0.1400	0	1
17	12	14	0.1231	0.2559	0	1
18	12	15	0.0662	0.1304	0	1
19	12	16	0.0945	0.1987	0	1
20	14	15	0.2210	0.1997	0	1
21	16	17	0.0824	0.1923	0	1
22	15	18	0.1073	0.2185	0	1
23	18	19	0.0639	0.1292	0	1
24	19	20	0.0340	0.0680	0	1
25	10	20	0.0936	0.2090	0	1
26	10	17	0.0324	0.0845	0	1
27	10	21	0.0348	0.0749	0	1
28	10	22	0.0727	0.1499	0	1
29	21	22	0.0116	0.0236	0	1
30	15	23	0.1000	0.2020	0	1
31	22	24	0.1150	0.1790	0	1
32	23	24	0.1320	0.2700	0	1
33	24	25	0.1885	0.3292	0	1
34	25	26	0.2544	0.3800	0	1
35	25	27	0.1093	0.2087	0	1
36	28	27	0	0.3960	0	0.968
37	27	29	0.2198	0.4153	0	1
38	27	30	0.3202	0.6027	0	1
39	29	30	0.2399	0.4533	0	1
40	8	28	0.0636	0.2000	0.0214	1
41	6	28	0.0169	0.0599	0.065	1

$S_{base} = 100\text{MVA}$

*R: Resistance, X: Reactance, B: Susceptance.

References

- [1] P. Kundur *et al.*, "Definition and classification of power system stability," *IEEE Transactions on Power Systems*, vol. 19, no. 3, pp. 1387–1401, Aug. 2004, doi: 10.1109/TPWRS.2004.825981.
- [2] P. Kessel and H. Glavitsch, "Estimating the voltage stability of a power system," *IEEE Transactions on Power Delivery*, vol. 1, no. 3, pp. 346–354, 1986, doi: 10.1109/TPWRD.1986.4308013.
- [3] M. Tahir, M. E. Nassar, R. El-Shatshat, and M. M. A. Salama, "A review of volt/var control techniques in passive and active power distribution networks," *2016 4th IEEE International Conference on Smart Energy Grid Engineering, SEGE 2016*, pp. 57–63, 2016, doi: 10.1109/SEGE.2016.7589500.
- [4] L. F. Ochoa, C. J. Dent, and G. P. Harrison, "Distribution network capacity assessment: Variable DG and active networks," *IEEE Transactions on Power Systems*, vol. 25, no. 1, pp. 87–95, 2010, doi: 10.1109/TPWRS.2009.2031223.
- [5] I. Dobson *et al.*, *Voltage Stability Assessment: Concepts, Practices and Tools*, no. January. 2002. [Online]. Available: http://resourcecenter.ieee-pes.org/files/2013/11/TR9_SP101PSS_Full_Content.pdf
- [6] M. Cupelli, C. Doig Cardet, and A. Monti, "Comparison of line voltage stability indices using dynamic real time simulation," *IEEE PES Innovative Smart Grid Technologies Conference Europe*, pp. 1–8, 2012, doi: 10.1109/ISGTEurope.2012.6465625.
- [7] Y. Amrane, M. Boudour, and M. Belazzoug, "A new Optimal reactive power planning based on Differential Search Algorithm," *International Journal of Electrical Power and Energy Systems*, vol. 64, pp. 551–561, 2015, doi: 10.1016/j.ijepes.2014.07.060.
- [8] M. Esmaili, E. C. Firozjaee, and H. A. Shayanfar, "Optimal placement of distributed generations considering voltage stability and power losses with observing voltage-related constraints," *Appl Energy*, vol. 113, pp. 1252–1260, 2014, doi: 10.1016/j.apenergy.2013.09.004.
- [9] Z. Wang, G. Xu, H. Wang, and J. Ren, "Distributed energy system for sustainability transition: A comprehensive assessment under uncertainties based on interval multi-criteria decision making method by coupling interval DEMATEL and interval VIKOR," *Energy*, vol. 169, pp. 750–761, 2019, doi: 10.1016/j.energy.2018.12.105.
- [10] P. G. McCormick and H. Suehrcke, "The effect of intermittent solar radiation on the performance of PV systems," *Solar Energy*, vol. 171, no. February, pp. 667–674, 2018, doi: 10.1016/j.solener.2018.06.043.
- [11] A. I. Nousedilis, G. C. Christoforidis, and G. K. Papagiannis, "Active power management in low voltage networks with high photovoltaics penetration based on prosumers' self-consumption,"

- Appl Energy*, vol. 229, no. April 2018, pp. 614–624, 2018, doi: 10.1016/j.apenergy.2018.08.032.
- [12] I. Triștiu, A. Iantoc, D. Poștovei, C. Bulac, and M. Arhip, “Theoretical analysis of voltage instability conditions in distribution networks,” in *2019 54th International Universities Power Engineering Conference (UPEC), Bucharest, Romania, 2019*, 2019, pp. 1–5.
- [13] M. Glavic and S. Greene, “Voltage stability in future power systems,” in *Encyclopedia of Electrical and Electronic Power Engineering*, Elsevier, 2023, pp. 209–223. doi: 10.1016/b978-0-12-821204-2.00141-0.
- [14] A. Chandra, A. K. Pradhan, and A. K. Sinha, “A comparative study of voltage stability indices used for power system operation,” *2016 21st Century Energy Needs - Materials, Systems and Applications (ICTFCEN), Kharagpur, India, 2016*, pp. 1–4, 2016.
- [15] J. Modarresi, E. Gholipour, and A. Khodabakhshian, “A comprehensive review of the voltage stability indices,” *Renewable and Sustainable Energy Reviews*, vol. 63, pp. 1–12, Sep. 2016, doi: 10.1016/J.RSER.2016.05.010.
- [16] H. Zaheb *et al.*, “A contemporary novel classification of voltage stability indices,” *Applied Sciences (Switzerland)*, vol. 10, no. 5, Mar. 2020, doi: 10.3390/app10051639.
- [17] A. J. Pujara and G. Vaidya, “Voltage stability index of radial distribution network,” *2011 International Conference on Emerging Trends in Electrical and Computer Technology, Nagercoil, India, 2011*, no. 3, pp. 180–185, 2011, doi: 10.1109/ICETECT.2011.5760112.
- [18] A. K. Sinha and D. Hazarika, “Comparative study of voltage stability indices in a power system,” *International Journal of Electrical Power and Energy System*, vol. 22, no. 8, pp. 589–596, 2000, doi: 10.1016/S0142-0615(00)00014-4.
- [19] H. H. Goh, Q. S. Chua, S. W. Lee, B. C. Kok, K. C. Goh, and K. T. K. Teo, “Evaluation for Voltage Stability Indices in Power System Using Artificial Neural Network,” *Procedia Eng*, vol. 118, pp. 1127–1136, 2015, doi: 10.1016/j.proeng.2015.08.454.
- [20] N. A. M. Ismail, A. A. M. Zin, A. Khairuddin, and S. Khokhar, “A comparison of voltage stability indices,” in *2014 IEEE 8th International Power Engineering and Optimization Conference (PEOCO2014), Langkawi, Malaysia, 2014*, pp. 30–34.
- [21] L. D. Arya, S. C. Choube, and M. Shrivastava, “Technique for voltage stability assessment using newly developed line voltage stability index,” *Energy Convers Manag*, vol. 49, no. 2, pp. 267–275, 2008, doi: 10.1016/j.enconman.2007.06.018.
- [22] A. R. R. Matavalam, S. M. H. Rizvi, A. K. Srivastava, and V. Ajjarapu, “Critical Comparative Analysis of Measurement Based Centralized Online Voltage Stability Indices,” *IEEE Transactions on Power Systems*, vol. 37, no. 6, pp. 4618–4629, Nov. 2022, doi: 10.1109/TPWRS.2022.3145466.
- [23] N. Shekhawat, A. K. Gupta, and A. Kumar Sharma, “Voltage Stability Assessment Using Line

- Stability Indices,” in *2018 3rd International Conference and Workshops on Recent Advances and Innovations in Engineering (ICRAIE), Jaipur, India, 2018*, pp. 1–4.
- [24] G. Meena, K. Verma, and A. Mathur, “FVSI Based Meta-heuristic Algorithm for Optimal Load Shedding to Improve Voltage Stability,” in *2022 IEEE 10th Power India International Conference, PIICON 2022*, Institute of Electrical and Electronics Engineers Inc., 2022. doi: 10.1109/PIICON56320.2022.10045119.
- [25] M. C. Pacis, I. J. M. Antonio, and I. J. T. Banaga, “Under Voltage Load Shedding Algorithm using Fast Voltage Stability Index (FVSI) and Line Stability Index (LSI),” in *2021 IEEE 13th International Conference on Humanoid, Nanotechnology, Information Technology, Communication and Control, Environment, and Management, HNICEM 2021*, Institute of Electrical and Electronics Engineers Inc., 2021. doi: 10.1109/HNICEM54116.2021.9731927.
- [26] S. Mokred, Y. Wang, and T. Chen, “Modern voltage stability index for prediction of voltage collapse and estimation of maximum load-ability for weak buses and critical lines identification,” *International Journal of Electrical Power and Energy Systems*, vol. 145, Feb. 2023, doi: 10.1016/j.ijepes.2022.108596.
- [27] I. G. Adebayo and Y. Sun, “A Comparison of Voltage Stability Indices for Critical Node Identification in a Power System,” in *2021 International Conference on Sustainable Energy and Future Electric Transportation, SeFet 2021*, Institute of Electrical and Electronics Engineers Inc., Jan. 2021. doi: 10.1109/SeFet48154.2021.9375674.
- [28] R. Chintakindi and A. Mitra, “Detecting Weak Areas in a Real-time Power System on a Static Load Model using Standard Line Voltage Stability Indices,” in *Proceedings of 2021 IEEE 2nd International Conference on Smart Technologies for Power, Energy and Control, STPEC 2021*, Institute of Electrical and Electronics Engineers Inc., 2021. doi: 10.1109/STPEC52385.2021.9718768.
- [29] A. Alshareef, R. Shah, N. Mithulananthan, and S. Alzahrani, “A new global index for short term voltage stability assessment,” *IEEE Access*, vol. 9, pp. 36114–36124, 2021, doi: 10.1109/ACCESS.2021.3061712.
- [30] S. Ratra, R. Tiwari, and K. R. Niazi, “Voltage stability assessment in power systems using line voltage stability index,” *Computers and Electrical Engineering*, vol. 70, pp. 199–211, Aug. 2018, doi: 10.1016/j.compeleceng.2017.12.046.
- [31] M. Furukakoi, O. B. Adewuyi, M. S. Shah Danish, A. M. Howlader, T. Senjyu, and T. Funabashi, “Critical Boundary Index (CBI) based on active and reactive power deviations,” *International Journal of Electrical Power and Energy Systems*, vol. 100, pp. 50–57, Sep. 2018, doi: 10.1016/j.ijepes.2018.02.010.
- [32] S. J. Chuang, C. M. Hong, and C. H. Chen, “Improvement of integrated transmission line transfer index for power system voltage stability,” *International Journal of Electrical Power and Energy Systems*, vol. 78, pp. 830–836, Jun. 2016, doi: 10.1016/j.ijepes.2015.11.111.

- [33] K. D. Dharmapala, A. Rajapakse, K. Narendra, and Y. Zhang, "Machine Learning Based Real-Time Monitoring of Long-Term Voltage Stability Using Voltage Stability Indices," *IEEE Access*, vol. 8, pp. 222544–222555, 2020, doi: 10.1109/ACCESS.2020.3043935.
- [34] S. Pérez-Londoño, L. F. Rodríguez, and G. Olivar, "A simplified voltage stability index (SVSI)," *International Journal of Electrical Power and Energy Systems*, vol. 63, pp. 806–813, 2014, doi: 10.1016/j.ijepes.2014.06.044.
- [35] S. Khunkitti and S. Premrudeepreechacharn, "Voltage Stability Improvement Using Voltage Stability Index Optimization," in *Proceedings of the 2020 International Conference on Power, Energy and Innovations, ICPEI 2020*, Institute of Electrical and Electronics Engineers Inc., Oct. 2020, pp. 193–196. doi: 10.1109/ICPEI49860.2020.9431536.
- [36] B. Ismail *et al.*, "New Line Voltage Stability Index (BVSI) for Voltage Stability Assessment in Power System: The Comparative Studies," *IEEE Access*, vol. 10, pp. 103906–103931, 2022, doi: 10.1109/ACCESS.2022.3204792.
- [37] A. F. Nasef, D. S. Osheba, H. A. Khattab, and S. Osheba, "Assessment of optimal allocation of renewable distributed generator sources in distribution network," *Engineering Reports*, vol. 2, no. 5, May 2020, doi: 10.1002/eng2.12158.
- [38] H. S. Salama and I. Vokony, "Voltage stability indices—A comparison and a review," *Computers and Electrical Engineering*, vol. 98, Mar. 2022, doi: 10.1016/j.compeleceng.2022.107743.
- [39] S. El Wejhani, M. Elleuch, S. Tnani, K. Ben Kilani, and G. Ennine, "Renewable Energy Integration in Power System: Clarification on Stability Indices," in *2022 IEEE International Conference on Electrical Sciences and Technologies in Maghreb, CISTEM 2022*, Institute of Electrical and Electronics Engineers Inc., 2022. doi: 10.1109/CISTEM55808.2022.10044066.
- [40] I. K. Otchere, B. Arhin, K. A. Kyeremeh, and E. A. Frimpong, "Investigation of Voltage Stability for Transmission Network with High Penetration of Wind Energy Sources," *Investigation of Voltage Stability for Transmission Network with High Penetration of Wind Energy Sources, 2020 IEEE PES/IAS PowerAfrica, Nairobi, Kenya, 2020*, pp. 1–5, 2020.
- [41] F. Ugranli and E. Karatepe, "Convergence of rule-of-thumb sizing and allocating rules of distributed generation in meshed power networks," *Renewable and Sustainable Energy Reviews*, vol. 16, no. 1. Elsevier Ltd, pp. 582–590, 2012. doi: 10.1016/j.rser.2011.08.024.
- [42] A. S. Hassan, E. S. A. Othman, F. M. Bendary, and M. A. Ebrahim, "Optimal integration of distributed generation resources in active distribution networks for techno-economic benefits," *Energy Reports*, vol. 6, pp. 3462–3471, Nov. 2020, doi: 10.1016/j.egyr.2020.12.004.
- [43] S. Essallah, A. Khedher, and A. Bouallegue, "Integration of distributed generation in electrical grid: Optimal placement and sizing under different load conditions," *Computers and Electrical Engineering*, vol. 79, Oct. 2019, doi: 10.1016/j.compeleceng.2019.106461.

- [44] S. Sinha, R. Roshan, M. A. Alam, and S. Banerjee, "Optimal Placement of D-STATCOM for Reduction of Power Loss and Improvement of Voltage Profile using Power Stability and Power Loss Indices in a Radial Distribution System," *2019 IEEE 5th International Conference for Convergence in Technology (I2CT), Bombay, India, 2019*, pp. 1–4, 2019.
- [45] R. Roshan, P. Samal, and P. Sinha, "Optimal placement of FACTS devices in power transmission network using power stability index and fast voltage stability index," in *2020 International Conference on Electrical and Electronics Engineering (ICE3), Gorakhpur, India, 2020*, pp. 246–251.
- [46] L. A. Paredes, M. G. Molina, and B. R. Serrano, "Optimal Location of an SVC in a Microgrid to Improve the Dynamic Voltage Stability," in *2021 IEEE URUCON, URUCON 2021*, Institute of Electrical and Electronics Engineers Inc., 2021, pp. 242–246. doi: 10.1109/URUCON53396.2021.9647244.
- [47] C. P. Steinmetz, "Power control and stability of electric generating stations," *Transactions of the American Institute of Electrical Engineers*, vol. 39, pp. 1215–1287, 1920, doi: 10.1109/T-AIEE.1920.4765322.
- [48] H. Review, "First Report of Power System Stability," *Transactions of the American Institute of Electrical Engineers*, vol. 56, no. 2, pp. 261–282, 1937, doi: 10.1109/T-AIEE.1937.5057521.
- [49] T. van Cutsem and C. Vournas, "Voltage stability of electric power systems," *Voltage Stability of Electric Power Systems*, pp. 1–378, 2008, doi: 10.1007/978-0-387-75536-6.
- [50] K. R. Padiyar and A. M. Kulkarni, "Dynamics and Control of Electric Transmission and Microgrids," *Dynamics and Control of Electric Transmission and Microgrids*, 2019, doi: 10.1002/9781119173410.
- [51] M. A. Pai and A. Stankovic, *Computational Techniques for Voltage Stability Assessment and Control*. 2007. doi: 10.1007/978-0-387-32935-2.
- [52] O. Alizadeh Mousavi, M. Bozorg, and R. Cherkaoui, "Preventive reactive power management for improving voltage stability margin," *Electric Power Systems Research*, vol. 96, pp. 36–46, 2013, doi: 10.1016/j.epsr.2012.10.005.
- [53] Prabha Kundur, "Prabha Kundur - Power System Stability and Control (part 1)-McGraw-Hill Professional (1994).pdf." 1994.
- [54] "Power System Voltage Stability," *IEEE Power Engineering Review*, vol. 15, no. 6. pp. 27–28, 1995. doi: 10.1109/MPER.1995.391560.
- [55] T. van Cutsem, "Voltage instability: Phenomena, countermeasures, and analysis methods," *Proceedings of the IEEE*, vol. 88, no. 2, pp. 208–227, 2000, doi: 10.1109/5.823999.
- [56] Y. Zhang, S. Rajagopalan, and J. Conto, "Practical voltage stability analysis," *IEEE PES General Meeting, PES 2010*, pp. 1–7, 2010, doi: 10.1109/PES.2010.5589892.

- [57] S. B. Bhaladhare, A. S. Telang, and P. P. Bedekar, "P-V , Q-V Curve – A Novel Approach for Voltage Stability Analysis," *National Conference on Innovative Paradigms in Engineering & Technology (NCIPET-2013)*, pp. 31–35, 2013.
- [58] R. Kumar, A. Mittal, N. Sharma, I. V. Duggal, and A. Kumar, "PV and QV curve analysis using series and shunt compensation," *PIICON 2020 - 9th IEEE Power India International Conference, 2020*, doi: 10.1109/PIICON49524.2020.9112917.
- [59] B. Gao, G. K. Morison, and P. Kundur, "Voltage Stability Evaluation using Modal Analysis," *IEEE Power Engineering Review*, vol. 12, no. 11, p. 41, 1992, doi: 10.1109/MPER.1992.161430.
- [60] C. W. Liu, M. C. Su, and S. S. Tsay, "Regression Tree for Stability Margin Prediction Using Synchrophasor Measurements measurements," *IEEE Transactions on Power Systems*, vol. 14, no. 2, pp. 685–692, 2012.
- [61] I. Musirin and T. K. Abdul Rahman, "Novel fast voltage stability index (FVSI) for voltage stability analysis in power transmission system," *2002 Student Conference on Research and Development: Globalizing Research and Development in Electrical and Electronics Engineering, SCORed 2002 - Proceedings*, pp. 265–268, 2002, doi: 10.1109/SCORED.2002.1033108.
- [62] H. Zaheb *et al.*, "A contemporary novel classification of voltage stability indices," *Applied Sciences (Switzerland)*, vol. 10, no. 5, pp. 1–15, 2020, doi: 10.3390/app10051639.
- [63] F. Karbalaei, H. Soleymani, and S. Afsharnia, "A comparison of voltage collapse proximity indicators," *2010 9th International Power and Energy Conference, IPEC 2010*, pp. 429–432, 2010, doi: 10.1109/IPEC.2010.5697034.
- [64] J. Modarresi, E. Gholipour, and A. Khodabakhshian, "A comprehensive review of the voltage stability indices," *Renewable and Sustainable Energy Reviews*, vol. 63, pp. 1–12, 2016, doi: 10.1016/j.rser.2016.05.010.
- [65] M. Moghavvemi and F. M. Omar, "Technique for contingency monitoring and voltage collapse prediction," *IEE Proceedings: Generation, Transmission and Distribution*, vol. 145, no. 6, pp. 634–640, 1998, doi: 10.1049/ip-gtd:19982355.
- [66] A. Mohamed and G. B. Jasmon, "A new clustering technique for power system voltage stability analysis," *Electric Machines and Power Systems*, vol. 23, no. 4, pp. 389–403, 1995, doi: 10.1080/07313569508955632.
- [67] M. Moghavvemi and M. O. Faruque, "Technique for assessment of voltage stability in Ill-conditioned radial distribution network," *IEEE Power Engineering Review*, vol. 21, no. 1, pp. 58–60, 2001, doi: 10.1109/39.893345.
- [68] A. Yazdanpanah-Goharrizi and R. Asghari, "A novel line stability index (NLSI) for voltage stability assessment of power systems," *Proceedings of the 7th WSEAS International Conference on Power Systems*, pp. 164–167, 2007.

- [69] M. Moghavvemi and O. Faruque, "Real-time contingency evaluation and ranking technique," *IEE Proceedings: Generation, Transmission and Distribution*, vol. 145, no. 5, pp. 517–523, 1998. doi: 10.1049/ip-gtd:19982179.
- [70] R. Kanimozhi and K. Selvi, "A novel line stability index for voltage stability analysis and contingency ranking in power system using fuzzy based load flow," *Journal of Electrical Engineering and Technology*, vol. 8, no. 4, pp. 694–703, 2013, doi: 10.5370/JEET.2013.8.4.694.
- [71] T. K. Chattopadhyay, S. Banerjee, and C. K. Chanda, "Impact of distributed generator on voltage stability analysis of distribution networks under critical loading conditions," *Proceedings of 2014 1st International Conference on Non Conventional Energy: Search for Clean and Safe Energy, ICONCE 2014*, pp. 288–291, 2014, doi: 10.1109/ICONCE.2014.6808728.
- [72] M. Nizam, A. Mohamed, and A. Hussain, "Dynamic voltage collapse prediction in power systems using support vector regression," *Expert Syst Appl*, vol. 37, no. 5, pp. 3730–3736, 2010, doi: 10.1016/j.eswa.2009.11.052.
- [73] F.A. Althowibi and M.W. Mustafa, "Line Voltage Stability Calculations in Power Systems," *Proceedings of the international conference on power and energy*, pp. 396–401, 2010.
- [74] T. K. Abdul Rahman and G. B. Jasmon, "A New Technique For Voltage Stability Analysis In A Power System and Improved Loadflow Algorithm For Distribution Network," 1995.
- [75] K. Joseph. Makasa and Ganesh K. Venayagamoorthy, "On-line Voltage Stability Load Index Estimation Based on PMU Measurements," *Proceedings of the IEEE power and energy society general meeting*, pp. 1–6, 2011.
- [76] Andreea-Georgiana IANȚOC, Constantin BULAC, Ion TRIȘTIU, Irina PICIOROAGĂ, and Dorian O. SIDEA, "Impact Analysis of Distributed Generation on Voltage Stability in Radial Distribution Systems," in *2019 International Conference on ENERGY and ENVIRONMENT (CIEM)*, 2019, pp. 510–514.
- [77] R. Tiwari, K. R. Niazi, and V. Gupta, "Line collapse proximity index for prediction of voltage collapse in power systems," *International Journal of Electrical Power and Energy Systems*, vol. 41, no. 1, pp. 105–111, Oct. 2012, doi: 10.1016/j.ijepes.2012.03.022.
- [78] M. M. Aman, G. B. Jasmon, H. Mokhlis, and A. H. A. Bakar, "Optimal placement and sizing of a DG based on a new power stability index and line losses," *International Journal of Electrical Power and Energy Systems*, vol. 43, no. 1, pp. 1296–1304, 2012, doi: 10.1016/j.ijepes.2012.05.053.
- [79] V. V. S. N. Murty and A. Kumar, "Optimal placement of DG in radial distribution systems based on new voltage stability index under load growth," *International Journal of Electrical Power and Energy Systems*, vol. 69, pp. 246–256, 2015, doi: 10.1016/j.ijepes.2014.12.080.
- [80] L. Wang, Y. Liu, and Z. Luan, "Power Transmission Paths Based Voltage Stability Assessment,"

- 2005.
- [81] G. Deng, Y. Sun, and J. Xu, "A new index of voltage stability considering distribution network," *Asia-Pacific Power and Energy Engineering Conference, APPEEC*, 2009, doi: 10.1109/APPEEC.2009.4918070.
- [82] "IEEE Guide for Identifying and Improving Voltage Quality in Power Systems," in *IEEE Std 1250-2018 (Revision of IEEE Std 1250-2011)*, vol., no., IEEE, pp. 1–63, 2018.
- [83] D. Das, H. S. Nagi, and D. P. Kothari, "Novel method for solving radial distribution networks," 1994.
- [84] "pg_tca30bus." http://labs.ece.uw.edu/pstca/pf30/pg_tca30bus.htm (accessed Jan. 11, 2023).
- [85] J. A. Sa'ed, Z. Wari, F. Abughazaleh, J. Dawud, S. Favuzza, and G. Zizzo, "Effect of demand side management on the operation of pv-integrated distribution systems," *Applied Sciences (Switzerland)*, vol. 10, no. 21, pp. 1–26, Nov. 2020, doi: 10.3390/app10217551.
- [86] S. Yari and H. Khoshkhou, "Assessment of line stability indices in detection of voltage stability status," *2017 IEEE International Conference on Environment and Electrical Engineering and 2017 IEEE Industrial and Commercial Power Systems Europe (EEEIC / I&CPS Europe)*, pp. 7–11, 2017, doi: 10.1109/EEEIC.2017.7977454.
- [87] P. IEEE Standards Coordinating Committee 21 (Fuel Cells, IEEE-SA Standards Board., and Institute of Electrical and Electronics Engineers., *IEEE standard for interconnecting distributed resources with electric power systems*. Institute of Electrical and Electronics Engineers, 2003.
- [88] M. M. N. N. I. A. W. N. S. M. S. L. J. A. I. A. Bazilah Ismail, "Voltage Stability Indices Studies on Optimal Location of Wind Farm in Distribution Network," in *2017 IEEE Conference on Energy Conversion (CENCON)*, 2017, pp. 111–116.
- [89] saac Kofi Otchere, Bernard Arhin, and Emmanuel Asuming Frimpong, "Investigation of Voltage Stability for Transmission Network with High Penetration of Wind Energy Sources," in *IEEE Power Engineering Society Conference and Exposition in Africa, PowerAfrica*, IEEE, 2020.
- [90] P. Mehta, P. Bhatt, and V. Pandya, "Optimal selection of distributed generating units and its placement for voltage stability enhancement and energy loss minimization," *Ain Shams Engineering Journal*, vol. 9, no. 2, pp. 187–201, Jun. 2018, doi: 10.1016/j.asej.2015.10.009.
- [91] Geethika Nannapaneni, Tarek Medalel Masaud, and Rajab Chaloo, "A Comprehensive Analysis of Voltage Stability Indices in the Presence of Distributed Generation," in *2015 IEEE Conference on Technologies for Sustainability (SusTech)*, 2015, pp. 96–102.
- [92] D. Q. Hung, N. Mithulananthan, and R. C. Bansal, "Analytical expressions for DG allocation in primary distribution networks," *IEEE Transactions on Energy Conversion*, vol. 25, no. 3, pp. 814–820, Sep. 2010, doi: 10.1109/TEC.2010.2044414.

- [93] J. A. Sa'ed, M. K. Jubran, S. Favuzza, and F. Massaro, "Reassessment of voltage stability for distribution networks in presence of DG," in *2016 IEEE 16th International Conference on Environment and Electrical Engineering (ICEEE)*., IEEE, 2016.
- [94] D. Q. Hung and N. Mithulanathan, "Multiple distributed generator placement in primary distribution networks for loss reduction," *IEEE Transactions on Industrial Electronics*, vol. 60, no. 4, pp. 1700–1708, 2013, doi: 10.1109/TIE.2011.2112316.
- [95] R. S. al Abri, E. F. El-Saadany, and Y. M. Atwa, "Optimal placement and sizing method to improve the voltage stability margin in a distribution system using distributed generation," *IEEE Transactions on Power Systems*, vol. 28, no. 1, pp. 326–334, 2013, doi: 10.1109/TPWRS.2012.2200049.